10-23-2018 2:00 PM

Bifurcation Analysis of Two Biological Systems: A Tritrophic Food Chain Model and An Oscillating Networks Model

Xiangyu Wang, *The University of Western Ontario*

Supervisor: Yu, Pei., *The University of Western Ontario*

A thesis submitted in partial fulfillment of the requirements for the Master of Science degree in Applied Mathematics

Abstract

In this thesis, we apply bifurcation theory to study two biological systems. Main attention is focused on complex dynamical behaviors such as stability and bifurcation of limit cycles. Hopf bifurcation is particularly considered to show bistable or even tristable phenomenon which may occur in biological systems. Recurrence is also investigated to show that such complex behavior is common in biological systems.

First we consider a tritrophic food chain model with Holling functional response types III and IV for the predator and superpredator, respectively. Main attention is focused on the stability and bifurcation of equilibria when the prey has a linear growth. Coexistence of different species is shown in the food chain, showing bistable or even tristable phenomenon. Hopf bifurcation is studied to show complex dynamics due to the existence of multiple limit cycles. In particular, normal form theory is applied to prove that three limit cycles can bifurcate from an equilibrium in the vicinity of a Hopf critical point.

Further investigation is focused on the recurrence behavior in oscillating networks of biologically relevant organic reactions. This model has one unique equilibrium solution. Analysis is first given to the stability and bifurcation of the equilibrium. Then, particular attention is focused on recurrence behavior of the system when the equilibrium become unstable. Numerical simulations are compared with the analytical predictions to show a very good agreement.

Keywords: Food chain model, oscillating network, organic reaction, stability, saddle-node bifurcation, Hopf bifurcation, limit cycle, bistable, tristable, recurrence

Acknowledgements

I would like to express the special appreciation to my supervisor Dr. Pei Yu, for his constant encouragement and guidance. I thank him for giving me the opportunity to study at Western University. His useful suggestions and instructive advice are necessary to complete the thesis.

I would also thank Dr. Xingfu Zou. His cheerful attitude encourage me a lot in my study. My course professors Dr. Greg Reid and Dr. Lindi Wahl lead me into the world of Applied Mathematics. Many thanks to their energy in teaching me. I am very grateful the administration of the department of Applied Mathematics. Also, Audrey Kager has provided huge support and assistance to me.

Finally, I dedicate my thesis to my parents and husband Laigang for their love and support.

Contents

List of Figures

List of Appendices

Chapter 1

Introduction

1.1 Overview

Bifurcation analysis has always played an important role in the study of practical dynamical systems, such as biological models, physical models, and chemical models. For example, as it has been shown, a railway vehicle has stable motion in low speeds, but when it reaches a high speed, the motion becomes unstable. The main purpose of nonlinear analysis on the dynamics of railway vehicles is to study bifurcation, nonlinear lateral stability and hunting behavior of vehicles in tangent track. As an indispensable part of bifurcation theory, Hopf bifurcation is a very important type of bifurcation and often occurs in almost all physical systems, yielding periodic oscillations. In particular, Hopf bifurcation can occur in many biological systems such as the Lotka-Volterra model of predator-prey interaction (known as paradox of enrichment), the Hodgkin-Huxley model for nerve membranes [1], the Selkov model of glycolysis, the Belousov-Zhabotinsky reaction and the Lorenz attractor. Thus, considering Hopf bifurcation is of great importance in studying biological and physical systems.

Hopf bifurcation is also known as Poincaré-Andronov-Hopf bifurcation, named after Henri Poincaré, Eberhard Hopf, and Aleksandr Andronov [2]. In the mathematical theory of bifurcations, Hopf bifurcation appears from a critical point at which the system's stability changes and a periodic motion arises. More precisely, Hopf bifurcation occurs in a dynamical system from an equilibrium solution when the linearized system contains a pair of purely imaginary eigenvalues at the equilibrium solution. With a general assumption for a dynamical system, the equilibrium solution loses its stability at a critical point and a family of small-amplitude limit cycle bifurcates from the equilibrium. Further, for post-critical behaviors, Hopf bifurcation can be classified as two types: supercritical and subcritical. Assume that a dynamical system undergoes a Hopf bifurcation from an equilibrium of the system, the normal form associated with the Hopf bifurcation can be written as

$$\frac{dz}{dt} = z[(\lambda + i) + c|z|^2], \tag{1.1}$$

where z, c are both complex and λ is a parameter. If we write $c = \alpha + i\beta$, α is called the first Lyapunov constant. There exists a unique limit cycle bifurcating from the equilibrium $z = 0$

for $\lambda > 0$, with the solution given by

$$z(t) = \sqrt{-\frac{\lambda}{\alpha}} e^{(1+\beta r^2)it}. \tag{1.2}$$

If $\alpha < 0$ (or $\alpha > 0$), then the bifurcation is called supercritical (or subcritical). Therefore, if the first Lyapunov constant (focus value) is negative, then the limit cycle is orbitally stable and the bifurcation is supercritical. Otherwise the limit cycle is unstable and the bifurcation is subcritical.

Recently, there have been many studies on the subject of Hopf bifurcation. Among them, the main research is focused on the analysis of limit cycles and stability. Yu *et al.* [34] studied a bacteriophage model that includes prophage, focusing on asymptotic behavior of the solutions, and proved the existence of a supercritical Hopf bifurcation and stable limit cycles. Zhang *et al.* [35] studied a newly autoimmune four-dimensional disease model, and proved the existence of a supercritical Hopf bifurcation, leading to a family of stable limit cycles. The study of Hopf bifurcation has also been used to investigate the behaviors in simple disease models arising in epidemiology, in-host disease and autoimmunity (e.g., see [36]). Recently, there are also some studies on the tritrophic food chain models, in which the coexistence of multiple species is shown by proving the existence of a stable limit cycle. For example, Francois and Llibre [11] used averaging theory to prove the existence of a stable periodic orbit contained in the region where all variables are positive. Castellanos *et al.* [8] studied linear growth of the prey and functional response of Holling type III [62] for the middle and top species, and showed a double zero-Hopf bifurcation in the positive octant of $\mathbb{R}^3$ using the averaging theory. In [4], the authors studied the case when the prey has linear growth, while the middle and top species have functional responses Holling types II and III [62], respectively, and proved the existence of a stable limit cycle in the region of interest. In [6], the authors considered the case when the prey has logistic growth, while the predator and superpredator have the functional responses Lotka-Volterra type and Holling type II [62], respectively, forming a differential system based on the Leslie-scheme. In the paper, the authors also computed the first Lyapunov coefficient explicitly and showed the existence of a stable limit cycle. Moreover, they demonstrated by simulation a strange attractor which provides evidence that the model exhibits chaotic dynamics.

In this thesis, our study focuses on the stability and bifurcation of limit cycles due to Hopf bifurcation. In particular, we consdier two models: a tritrophic food chain model and an oscillating networks model. For the food chain model, we mainly investigate the case when the model is characterized by that the prey growth rate is linear in the absence of the predators, while the functional responses for the middle and top species in the chain are Holling type III and Holling type IV, respectively. For the oscillating network model, our main attention is focused on Hopf bifurcation and the reccurence phenomenon induced by Hopf bifurcation.

To study our two models, we need the basis of stability and bifurcation theory for nonlinear dynamical systems. In the following, we briefly introduce some of the fundamental theory and methodology.

1.1.1 Linear theory

Firstly, we present some results and formulas for general dynamical systems to study the stability of equilibrium solutions. Consider the general nonlinear differential system:

$$\dot{x} = f(x,\mu), \quad x \in R^n, \ \ \mu \in R^m, \ \ f: \ R^{n+m} \longmapsto R^n, \tag{1.3}$$

where the dot denotes differentiation with respect to time t, x and μ are the n-dimensional state variable and m-dimensional parameter variable, respectively. Assume that the nonlinear function $f(x,\mu)$ is analytic with respect to x and μ. Suppose that an equilibrium solution of Eq.(1.3) is given in the form of $x_e = x_e(\mu)$, which is determined from $f(x,\mu) = 0$. In order to analyze the stability of x_e, evaluating the Jacobian of system (1.3) at $x = x_e(\mu)$ yields $J(\mu) = D_x f|_{x=x_e(\mu)}$. If all eigenvalues of $J(\mu)$ have nonzero real parts, then the system is said to be hyperbolic, that means no complex dynamics exists in the vicinity of the equilibrium. Otherwise, at least one of the eigenvalues of $J(\mu)$ has zero real part at a critical point, defined by $\mu = \mu_c$, and bifurcations may occur from $x_e(\mu)$. To determine the stability of the equilibrium, we firstly find the eigenvalues of the Jacobian $J(\mu)$, which are the roots of the characteristic polynomial equation:

$$\begin{aligned} P_n(\lambda) &= \det[\lambda I - J(\mu)] \\ &= \lambda^n + a_1(\mu)\lambda^{n-1} + a_2(\mu)\lambda^{n-2} + \cdots + a_{n-1}(\mu)\lambda + a_n(\mu) = 0. \end{aligned} \tag{1.4}$$

For a fixed value of μ, if all the roots of the polynomial $P_n(\lambda)$ have negative real part, then the equilibrium is asymptotically stable for this value of μ. If at least one of the eigenvalues has zero real part as μ is varied to cross a critical point μ_c, then the equilibrium becomes unstable at μ_c and bifurcation occurs from this critical point. When all the roots of $P_n(\lambda)$ have negative real part, we call $P_n(\lambda)$ a stable polynomial, otherwise an unstable polynomial.

In general, for $n \geqslant 3$, it is hard to find the roots of $P_n(\lambda)$. Thus we use the Routh-Hurwitz Criterion [46] to analyze the local stability of the equilibrium solution $x = x_e(\mu)$. The criterion gives necessary and sufficient conditions under which the equilibrium is locally asymptotically stable, i.e. all the roots of the the characteristic polynomial $P_n(\lambda)$ have negative real part. These conditions are given by

$$\Delta_i(\mu) > 0, \quad i = 1, 2, \ldots, n, \tag{1.5}$$

where $\Delta_i(\mu)$ is called the ith-principal minor of the Hurwitz arrangements of order n, defined as follows (here, order n means that there are n coefficients a_i ($i = 1, 2, \ldots, n$) in Eq. (1.4), which construct the Hurwitz principal minors):

$$\begin{aligned} &\Delta_1 = a_1, \\ &\Delta_2 = \det\begin{bmatrix} a_1 & 1 \\ a_3 & a_2 \end{bmatrix}, \\ &\Delta_3 = \det\begin{bmatrix} a_1 & 1 & 0 \\ a_3 & a_2 & a_1 \\ a_5 & a_4 & a_3 \end{bmatrix}, \\ &\ldots, \\ &\Delta_n = a_n \Delta_{n-1}. \end{aligned} \tag{1.6}$$

Assume that as μ is varied to reach a critical point $\mu = \mu_c$, at least one of Δ_i's becomes zero. Then the fixed point $x_e(\mu_c)$ becomes unstable, and μ_c is called critical point. It can be seen from Eq. (1.5) that if $a_n(\mu) = 0$, but other Hurwitz arrangements are still positive (i.e. $\Delta_n = 0$, $\Delta_i(\mu) > 0$, $i = 1, 2, \ldots, (n-1)$), then $P_n(\lambda) = 0$ has one zero root. In this case, system (1.3) has a simple zero singularity and a static bifurcation occurs from x_e. In other cases, for example, Hopf bifurcation occurs at a critical point when $P_n(\lambda) = 0$ has a pair of purely imaginary eigenvalues $\pm i\omega$ ($\omega > 0$) at this point. However, the pair of purely imaginary eigenvalues are often difficult to be determined explicitly for high dimensional systems. Here, we present the following theorem without computing the eigenvalues of the Jacobian of a general system. The theorem gives the necessary and sufficient conditions for determining a Hopf critical point based on the Hurwitz criterion. Its proof can be found in [57].

Theorem 1.1.1 [57] The necessary and sufficient conditions for system (1.3) to have a Hopf bifurcation at an equilibrium solution $x = x_e$ is $\Delta_{n-1} = 0$, with other Hurwitz conditions being still held, i.e. $a_n > 0$ and $\Delta_i > 0$, for $i = 1, \ldots, n-2$.

Next, we present a method for computing focus values. There are many methods developed for computing the focus values of planar vector fields, such as Poincaré Takens method [16], the perturbation method [58], the singular point value method [23], etc. But, for higher dimensional dynamical systems, the computation is much involved. In the next two subsections, we briefly introduce the method of normal forms for computing the focus values of general n-dimension dynamical systems. The general normal form theory can be found in [16, 10] and computations using computer algebra systems can be found in [17, 29].

1.1.2 Normal form theory

Consider the following general n-dimensional differential system:

$$\dot{z} = Az + f(z), z \in R^n, f : R^n \to R^n, \tag{1.7}$$

where Az and $f(z)$ represent the linear and nonlinear parts of the system, respectively. We assume that $z = 0$ is a fixed point of the system, which implies that $f(0) = Df(0) = 0$. It is also assumed that $f(z)$ is analytic and can be expanded in Taylor series about z, and system (1.7) only contains stable center manifolds. In the computation of normal forms, the first step is usually to introduce a linear transformation into (1.7) such that the linear part of (1.7) can be changed into the Jordan canonical form. Without loss of generality, suppose that under the linear transformation $z = T(x, y)$, system (1.7) becomes

$$\begin{aligned} \dot{x} &= J_1 x + f_1(x, y), \quad x \in R^k, \quad f_1 : R^n \to R^k, \\ \dot{y} &= J_2 y + f_2(x, y), \quad y \in R^{n-k}, \quad f_2 : R^n \to R^{n-k}, \end{aligned} \tag{1.8}$$

where J_1 =diag$(\lambda_1, \lambda_2, \cdots, \lambda_k)$, and J_2 =diag$(\lambda_{k+1}, \lambda_{k+2}, \cdots, \lambda_n)$, with $\mathrm{Re}(\lambda_j) = 0$, $j = 1, 2, \cdots, k$ and $\mathrm{Re}(\lambda_j) < 0$, $j = k+1, \cdots, n$.

Next, we apply center manifold theory [5] to system (1.8), yielding to that y can be expressed as $y = H(x)$, satisfying $H(0) = DH(0) = 0$. Therefore, the first equation of (1.8) can be rewritten as

$$\dot{x} = J_1 x + f_1(x, H(x)) = J_1 x + f_1^2(x) + f_1^3(x) + \cdots + f_1^s(x) + \cdots, \tag{1.9}$$

where $f_1^j \in M_j$, $j = 2, 3, \ldots$, M_j defining a linear space of vector fields whose elements are homogeneous polynomials of degree j. Equation (1.9) describes the dynamics on the center manifold of system (1.8), and $H(x)$ can be determined from the following equation:

$$DH(x)[J_1 x + f_1(x, H(x))] - J_2(H(x)) - f_2(x, H(x)) = 0. \tag{1.10}$$

Next, by using normal form theory, we introduce the near-identity transformation:

$$x = u + Q(u) = u + q^2(u) + q^3(u) + \cdots + q^s(u) + \cdots, \tag{1.11}$$

where $q^j \in M_j$, $j = 2, 3, \ldots$ into (1.9) to obtain the normal form,

$$\dot{u} = J_1 u + C(u) = J_1 u + c^2(u) + c^3(u) + \cdots + c^s(u) + \cdots, \tag{1.12}$$

where $c^j \in M_j$, $j = 2, 3, \ldots$

In the view point of computation, computing center manifold and normal form seems to be straightforward. However, to design an efficient algorithm is not an easy task. Recently, an explicit recursive formula has been developed for computing the normal form together with center manifold for general n-dimensional differential systems associated with semisimple singularities. We omit the detailed formulas and algorithms, as well as the Maple program here, which can be found in [29].

1.1.3 Bifurcation of multiple limit cycles

Now we turn to discuss how to determine the maximal number of limit cycles which may bifurcate from a Hopf critical point. Suppose that we have obtained the normal form of system (1.7), given in the polar coordinates up to the $(2k + 1)$th order term:

$$\begin{aligned} \dot{r} &= r(v_0 + v_1 r^2 + v_2 r^4 + \cdots + v_k r^{2k}), \\ \dot{\theta} &= \omega_c + t_1 r^2 + t_2 r^4 + \cdots + t_k r^{2k}, \end{aligned} \tag{1.13}$$

where r and θ denote the amplitude and phase of motion, respectively. v_k and t_k are expressed in terms of the original system's coefficients. v_k is called the kth-order focus value of the origin. The zero-order focus value v_0 is obtained from linear analysis.

To find k small-amplitude limit cycles of system (1.7) around the origin, we first find the conditions based on the original system's coefficients such that $v_0 = v_1 = v_2 = \cdots = v_{k-1} = 0$ (note that $v_0 = 0$ is automatically satisfied at the critical point), but $v_k \neq 0$. Then appropriate small perturbations are performed to prove the existence of k limit cycles. In the following theorem, we give sufficient conditions for the existence of small-amplitude limit cycles. (The proof can be found in [17].)

Theorem 1.1.2 [17] Suppose that the focus values depend on k parameters, expressed as

$$v_j = v_j(\epsilon_1, \epsilon_2, \cdots, \epsilon_k), \quad j = 0, 1, \cdots, k, \tag{1.14}$$

satisfying

$$\begin{aligned} &v_j(0, \cdots, 0) = 0, \quad j = 0, 1, \cdots, k-1, \quad v_k(0, \cdots, 0) \neq 0, \\ &\text{and} \quad \det\left[\frac{\partial(v_0, v_1, \cdots, v_{k-1})}{\partial(\epsilon_1, \epsilon_2, \cdots, \epsilon_k)}(0, \cdots, 0)\right] \neq 0. \end{aligned} \tag{1.15}$$

Then, for any given $\epsilon_0 > 0$, there exist $\epsilon_1, \epsilon_2, \cdots, \epsilon_k$ and $\delta > 0$ with $|\epsilon_j| < \epsilon_0, j = 1, 2, \cdots, k$ such that the equation $\dot{r} = 0$ has exactly k real positive roots (i.e. system (2.1) has exactly k limit cycles) in a δ-ball withe its center at the origin.

1.2 Two biological models studied in the thesis

This thesis is focused on the study of a tritrophic food chain model and an oscillating networks model of biologically relevant organic reactions. Particular attention is given to stability of equilibrium solutions and bifurcations.

1.2.1 A tritrophic food chain model

The general tritrophic food chain model with three species is described by the following three ordinary differential equations [7]:

$$\begin{aligned} \frac{dx}{dt} &= h(x) - f(x)y, \\ \frac{dy}{dt} &= c_1 y f(x) - g(y)z - \mu y, \\ \frac{dz}{dt} &= c_3 g(y)z - d_2 z, \end{aligned} \tag{1.16}$$

where x, y and z represent respectively the densities of the bottom, the middle and the top species in the chain. The function $h(x)$ represents the growth rate of prey in the absence of the other species, and $h(x)$ is assumed linear in this study. The functions $f(x)$ and $g(y)$ are the functional responses of the predator y and superpredator z, respectively. All the parameters are positive. The parameters c_1 and c_3 represent the benefits from the consumption of food, and the parameters μ and d_2 represent the mortality rate of the corresponding predators. For ecological study, the region of interest in $\mathbb{R}^3$ is the positive octant $\Omega = \{(x, y, z) \in \mathbb{R}^3 | x > 0, y > 0, z > 0\}$.

We consider the case when f is Holling type III and g is Holling type IV, which are given explicitly in the form of

$$f(x) = \frac{a_1 x^2}{x^2 + b_1}, \quad g(y) = \frac{a_2 y}{y^2 + b_2}, \tag{1.17}$$

where a_1, b_1, a_2, b_2 are positive parameters.

1.2.2 An oscillating networks model of biologically relevant organic reactions

To study oscillations in oscillating networks, a simple kinetic model is constructed in [54], described by the following three ordinary differential equations:

$$\begin{aligned} \frac{dA}{dt} &= k_1 SA - k_2 IA - k_3 A - k_0 A + k_4 S, \\ \frac{dI}{dt} &= k_0 I_0 - k_0 I - k_2 IA, \\ \frac{dS}{dt} &= k_0 S_0 - k_0 S - k_4 S - k_1 SA, \end{aligned} \tag{1.18}$$

where A = [RSH], I = [maleimide], S = [AlaSEt], I_0 and S_0 are the concentrations of maleimide and AlaSEt fed into the reactor, respectively, k_i, $i = 1, 2, 3, 4$, are rate constants and k_0 is the space velocity. From the linear stability analysis of this model [39], we find that increasing k_0 from lower to higher values causes two transitions. The first one is from a stable focus to a stable orbit via an Andronov-Hopf bifurcation [48], and the second one is from a stable orbit to a single stable equilibrium via a saddle-node or fold bifurcation [48].

1.2.3 Outline of the thesis

In Chapter 2, we focus on Hopf bifurcation in a tritrophic food chain model (1.16) with Holling functional response types III and IV. We provide a summary on the linear analysis of system (1.16). And we find three limit cycles around the Hopf singular point in system (1.16) by using normal form theory. Conclusion and discussions are presented at the end of this chapter.

In Chapter 3, we are devoted to the stability analysis of the equilibria in an oscillating networks model of biologically relevant organic reactions (1.18). We first present a summary on the stability of equilibria of the model by the Routh-Hurwitz Cirterion, and then identify saddle-node and Hopf bifurcations arising from the equilibrium. Numerical simulations are given to show the good agreement between simulations and analytical predictions. Conclusion and discussions are drawn at the end of this chapter.

Finally, we conclude the thesis in Chapter 4 and also disucss some potential future research.

Chapter 2

Multiple Limit Cycles in a Food Chain Model

2.1 Introduction

After the pioneering work of Lotka and Volterra [24, 30], the study of ditrophic food chains has received and been continuously receiving much attention in mathematical ecology. The classical ecological models of interacting populations often have focused on two species. Continuous time models of two interacting species, usually called prey-predator models, have been analyzed extensively, and some notable achievements have been made, for example, see [3, 21]. Mathematically, these models can exhibit only two basic patterns: Trajectories approach a steady state or a limit cycle. However, the ecological communities in nature have been observed to exhibit much more complex dynamics. Price *et al.* [28] argued that community behavior must be based on three or more trophic levels. Continuous time models with three species have been reported to have more complicated patterns. Existence of limit cycles, multiplicity of attractors, and catastrophic bifurcations are the characteristics of the models which have been used to explain complex behaviors observed in the field. The research in the past two decades has demonstrated that the complex dynamical behavior, including quasi-periodic motion or even chaos, can arise in continuous time ecological models with three or more species. Much attention has been paid to the study of the transition from periodic oscillation to chaotic motion. Understanding the mechanism of generating such behaviors constitutes an exercise of paramount importance. In the late 1970s, some interest in the mathematics of tritrophic food chain models emerged. One important model is called tritrophic food chain because each population except the lowest eats only the one on the immediate lower trophic level [12]. Our attention in this article is to investigate whether or not three species can exist simultaneously. The typical ecological interaction has been studied from a mathematical point of view through a differential equation system, showing the coexistence of species translating to the existence of a stable limit cycle. Some authors dealt with the problem of persistence [12, 13], but did not provide information on the number and the geometry of the attractors. Hogeweg and Hesper [20] showed through simulation that a particular food chain model can behave chaotically, however, this paper did not receive much attention. Later, Hastings and Powell showed in [18] that food chains behave chaotically on a "tea-cup" strange attractor, and the three populations

have diversified time responses increasing from bottom to top. Around the same time, Muratori and Rinaldi [26] performed a singular perturbation analysis to confirm that the tea-cup geometry is the result of the interaction between high frequency (prey-predator) oscillation and low frequency (predator-top-predator) oscillation. Since then, particular effort has been devoted to the study of the complex dynamics of food chain systems, and bifurcation analysis has been the major tool of investigation.

The general tritrophic food chain model with three species is described by the following three ordinary differential equations [7]:

$$\begin{aligned} \frac{dx}{dt} &= h(x) - f(x)y, \\ \frac{dy}{dt} &= c_1 y f(x) - g(y)z - \mu y, \\ \frac{dz}{dt} &= c_3 g(y)z - d_2 z, \end{aligned} \tag{2.1}$$

where x, y and z represent respectively the densities of the bottom, the middle and the top species in the chain. The function $h(x)$ represents the growth rate of prey in the absence of the other species, and $h(x)$ is assumed linear in this study. The functions $f(x)$ and $g(y)$ are the functional responses of the predator y and superpredator z, respectively. All the parameters are positive. The parameters c_1 and c_3 represent the benefits from the consumption of food, and the parameters μ and d_2 represent the mortality rate of the corresponding predators. For ecological study, the region of interest in $\mathbb{R}^3$ is the positive octant $\Omega = \{(x, y, z) \in \mathbb{R}^3 | x > 0, y > 0, z > 0\}$.

In this chapter, we consider the case when f is Holling type III and g is Holling type IV, which are given explicitly in the form of

$$f(x) = \frac{a_1 x^2}{x^2 + b_1}, \quad g(y) = \frac{a_2 y}{y^2 + b_2}, \tag{2.2}$$

where a_1, b_1, a_2, b_2 are positive parameters.

The rest of the chapter is organized as follows. In section 2.2, we provide a linear analysis of system (2.1), in particular on the stability and bifurcation of the positive equilibrium. In section 2.3, we prove the existence of three limit cycles around the positive equilibrium, arising from Hopf bifurcation. In section 2.4, numerical simulation is presented in good agreement with our analytical theory. Finally, the conclusion and discussion is drawn in section 2.5.

2.2 Bifurcation analysis of system (2.1)

In this section, we consider the differential system (2.1) where the functional responses are given in (2.2) and the growth rate of prey is linear. So, the function h is written as $h(x) = \rho x$

and the differential system that we will analyze has the form,

$$\begin{aligned}
\dot{x} &= \left(\rho - \frac{a_1 xy}{b_1 + x^2}\right) x, \\
\dot{y} &= \left(-\mu + \frac{a_1 c_1 x^2}{b_1 + x^2} - \frac{a_2 z}{b_2 + y^2}\right) y, \\
\dot{z} &= \left(-d_2 + \frac{a_2 c_3 y}{b_2 + y^2}\right) z.
\end{aligned} \tag{2.3}$$

It is obvious that $p_b = (0, 0, 0)$ is a boundary equilibrium solution of system (2.3). The Jacobian matrix of system (2.3) evaluated at the equilibrium p_b is given by

$$\begin{bmatrix} \rho & 0 & 0 \\ 0 & -\mu & 0 \\ 0 & 0 & -d_2 \end{bmatrix},$$

which clearly shows that p_b is a saddle point.

Because it is hard to obtain the explicit expression of the positive equilibrium solution of system (2.3), we derive the conditions based on the system parameters for the existence of the positive equilibrium in the region of interest. Moreover, we study the stability and find the conditions under which Hopf bifurcation occurs from the positive equilibrium. In [7], the authors have given the conditions for the existence of the positive equilibrium, and a single limit cycle bifurcating from this positive equilibrium. Here, our main result is to prove the existence of three limit cycles. First, we cite some results from [7].

It should be noted that for practical systems proving the existence of a single limit cycle is usually not difficult , but proving the existence of two limit cycles is quite challenge. It is extremely difficult to prove the existence of three limit cycles. Very few articles have been published to discuss the existence of three limit cycles, for example, see [33, 14] .

Lemma 2.2.1 [7] For system (2.6) with positive parameters, the point $p_0 = (x_0, y_0, z_0) \in \Omega$ is an equilibrium if and only if the parameters a_1, b_2 and the third coordinate of p_0 satisfy

$$\begin{aligned}
&a_1 = \frac{\rho(b_1 + x_0^2)}{x_0 y_0}, \quad b_2 = \frac{y_0}{d_2}(a_2 c_3 - d_2 y_0), \quad z_0 = \frac{c_3}{d_2}(-\mu y_0 + c_1 x_0 \rho), \\
&y_0 < \frac{a_2 c_3}{d_2}, \quad -\mu y_0 + c_1 x_0 \rho > 0.
\end{aligned} \tag{2.4}$$

Corollary 2.2.2 [7] *With the conditions given as in Lemma* 2.2.1, if

$$c_1 = \frac{k_1 + \mu c_3 y_0}{c_3 x_0 \rho}, \quad y_0 < \frac{a_2 c_3}{d_2} \tag{2.5}$$

with $k_1 > 0$, then $z_0 > 0$ and the equilibrium is inside Ω, given in the form of $p_0 = (x_0, y_0, \frac{k_1}{d_2})$.

With the parameter values given in Lemma 2.2.1 and Corollary 2.2.2, system (2.3) becomes

$$\begin{aligned}
\dot{x} &= \rho x - \frac{\rho x^2 y(b_1 + x_0^2)}{x_0 y_0 (b_1 + x^2)}, \\
\dot{y} &= -\frac{a_2 d_2 yz}{y_0(a_2 c_3 - d_2 y_0) + d_2 y^2} + \frac{x^2 y(b_1 + x_0^2)(k_1 + \mu c_3 y_0)}{c_3 x_0^2 y_0 (b_1 + x^2)} - \mu y, \\
\dot{z} &= d_2 z \left(\frac{a_2 d_2 c_3 y}{y_0(a_2 c_3 - d_2 y_0) + d_2 y^2} - 1 \right).
\end{aligned} \tag{2.6}$$

The Jacobian matrix of system (2.6) evaluated at $p_0 = (x_0, y_0, \frac{k_1}{d_2})$ is given as follows:

$$\mathrm{J}_{\mathrm{p}_0} = \begin{bmatrix} \dfrac{(x_0^2 - b_1)\rho}{x_0^2 + b_1} & -\dfrac{x_0 \rho}{y_0} & 0 \\ \dfrac{2b_1(k_1 + \mu c_3 y_0)}{c_3 x_0^2 (b_1 + x_0^2)} & \dfrac{2d_2 k_1}{a_2 c_3^2} & -\dfrac{d_2}{c_3} \\ 0 & \dfrac{k_1(a_2 c_3 - 2d_2 y_0)}{a_2 c_3 y_0} & 0 \end{bmatrix}.$$

Which, in turn, yields a cubic characteristic polynomial, given by

$$P_1(\lambda) = \lambda^3 + A_1 \lambda^2 + A_2 \lambda + A_3 = 0, \tag{2.7}$$

where the coefficients $A_1,\ A_2,\ A_3$ are expressed in terms of the parameters in system (2.6) as

$$\begin{aligned}
A_1 &= \frac{c_3^2 \rho (b_1 - x_0^2) a_2 - 2d_2 k_1 (b_1 + x_0^2)}{(b_1 + x_0^2) c_3^2 a_2}, \\
A_2 &= \frac{1}{(b_1 + x_0^2) c_3^2 a_2 y_0} \{ [(-2y_0 d_2^2 + (a_2 c_3 - 2\rho y_0) d_2 \\
&\quad + 2a_2 c_3 \rho) b_1 + d_2 x_0^2 (a_2 c_3 - 2d_2 y_0 + 2\rho y_0)] k_1 + 2a_2 b_1 c_3^2 \mu \rho y_0 \}, \\
A_3 &= \frac{d_2 k_1 \rho (b_1 - x_0^2)(a_2 c_3 - 2d_2 y_0)}{(b_1 + x_0^2) c_3^2 a_2 y_0}.
\end{aligned} \tag{2.8}$$

Based on the characteristic polynomial (2.7), we consider possible bifurcation from the equilibrium p_0, including both static and dynamic (Hopf) bifurcations. The static bifurcation occurs when $P_1(\lambda) = 0$ has zero roots (zero eigenvalues). Thus we let $A_3 = 0$ to get $b_1 = x_0^2$, which yields $A_1 < 0$. Thus, the static bifurcation occurs in the unstable region, which is not interesting physically.

Theorem 2.2.3 *In system* (2.6)*, if one of the following conditions is satisfied,*

$$\begin{aligned}
&\text{I)}\ \ 0 < x_0 < \sqrt{b_1},\ \ 0 < y_0 < \frac{a_2 c_3}{2d_2},\ \ k_1 \le k_{\mathrm{L}},\ \ \mu > 0; \\
&\text{II)}\ \ 0 < x_0 < \sqrt{b_1},\ \ 0 < y_0 < \frac{a_2 c_3}{2d_2},\ \ k_{\mathrm{L}} < k_1 < k_{\mathrm{U}},\ \ \mu > \mu_0;
\end{aligned} \tag{2.9}$$

then the equilibrium $p_0 = (x_0, y_0, \frac{k_1}{d_2})$ *is local asymptotically stable. Here,*

$$k_{\mathrm{L}} = \frac{a_2c_3^2\rho^2(b_1 - x_0^2)[b_1(a_2c_3 - d_2y_0) + d_2y_0x_0^2]}{d_2(b_1 + x_0^2)[d_2(b_1 + x_0^2)(a_2c_3 - 2d_2y_0) + 2d_2\rho y_0x_0^2 + 2b_1\rho(a_2c_3 - d_2y_0)]},$$
$$k_{\mathrm{U}} = \frac{c_3^2\rho(b_1 - x_0^2)a_2}{2d_2(b_1 + x_0^2)}.$$

Proof According to the Hurwitz criterion, first we have

$$\begin{aligned}
&A_1 > 0 \Longrightarrow\ c_3^2\rho(b_1 - x_0^2)a_2 > 0 \Longleftrightarrow\ b_1 - x_0^2 > 0 \Longrightarrow\ 0 < x_0 < \sqrt{b_1};\\
&A_1 > 0 \Longrightarrow\ c_3^2\rho(b_1 - x_0^2)a_2 - 2d_2k_1(b_1 + x_0^2) > 0 \Longrightarrow\ k_1 < \frac{c_3^2\rho(b_1 - x_0^2)a_2}{2d_2(b_1 + x_0^2)} \Longleftrightarrow\ k_1 < k_{\mathrm{U}};\\
&A_3 > 0 \Longrightarrow\ (b_1 - x_0^2)(a_2c_3 - 2y_0d_2) > 0 \Longrightarrow\ 0 < y_0 < \frac{a_2c_3}{2d_2}.
\end{aligned} \tag{2.10}$$

Then, we compute $\Delta_2 = A_1A_2 - A_3$ to obtain

$$\begin{aligned}
\Delta_2 \quad &= \frac{2}{(b_1 + x_0^2)^2c_3^4a_2^2y_0}\Delta_{2a},\\
\Delta_{2a} \quad &= (b_1 + x_0^2)y_0\rho c_3^4b_1a_2^2A_1\mu - k_1\{-2y_0(x_0^2 + b_1)d_2^2 + [(a_2c_3 - 2\rho y_0)b_1\\
&\quad + x_0^2(a_2c_3 + 2\rho y_0)]d_2 + 2a_2b_1c_3\rho\}d_2(x_0^2 + b_1)(k_1 - k_{\mathrm{L}}).
\end{aligned} \tag{2.11}$$

Now, solving Δ_{2a} for μ, we obtain the critical value,

$$\mu_{\mathrm{H}} = \frac{k_1[d_2(b_1 + x_0^2)(a_2c_3 - 2y_0d_2 + 2\rho y_0) + 2b_1\rho(a_2c_3 - 2d_2y_0)](k_1 - k_{\mathrm{L}})}{2b_1a_2c_3^2\rho y_0(k_{\mathrm{U}} - k_1)}. \tag{2.12}$$

Further, it can be verified that $k_{\mathrm{L}} < k_{\mathrm{U}}$:

$$\begin{aligned}
&k_{\mathrm{L}} < k_{\mathrm{U}}\\
&\Longleftrightarrow \frac{a_2c_3^2\rho^2(b_1 - x_0^2)[b_1(a_2c_3 - d_2y_0) + d_2y_0x_0^2]}{d_2(b_1 + x_0^2)[d_2(b_1 + x_0^2)(a_2c_3 - 2y_0d_2) + 2d_2\rho y_0x_0^2 + 2b_1\rho(a_2c_3 - d_2y_0)]} < \frac{c_3^2\rho(b_1 - x_0^2)a_2}{2d_2(b_1 + x_0^2)},\\
&\Longleftrightarrow \frac{\rho[b_1(a_2c_3 - d_2y_0) + d_2y_0x_0^2]}{[d_2(b_1 + x_0^2)(a_2c_3 - 2y_0d_2) + 2d_2\rho y_0x_0^2 + 2b_1\rho(a_2c_3 - d_2y_0)]} < \frac{1}{2},\\
&\Longleftrightarrow 2\rho[b_1(a_2c_3 - d_2y_0) + d_2y_0x_0^2] < [d_2(b_1 + x_0^2)(a_2c_3 - 2y_0d_2) + 2d_2\rho y_0x_0^2 + 2b_1\rho(a_2c_3 - d_2y_0)],\\
&\Longleftrightarrow d_2(b_1 + x_0^2)(a_2c_3 - 2y_0d_2) > 0.
\end{aligned} \tag{2.13}$$

Thus, besides $A_1 > 0$, $A_2 > 0$, $A_3 > 0$ under the conditions given in (2.10), the above discussion shows that $\Delta_2 > 0$ for $k_1 \le k_L$ ($\mu > 0$) or $k_L < k_1 < k_U$ ($\mu > \mu_{\mathrm{H}}$). Hence,

$$\begin{aligned}
&\text{if } k_1 \le k_{\mathrm{L}} \Longrightarrow \Delta_2 > 0 \text{ for } \mu > 0 \Longrightarrow \text{equilibrium point is stable, or}\\
&\text{if } k_{\mathrm{L}} < k_1 < k_{\mathrm{U}} \Longrightarrow \Delta_2 > 0 \text{ for } \mu > \mu_0 \Longrightarrow \text{equilibrium point is stable.}
\end{aligned} \tag{2.14}$$

Next, we derive the conditions for Hopf bifurcation. According to Theorem 1.1.1, Hopf bifurcation occurs from the equilibrium p_0 at $\mu = \mu_{\mathrm{H}} > 0$ when the following conditions hold,

$$0 < x_0 < \sqrt{b_1},\ \ k_{\mathrm{L}} < k_1 < k_{\mathrm{U}},\ \ 0 < y_0 < \frac{a_2 c_3}{2d_2}. \tag{2.15}$$

Under the conditions in (2.15), we rewrite $P_1(\lambda)$ as

$$P_1(\lambda) = \frac{F_1 F_2}{y_0 a_2 c_3^2 [a_2 c_3^2 \rho(b_1 - x_0^2) - 2k_1 d_2(b_1 + x_0^2)](b_1 + x_0^2)}, \tag{2.16}$$

where

$$\begin{aligned} F_1 &= a_2 c_3^2 (b_1 + x_0^2)\left[\lambda + \frac{2d_2(k_{\mathrm{U}} - k_1)}{a_2 c_3^2}\right], \\ F_2 &= 2y_0 d_2 (b_1 + x_0^2)(k_{\mathrm{U}} - k_1)\left[\lambda^2 + \frac{\rho k_1 (b_1 - x_0^2)(a_2 c_3 - 2d_2 y_0)}{2y_0(b_1 + x_0^2)(k_{\mathrm{U}} - k_1)}\right]. \end{aligned} \tag{2.17}$$

Thus, we can get the three roots (three eigenvalues) of $P_1(\lambda)$ as α and $\pm\omega i$, where

$$\begin{aligned} \alpha &= -\frac{2d_2(k_{\mathrm{U}} - k_1)}{a_2 c_3^2}, \\ \omega_{\mathrm{H}} &= \sqrt{\frac{\rho k_1 (b_1 - x_0^2)(a_2 c_3 - 2d_2 y_0)}{2y_0(b_1 + x_0^2)(k_{\mathrm{U}} - k_1)}}, \end{aligned} \tag{2.18}$$

satisfying $\alpha < 0$ and $\omega_{\mathrm{H}} > 0$ for $0 < k_1 < k_{\mathrm{U}}$.

In order to make the normal form computation feasible for the Hopf bifurcation, we further set

$$x_0 = \sqrt{X_0},\ \ X_0 > 0,\ \ k_1 = k_{\mathrm{L}} + \tfrac{1}{2}(k_{\mathrm{U}} - k_{\mathrm{L}}),\ \ y_0 = \frac{a_2 c_3}{4d_2},\ \ b_1 = x_0^2 + B_1, B_1 > 0. \tag{2.19}$$

Then, we can rewrite $k_{\mathrm{L}},\ k_{\mathrm{U}},\ A_1,\ A_2,\ A_3,\ \mu_{\mathrm{H}},\ \alpha$ *and* ω as

$$\begin{aligned} k_{\mathrm{L}} &= \frac{B_1 \rho^2 c_3^2 a_2 (3B_1 + 4X_0)}{2d_2[(d_2 + 3\rho)B_1 + 2X_0(d_2 + 2\rho)](2X_0 + B_1)}, \\ k_{\mathrm{U}} &= \frac{c_3^2 \rho B_1 a_2}{2d_2(2X_0 + B_1)}, \\ A_1 &= \frac{B_1 \rho d_2}{2[(d_2 + 3\rho)B_1 + 2X_0(d_2 + \rho)]}, \\ A_2 &= \frac{(d_2 + 6\rho)B_1 + 2X_0(d_2 + 4\rho)B_1\rho}{(2X_0 + B_1)^2}, \\ A_3 &= \frac{d_2 \rho^2 B_1^2[(d_2 + 6\rho)B_1 + 2X_0(d_2 + 4\rho)]}{2[(d_2 + 3\rho)B_1 + 2X_0(d_2 + 2\rho)](2X_0 + B_1)^2}, \\ \alpha &= -\frac{B_1 \rho d_2}{2[(d_2 + 3\rho)B_1 + 2X_0(d_2 + 2\rho)]}, \\ \mu_{\mathrm{H}} &= \frac{[(d_2 + 6\rho)B_1 + 2X_0(d_2 + 4\rho)]B_1}{4(X_0 + B_1)(2X_0 + B_1)}, \\ \omega_{\mathrm{H}} &= \frac{\sqrt{[(d_2 + 6\rho)B_1 + 2X_0(d_2 + 4\rho)]B_1\rho}}{2X_0 + B_1}, \end{aligned} \tag{2.20}$$

satisfying $A_1 > 0,\ A_2 > 0,\ A_3 > 0,\ \Delta_2 = 0,\ \alpha < 0,\ \mu_{\rm H} > 0,\ \omega_{\rm H} > 0$, as expected.

2.3 Existence of three limit cycles around p_0

In this section, we will present our main result. We will apply normal form theory to show that at least three small-amplitude limit cycles can bifurcate from the equilibrium p_0.

Theorem 2.3.1 *For system* (2.6)*, at least three small-amplitude limit cycles can bifurcate from the equilibrium* p_0.

Proof In order to study the limit cycle bifurcation around the equilibrium p_0 near the critical point $\mu = \mu_{\rm H}$, we need to compute the focus values. To achieve this, we use the following transformation,

$$\begin{aligned} x &= x_0 + T_{11}u + T_{12}v + T_{13}w, \\ y &= y_0 + T_{21}u + T_{22}v + T_{23}w, \\ z &= z_0 + T_{31}u + T_{32}v + T_{33}w, \end{aligned} \tag{2.21}$$

where

$$\begin{aligned} T_{11} &= -\frac{8d_2(2X_0+B_1)\sqrt{X_0}[(d_2+3\rho)B_1+2X_0(d_2+2\rho)]}{c_3^2a_2[(d_2+7\rho)B_1+2X_0(d_2+4\rho)]B_1}, \\ T_{12} &= -\frac{8d_2(2X_0+B_1)^2\sqrt{X_0}[(d_2+3\rho)B_1+2X_0(d_2+2\rho)]\omega_{\rm H}}{c_3^2[(d_2+6\rho)B_1+2X_0(d_2+4\rho)]a_2[(d_2+7\rho)B_1+2X_0(d_2+4\rho)]B_1}, \\ T_{13} &= \frac{x_0\rho(-a_2c_3^2\rho x_0^2+a_2b_1c_3^2\rho-2d_2k_1x_0^2-2b_1d_2k_1)c_3a_2}{2(a_2c_3x_0^2-2d_2x_0^2y0+a_2b_1c_3-2b_1d_2y0)k_1^2d_2}, \\ T_{21} &= 0, \\ T_{22} &= \frac{2[(d_2+3\rho)B_1+2X_0(d_2+2\rho)](2X_0+B_1)\omega_{\rm H}}{\rho c_3[(d_2+6\rho)B_1+2X_0(d_2+4\rho)]B_1}, \\ T_{23} &= -\frac{y_0(-a_2c_3^2\rho x_0^2+a_2b_1c_3^2\rho-2d_2k_1x_0^2-2b_1d_2k_1)}{(a_2c_3x_0^2-2d_2x_0^2y_0+a_2b_1c_3-2b_1d_2y_0)c_3k_1}, \\ T_{31} &= 1, \\ T_{32} &= 0, \\ T_{33} &= 1, \end{aligned} \tag{2.22}$$

to transform system (2.6) to a new system expanded in the form of

$$\begin{aligned} \dot{u} &= v + \sum_{i+j+k=2}^{5} a_{ijk}u^iv^jw^k, \\ \dot{v} &= -u + \sum_{i+j+k=2}^{5} b_{ijk}u^iv^jw^k, \\ \dot{w} &= c_{001}w_{\rm H} + \sum_{i+j+k=2}^{5} c_{ijk}u^iv^jw^k, \end{aligned} \tag{2.23}$$

where the coefficients a_{ijk}, b_{ijk} and c_{ijk} are expressed in term of the parameters in system (2.6).

Then, using the Maple program in [29], we get the first three focus values as follows:

$$
\begin{aligned}
V_1 &= -(B_1d_2+3B_1\rho+2X_0d_2+4X_0\rho)^2/[2B_1^3\rho(B_1d_2+7B_1\rho+2X_0d_2+8X_0\rho)(4B_1^3d_2^3\\
&+49B_1^3d_2^2\rho+180B_1^3d_2\rho^2+216B_1^3\rho^3+24B_1^2X_0d_2^3+260B_1^2X_0d_2^2\rho+840B_1^2X_0d_2\rho^2\\
&+864B_1^2X_0\rho^3+48B_1X_0^2d_2^3+452B_1X_0^2d_2^2\rho+1280B_1X_0^2d_2\rho^2+1152B_1X_0^2\rho^3+32X_0^3d_2^3\\
&+256X_0^3d_2^2\rho+640X_0^3d_2\rho^2+512X_0^3\rho^3)(16B_1^3d_2^3+193B_1^3d_2^2\rho+720B_1^3d_2\rho^2+864B_1^3\rho^3\\
&+96B_1^2X_0d_2^3+1028B_1^2X_0d_2^2\rho+3360B_1^2X_0d_2\rho^2+3456B_1^2X_0\rho^3+192B_1X_0^2d_2^3\\
&+1796B_1X_0^2d_2^2\rho+5120B_1X_0^2d_2\rho^2+4608B_1X_0^2\rho^3+128X_0^3d_2^3+1024X_0^3d_2^2\rho\\
&+2560X_0^3d_2\rho^2+2048X_0^3\rho^3)c_3^2]V_{1a},\\
V_2 &= -2(B_1d_2+3B_1\rho+2X_0d_2+4X_0\rho)^4d_2/[9c_3^6a_2^2(36B_1^3d_2^3+433B_1^3d_2^2\rho+1620B_1^3d_2\rho^2\\
&+1944B_1^3\rho^3+216B_1^2X_0d_2^3+2308B_1^2X_0d_2^2\rho+7560B_1^2X_0d_2\rho^2+7776B_1^2X_0\rho^3\\
&+432B_1X_0^2d_2^3+4036B_1X_0^2d_2^2\rho+11520B_1X_0^2d_2\rho^2+10368B_1X_0^2\rho^3+288X_0^3d_2^3\\
&+2304X_0^3d_2^2\rho+5760X_0^3d_2\rho^2+4608X_0^3\rho^3)(2X_0+B_1)(16B_1^3d_2^3+193B_1^3d_2^2\rho+720B_1^3d_2\rho^2\\
&+864B_1^3\rho^3+96B_1^2X_0d_2^3+1028B_1^2X_0d_2^2\rho+3360B_1^2X_0d_2\rho^2+3456B_1^2X_0\rho^3+192B_1X_0^2d_2^3\\
&+1796B_1X_0^2d_2^2\rho+5120B_1X_0^2d_2\rho^2+4608B_1X_0^2\rho^3+128X_0^3d_2^3+1024X_0^3d_2^2\rho+2560X_0^3d_2\rho^2\\
&+2048X_0^3\rho^3)^3\rho^3B_1^7(B_1d_2+7B_1\rho+2X_0d_2+8X_0\rho)^2(4B_1^3d_2^3+49B_1^3d_2^2\rho+180B_1^3d_2\rho^2\\
&+216B_1^3\rho^3+24B_1^2X_0d_2^3+260B_1^2X_0d_2^2\rho+840B_1^2X_0d_2\rho^2+864B_1^2X_0\rho^3+48B_1X_0^2d_2^3\\
&+452B_1X_0^2d_2^2\rho+1280B_1X_0^2d_2\rho^2+1152B_1X_0^2\rho^3+32X_0^3d_2^3+256X_0^3d_2^2\rho+640X_0^3d_2\rho^2\\
&+512X_0^3\rho^3)^3(B_1d_2+6B_1\rho+2X_0d_2+8X_0\rho)^2]V_{2a},\\
V_3 &= -d_2^2(B_1d_2+3B_1\rho+2X_0d_2+4X_0\rho)^6/[648(B_1d_2+6B_1\rho+2X_0d_2+8X_0\rho)^4B_1^{11}\rho^5(B_1d_2\\
&+7B_1\rho+2X_0d_2+8X_0\rho)^3c3^10a_2^4(64B_1^3d_2^3+769B_1^3d_2^2\rho+2880B_1^3d_2\rho^2+3456B_1^3\rho^3\\
&+384B_1^2X_0d_2^3+4100B_1^2X_0d_2^2\rho+13440B_1^2X_0d_2\rho^2+13824B_1^2X_0\rho^3+768B_1X_0^2d_2^3\\
&+7172B_1X_0^2d_2^2\rho+20480B_1X_0^2d_2\rho^2+18432B_1X_0^2\rho^3+512X_0^3d_2^3+4096X_0^3d_2^2\rho\\
&+10240X_0^3d_2\rho^2+8192X_0^3\rho^3)(36B_1^3d_2^3+433B_1^3d_2^2\rho+1620B_1^3d_2\rho^2+1944B_1^3\rho^3\\
&+216B_1^2X_0d_2^3+2308B_1^2X_0d_2^2\rho+7560B_1^2X_0d_2\rho^2+7776B_1^2X_0\rho^3+432B_1X_0^2d_2^3\\
&+4036B_1X_0^2d_2^2\rho+11520B_1X_0^2d_2\rho^2+10368B_1X_0^2\rho^3+288X_0^3d_2^3+2304X_0^3d_2^2\rho+5760X_0^3d_2\rho^2\\
&+4608X_0^3\rho^3)^2(2X_0+B_1)^2(4B_1^3d_2^3+49B_1^3d_2^2\rho+180B_1^3d_2\rho^2+216B_1^3\rho^3+24B_1^2X_0d_2^3\\
&+260B_1^2X_0d_2^2\rho+840B_1^2X_0d_2\rho^2+864B_1^2X_0\rho^3+48B_1X_0^2d_2^3+452B_1X_0^2d_2^2\rho+1280B_1X_0^2d_2\rho^2\\
&+1152B_1X_0^2\rho^3+32X_0^3d_2^3+256X_0^3d_2^2\rho+640X_0^3d_2\rho^2+512X_0^3\rho^3)^5(16B_1^3d_2^3+193B_1^3d_2^2\rho\\
&+720B_1^3d_2\rho^2+864B_1^3\rho^3+96B_1^2X_0d_2^3+1028B_1^2X_0d_2^2\rho+3360B_1^2X_0d_2\rho^2+3456B_1^2X_0\rho^3\\
&+192B_1X_0^2d_2^3+1796B_1X_0^2d_2^2\rho+5120B_1X_0^2d_2\rho^2+4608B_1X_0^2\rho^3+128X_0^3d_2^3+1024X_0^3d_2^2\rho\\
&+2560X_0^3d_2\rho^2+2048X_0^3\rho^3)^5]V_{3a},
\end{aligned}
$$

where V_{1a}, V_{2a} and V_{3a} are polynomials in X_0, d_2, ρ and B_1, and V_{1a} and V_{2a} are listed in Appendix.

From computation, we can choose X_0 as a free parameter to express other parameters as

$$d_2 = D_2X_0, \;\; \rho = RD_2X_0, \;\; B_1 = BX_0.$$

Then, we get

$$V_{1a} = D_2^7X_0^{16}V_{1b}, \;\; V_{2a} = D_2^{26}X_0^{56}V_{2b}, \;\; V_{3a} = D_2^{48}X_0^{102}V_{3b},$$

where V_{1b}, V_{2b} and V_{3b} are expressed in term of R and B.

Using the Maple built-in command, we eliminate R from $V_{1b} = V_{2b} = 0$ to obtain

$$\begin{aligned} V_{12b} &= \text{resultant}(\text{V}_{1\text{b}}, \text{V}_{2\text{b}}, \text{R}) \\ &= -209305557128275993010925074939984178315264B^4 6(B+1)^2(B+2)^{182} \\ &\quad \times(3B+4)^{50}(8+9B)^3(15B+16)^2(23B+24)^2(3B^2+8B+8)F_1F_2^2F_3^2F_4^2F_5, \end{aligned} \tag{2.24}$$

where

$$\begin{aligned} F_1 = \;& 147B^5 + 874B^4 + 1668B^3 + 1104B^2 + 24B - 128, \\ F_2 = \;& 9279B^6 + 32016B^5 + 38156B^4 + 10960B^3 - 10700B^2 - 4864B + 2048, \\ F_3 = \;& 59193B^7 + 227328B^6 - 393560B^5 - 3227552B^4 - 5745904B^3 - 4141440B^2 \\ & -1167360B - 98304, \\ F_4 = \;& 265186629B^{14} + 3162608064B^{13} + 18146078748B^{12} + 65973784152B^{11} \\ & +166528741076B^{10} + 297577658208B^9 + 366510497088B^8 + 283043369216B^7 \\ & +89715855360B^6 - 57877204992B^5 - 76036567040B^4 - 27416985600B^3 \\ & +3643146240B^2 + 5555355648B + 1233125376, \end{aligned} \tag{2.25}$$

and F_5 can be found in the Appendix.

Then, we can find seven real positive roots from the polynomial equation $V_{12b} = 0$, however, only one satisfies $V_1 = V_2 = 0$. This solution is given by

$$B = 0.1268297707\cdots, \;\; R = 0.235165980\cdots. \tag{2.26}$$

under which $V_1 = V_2 = 0$, $V_3 = -(2.677759596\cdots)\times 10^{10}\dfrac{D_2^5X_0^6}{c_3^{10}a_2^4} < 0$.

Further, a simple computation shows that

$$\det\left[\frac{\partial(V_1, V_2)}{\partial(B, R)}\right] = (5.650407050\cdots)\times 10^{11}\frac{D_2^4X_0^6}{a_2^2c_3^8} \neq 0.$$

Thus, according to Theorem 1.1.2, two small-amplitude limit cycles can bifurcate from the equilibrium point p_0 in the system (2.6). Finally, a linear small perturbation on μ from μ_{H} is applied to obtain an additional small-amplitude limit cycle, giving a total of three limit cycles around the equilibrium p_0.

2.4 Simulation of three limit cycles

In this section, we simulate the three limit cycles bifurcating from the equilibrium p_0. Since $V_3 < 0$, the outer-most and inner-most limit cycles are stable and the middle one is unstable, and the equilibrium p_0 must be unstable. Note that all the three limit cycles and located on a 2-dimensional invariant manifold near the equilibrium p_0.

Set $D_2 = 1, X_0 = 1, a_2 = 2, c_3 = 10$. The equilibrium point becomes $p_0 = (1, 5, \frac{50RB(6BR+B+8R+2)}{(2+B)(3BR+B+4R+2)})$. Now, we perturb the parameters B and R as

$$B = B_c - 0.000036455\cdots, \quad R = R_c - 0.000124549\cdots, \tag{2.27}$$

under which the system (2.6) becomes

$$\begin{aligned}
\dot{x} = \; & (0.235041430\cdots)x^3y^2 + (17.62810726\cdots)x^3 - (0.099976908\cdots)x^2y^3 \\
& -(7.498268139\cdots)x^2y + (0.264843112\cdots)xy^2 + (19.86323342\cdots)x, \\
\dot{y} = \; & (0.101911014\cdots)x^2y^3 + (7.643326115\cdots)x^2y - (0.062388356\cdots)y^3 - 2x^2yz \\
& -(4.679126724\cdots)y - (2.253586630\cdots)yz, \\
\dot{z} = \; & -x^2y^2z + 20yx^2z - 75x^2z - (1.126793315\cdots)zy^2 + (22.53586630\cdots)yz \\
& -(84.50949863\cdots)z.
\end{aligned} \tag{2.28}$$

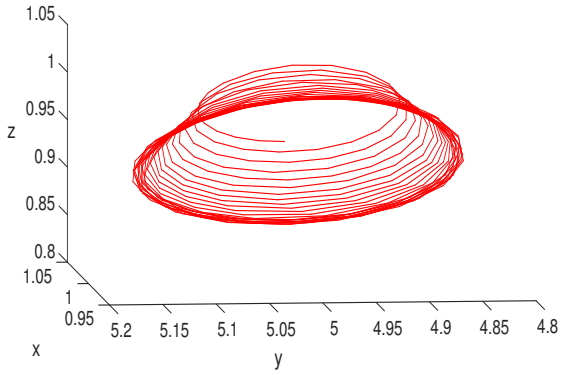

Figure 2.1: Simulation of system (2.28) showing the inner-most stable limit cycle.

2.5 Conclusion and discussion

In this chapter, we have considered a tritrophic food chain model with functional response Holling types III and IV for the predator and superpredator, respectively. We have studied the stability and bifurcation of the positive equilibrium when the prey has linear growth. We have applied center manifold and normal form theory to give a detailed analysis on the Hopf bifurcation.

Moreover, we have investigated the bifurcation of multiple limit cycles, which can cause complex dynamics in biological systems. We have particularly shown that the food chain

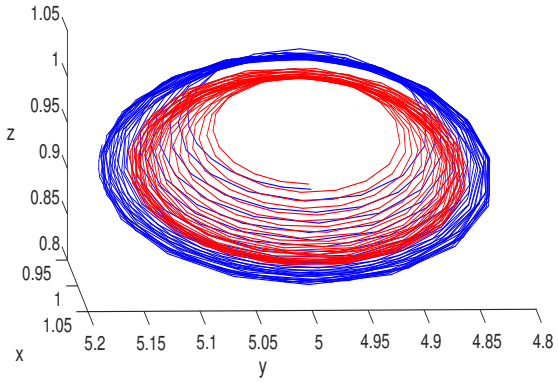

Figure 2.2: Simulation of system (2.28) showing the inner-most stable (in red) and the middle unstable limit cycle (in blue).

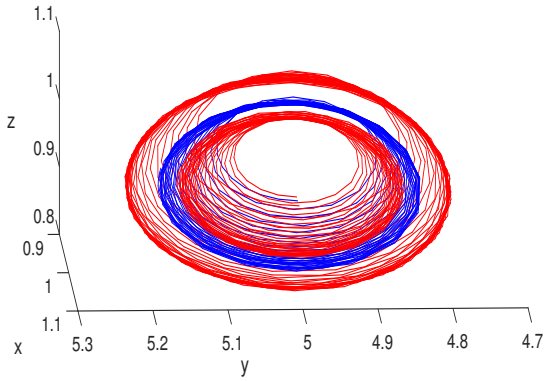

Figure 2.3: Simulation of system (2.28), showing all the limit cycles with inner-most and outer-most ones stable (in red) and middle one unstable (in blue).

model can exhibit at least three limit cycles due to Hopf bifurcation, which may explain how complex dynamical behavior occurs in such food chain systems. The numerical example shows that it is possible to have bistable phenomenon consisting of two stable limit cycles (the inner-most and outer-most ones), restricted to a center manifold. Since periodic and quasi-periodic oscillations are often observed in real biological systems, it is anticipated that the multiple limit cycle bifurcation studied in this chapter may lead to establishing a good methodology for investigating such complex dynamical behaviors. We hope that the method presented in this chapter can be used to study other nonlinear dynamical systems, and promote further research in this field.

Chapter 3

Recurrence Phenomenon in Oscillating Networks

3.1 Introduction

Today organic chemical reaction networks become more and more important in life and play a central role in their origins [38, 52, 53]. Network dynamics regulates cell division [55, 40, 56], circadian rhythms [43], nerve impulses [41] and chemotaxis [50], and provide guidelines for the development of organisms [49]. In chemical reactions, out-of-equilibrium networks have the potential to display emergent network dynamics such as spontaneous pattern formation, bistability and periodic oscillations. However, it has been noted that the principle of organic reaction networks developing complex behaviors is still not completely understood. In [54], a biologically related network organic reaction was developed, which exhibted bistability and oscillations in the concentrations of organic thiols and amides. Oscillations are generated from the interaction between three sub networks: an autocatalytic cycle that produces thiols and amides from thioesters and dialkyl disulfides; a trigger that controls autocatalytic growth; and inhibitory processes that remove activating thiol species that are generated during the autocatalytic cycle. Previous studies proved oscillations and bistability using highly evolved biomolecules or inorganic molecules of questionable biochemical relevance (for example, those used in Belousov-Zhabotinskii-type reactions)[37, 44], while the organic molecules used in [54] are related to metabolism, which is similar to those found in early Earth. The network considered in [54] can be modified to study the influence of molecular structure on the dynamics of reaction networks, and may possibly lead to the design of biomimetic networks and of synthetic self-regulating and evolving chemical systems.

Numerical simulations given in [54] has shown that that space velocities (defined as the ratio of the flow rate and the reactor volume and given in units of per second) in the range 0.0001-0.01/s would produce hysteresis. In order to test the result of simulations, the authors of [54] studied the total concentration of thiols during stepwise changes. In particular, they started from a low flow rate, then rised to a high flow rate, and finally returned to the low flow rate. To activate the autocatalytic pathway, one needs to use high thiol concentrations which are generated through self-amplification [of CSH (cysteamine)], requiring the space velocities to be lowered to 0.0005/s. It has been observed that when the space velocity reaches 0.006/s,

the system transitions will be out of the self-amplifying state. Such limits may explain the self-amplification which requires maleimide to be removed from the CSTR (continuously stirred tank reactor) more rapidly than it is added through the inlet port; while when the termination of self-amplification starts, free thiols should be removed from the CSTR by transporting out from the outlet port more rapidly than they are produced. Noticed from the model prediction, an increase of maleimide concentration reduced the bistable limit flow velocity. This chemical reaction network shows a general process to convert any quadratic autocatalytic system into a bistable switch. In [39], Epstein and Pojman found that bistable systems could generate oscillations in the presence of an inhibition reaction. In the system studied in [54], they choose acrylamide as an inhibitor, and tested this system with acrylamide in batch, which exhibited a oscillation (that is, one peak) in the concentration of free thiols. Moreover NMR (nuclear magnetic resonance) analysis has shown that the oscillation is triggered when the maleimide is removed. With a combination of numerical simulations and experiments in the CSTR under different flow rates, they found the conditions under which the addition of acrylamide can produce sustained oscillations in RSH (organic thiols). To determine how the changes in flow rate affect oscillations, the authors of [54] further examined the influence of flow rate on the stability, period and amplitude of oscillations. It showed that period increases nonlinearly with space velocity, while the amplitude increases linearly.

Recently, the recurrence phenomenon has received great attention. For example, Zhang *et al*. [60] studied the recurrence phenomenon of a newly autoimmune disease model. The newly developed 4-dimensional model exhibits recurrent dynamics, which are preserved in a reduced and rescaled 3-dimensional model as well. They analyzed the dynamics underlying this behavior in both the 4-dimensional and 3-dimensional models, and further proved that the recurrent behavior arises due to Hopf bifurcation. Moreover, some other disease models also show recurrent behavior, which was found in multifocal osteomyelitis [45, 47], eczema [42] and subacute discoid lupus erythematosus [51]. Actually, the subtypes of some diseases are clinically classified based on the patterns of this recurrent behavior [61]. Thus, an improved understanding of recurrence phenomenon in autoimmune disease is important to promoting correct diagnosis, patient management, and treatment decisions. Possibly, the recurrence phenomenon may be used to realistically explain complex dynamics in some real physical systems, and an improved understanding of recurrent dynamics in organic reactions may promote correct classification, management and utilization of energy resources.

To explain the trends in period and amplitude of oscillating networks, and the nature of bifurcations at low and high limiting space velocities, a simple kinetic model has been constructed in [54] to enable qualitative analysis on dynamic behaviors. The model simplifies the autocatalytic thiol network to bimolecular autocatalytic production of thiols from thioester, and considers the concentrations of CSSC (cystamine) and acrylamide ([CSSC] and [acrylamide]) as constants:

$$\begin{aligned}
\frac{dA}{dt} &= k_1 S A - k_2 I A - k_3 A - k_0 A + k_4 S, \\
\frac{dI}{dt} &= k_0 I_0 - k_0 I - k_2 I A, \\
\frac{dS}{dt} &= k_0 S_0 - k_0 S - k_4 S - k_1 S A,
\end{aligned} \tag{3.1}$$

where A = [RSH], I = [maleimide], S = [AlaSEt], I_0 and S_0 are the concentrations of maleimide and AlaSEt fed into the reactor, respectively, $k_i, i = 1, 2, 3, 4$, are rate constants and k_0 is the space velocity. From linear analysis [39] of this model, we find that increasing k_0 from low to high values causes two transitions. First, the system taking the transition from having a stable focus (damped oscillations) to a stable orbit (sustained oscillations) via an Andronov-Hopf bifurcation [48]. Second, the system transits from having a stable orbit to a single stable equilibrium (a stable 'node'-an equilibrium in which the system, when perturbed, returns directly to the stable state, as opposed to orbiting around it) via a saddle-node or fold bifurcation [48].

In this chapter, we focus on the stability analysis of equilibria. The rest of the chapter is organized as follows. In the next section, we identify the saddle-node and Hopf bifurcations arising from the equilibrium and use simulation to verify the analytical predictions. Further, analysis on the Hopf bifurcation and in particular the post-critical oscillation are given in section 3.3. Numerical simulation to show the recurrence phenomenon is presented in section 3.4, which agrees very well with the experimental results given in [54]. The conclusion and discussion is drawn in Section 3.5

3.2 Stability and bifurcation: linear analysis

In this section, we present a linear analysis for model (3.1) based on the results established for general nonlinear dynamical systems in the previous section. The equilibrium solution of model (3.1) is obtained by simply setting $\dot{A} = \dot{I} = \dot{S} = 0$ and solving the resulting algebraic equations, which yields an equilibrium solution E_1, given by

$$E_1 = \left(A_1, \frac{I_0 k_0}{A_1 k_2 + k_0}, \frac{S_0 k_0}{A_1 k_1 + k_0 + k_4}\right), \tag{3.2}$$

where A_1 is determined from the equation:

$$\frac{k_1 k_0 S_0 A_1}{k_0 + k_4 + k_1 A_1} - \frac{k_2 k_0 I_0 A_1}{k_0 + k_2 A_1} - (k_0 + k_3)A_1 + \frac{k_4 k_0 S_0}{k_0 + k_4 + k_1 A_1} = 0, \tag{3.3}$$

which is equivalent to:

$$\begin{aligned}&(k_1 k_2 k_3 + k_1 k_2 k_0)A_1^3 + [k_0^2(k_1 + k_2) + k_0(k_1 k_2 I_0 + k_2 k_3 + k_2 k_4 + k_1 k_3 - k_1 k_2 S_0) + k_2 k_3 k_4]A_1^2 \\ &+[k_0^3 + k_0^2(k_2 I_0 + k_3 + k_4 - k_1 S_0) + k_0(k_2 k_4 I_0 + k_3 k_4 - k_2 k_4 S_0)]A_1 - k_4 k_0^2 S_0 = 0\end{aligned} \tag{3.4}$$

The data obtained from the experiments [54] for the model are given below,

$$\begin{aligned}&S_0 = 0.05M, \qquad I_0 = 0.01M, \qquad k_1 = 0.25 s^{-1} M^{-1}, \\ &k_2 = 300 s^{-1} M^{-1}, \quad k_3 = 0.0035 s^{-1}, \quad k_4 = 7 \times 10^{-5} s^{-1},\end{aligned} \tag{3.5}$$

under which system (3.4) becomes

$$\begin{aligned}F(A_1, k_0) = \; &(\frac{21}{80} + 75k_0)A_1^3 + (\frac{1201}{4}k_0^2 - \frac{617}{320}k_0 + \frac{147}{2000000})A_1^2 + (k_0^3 \\ &+\frac{299107}{100000}k_0^2 - \frac{167951}{200000000}k_0)A_1 - \frac{7}{2000000}k_0^2 = 0.\end{aligned} \tag{3.6}$$

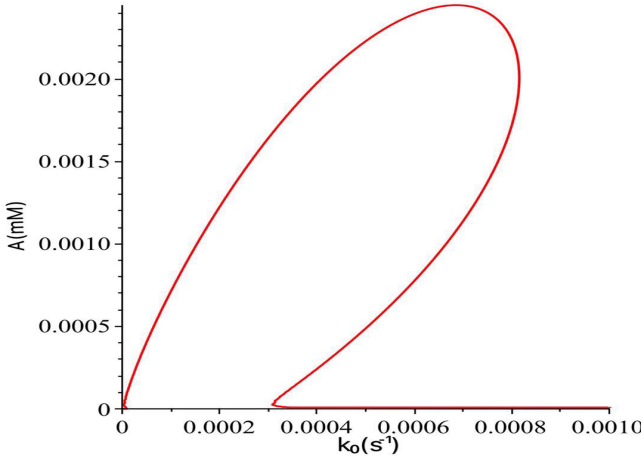

Figure 3.1: The component A_1 of the equilibrium solution E_1, satisfying $F(A_1, k_0) = 0$.

Note that the rational numbers given in the above equation are obtained by transforming the numbers in digital format for convenience of computation. The graph depicted in Figure 1 shows the component A of the equilibrium solution E_1, satisfying $F(A_1, k_0) = 0$.

Next, we consider the stability of equilibrium solution E_1, and give a complete bifurcation classification. Evaluating the Jacobian of (3.1) at E_1 yields a cubic characteristic polynomial, given by

$$P_1(\lambda, A_1, k_0) = \lambda^3 + a_1(A_1, k_0)\lambda^2 + a_2(A_1, k_0)\lambda + a_3(A_1, k_0) = 0, \tag{3.7}$$

where the coefficients $a_1(A_1, k_0)$, $a_2(A_1, k_0)$ and $a_3(A_1, k_0)$, expressed in terms of A_1 and k_0, are given below:

$$\begin{aligned}
a_1(A_1,k_0)=&\frac{1}{(30000000\,A_1+100000\,k_0)(25000\,A_1+100000\,k_0+7)}[30000000000\,{k_0}^3\\
&+(12010000000000\,A_1+29912800000){k_0}^2+(903750625000000\,{A_1}^2\\
&-18440900000\,A_1+2102499)k_0+225187500000000\,{A_1}^3+65730000000\,{A_1}^2\\
&+749700\,A_1],\\
a_2(A_1,k_0)=&\frac{1}{200000000(300A_1+k_0)(25000A_1+100000k_0+7)}[600000000000000k_0^4\\
&+(300250000000000000A_1+119647000000000)k_0^3+(36120025000000000000A_1^2\\
&-113586100000000A_1+12614896000)k_0^2+(13511250000000000000A_1^3\\
&-15796615625000000A_1^2+8070650000A_1+294343)k_0+1125000000000000000A_1^4\\
&+16393125000000000A_1^3+4505550000000A_1^2+102900A_1],\\
a_3(A_1,k_0)=&\frac{1}{200000000(300A_1+k_0)(25000A_1+100000k_0+7)}[1125000000000000000A_1^4k_0\\
&+900750000000000000A_1^3k_0^2+180600125000000000000A_1^2k_0^3+12010000000000000A_1k_0^4\\
&+2000000000000k_0^5+3937500000000000A_1^4+32156250000000000A_1^3k_0\\
&-159228256250000000A_1^2k_0^2-76284300000000A_1k_0^3+59822800000000k_0^4\\
&+2205000000000A_1^3+892290000000A_1^2k_0+80412500000A_1k_0^2+8409898000k_0^3\\
&+308700000A_1^2+2058000A_1k_0+294343k_0^2].
\end{aligned} \tag{3.8}$$

Based on the characteristic polynomial (3.7), we consider possible bifurcations from E_1, including both static and dynamical (Hopf) bifurcations. First, we consider static bifurcation, which occurs when $P_1(\lambda, A_1, k_0) = 0$ has zero roots (zero eigenvalues). The simplest case is single zero, i.e. when $a_3(A_1, k_0) = 0$, and A_1 should simultaneously satisfy $F(A_1, k_0) = 0$ (see Eq. (3.6)). Thus, we obtain

$$\begin{aligned}
A_{1s}(k_{0s}) = -[&k_{0s}(1439039800000000000000000000000k_{0s}^6 \\
&+ 428288040277200000000000000000k_{0s}^5 - 62132768901471980000000000000k_{0s}^4 \\
&+ 26803869391772030000000000k_{0s}^3 + 3631431743948809500000k_{0s}^2 \\
&+ 1210694204622124250k_{0s} \\
&+ 15045612346947)]/[43164005995000000000000000000000k_{0s}^6 \\
&- 1302173146462753500000000000000000k_{0s}^5 \\
&+ 29971751440639244750000000000000k_{0s}^4 \\
&- 208788356270006416250000000000k_{0s}^3 - 51116621703491955625000000k_{0s}^2 \\
&+ 233617980290310525000k_{0s} + 2178822504600000],
\end{aligned} \tag{3.9}$$

where k_{0s} is determined from the equation,

$$\begin{aligned}
F_2(k_{0s}) = \; &1437601000000000000000000000000000000k_{0s}^8 \\
&+8567031085140000000000000000000000000k_{0s}^7 \\
&+1266832833449568490000000000000000000k_{0s}^6 \\
&-3016017614668520296000000000000000000k_{0s}^5 \\
&+2922708873924575222500000000000000k_{0s}^4 \\
&-7958153479149473250000000000k_{0s}^3 \\
&-3776310372076908509375000k_{0s}^2 \\
&+6325840519419858150000k_{0s} + 610426123747209.
\end{aligned} \tag{3.10}$$

Solving $F_2(k_{0s}) = 0$ for k_{0s} yields four positive real solutions. Then, substituting the four solutions into $A_{1s}(k_{0s})$ using (3.9), we get four values of $A_{1s}(k_{0s})$, and two of them are positive, which yield two critical values (see the two circles in Figure 2): $(k_{0sn}, A_{1sn}) = (0.000308266\cdots, 0.000026398\cdots)$ and $(0.000815525\cdots, 0.002006192\cdots)$. By verifying the changes of the stability on both sides of the critical points on the curve $F(k_0, A_1) = 0$, we find that the first one defines a saddle-node bifurcation. For example, we select $A_1 = 0.000027$ (above the critical point), the corresponding value of k_0 is equal to $0.000308273\cdots$, under which the eigenvalues defined by equation (3.7) are $0.0000199\cdots$, $-0.000249107\cdots$ and $-0.112353614\cdots$, implying that the corresponding equilibrium solution is unstable. When we select $A = 0.000025$ (below the critical point), the corresponding k_0 is equal to $0.000308308\cdots$, for which the eigenvalues are $-0.000046078\cdots$, $-0.000244614\cdots$ and $-0.120143088\cdots$, indicating that the corresponding equilibrium solution is locally asymptotically stable.

Next, we turn to consider Hopf bifurcation which may occur from the equilibrium E_1. To achieve this, we apply Theorem 2.1 to the equilibrium E_1, where A_1 satisfies the polynomial equation $F(A_1, k_0) = 0$ in (3.6). Based on the cubic characteristic polynomial $P_1(\lambda, A_1, k_0) = 0$

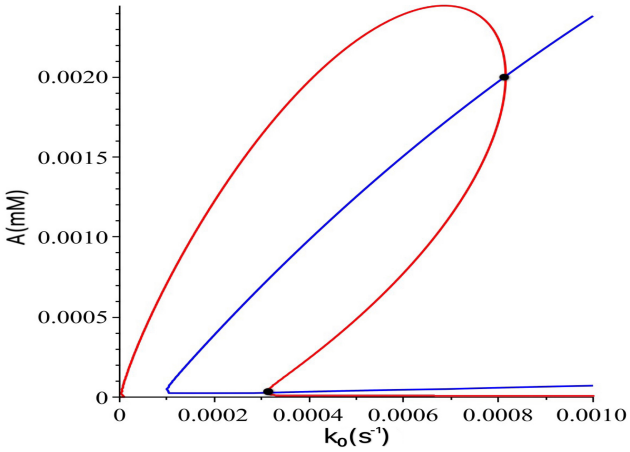

Figure 3.2: The graphs of $a_3(A_1, k_0) = 0$ and $F(A_1, k_0) = 0$.

(see Eq. (3.7)), we apply the formula, $\Delta_2(A_1, k_0) = a_1a_2 - a_3$, to solve the two polynomial equations, $\Delta_2 = 0$ and $F(A_1, k_0) = 0$, together with the parameter values given in (3.5), yielding three candidates for Hopf critical points: $(k_{0H1}, A_{H1}) = (0.000176806\cdots, 0.001114785\cdots)$, $(0.000254830\cdots, -0.000029768\cdots)$ and $(0.000309121\cdots, 0.000033790\cdots)$. We only consider the biologically meaningful points with two positive entries to get two possible Hopf critical points (k_{0H1}, A_{H1}) and (k_{0H3}, A_{H3}). For these two sets of solutions, we need to check if the eigenvalues defined by equation (3.7) contain a pair of purely imaginary eigenvalues and a negative eigenvalue. By a simple calcualtion, we find that the unique Hopf critical point is $(k_{0H}, A_H) = (0.000176806\cdots, 0.001114785\cdots)$, which is shown in Figure 3. Note that at the critical point (k_{0H}, A_H), other stability conditions given in Theorem 2.1 are still satisfied.

As a matter of fact, by using these given parameter values, we may numerically compute the Jacobian of system (3.1) at the equilibrium E_1 to obtain a purely imaginary pair and one negative real eigenvalues: $\pm 0.001087856i\cdots$ and $-0.336194209\cdots$. Therefore, on the equilibrium solution curve defined by $F(k_0, A_1) = 0$ (see Figure 4), the equilibrium E_1 is stable from the origin to the Hopf point (k_{0H}, A_H), and unstable from (k_{0H}, A_H) to the saddle-node bifurcation point (k_{0sn}, A_{1sn}), and then returns to stable from the saddle-node bifurcation point, as shown in Figure 3.4.

We have used the MATCONT in Matlab to obtain the numerical bifurcation diagram, as depicted in Figure 3.5, which agrees with that as given in Figure 3.1.

3.3 Normal form of Hopf bifurcation and limit cycles

In this section, we will further study the Hopf bifurcation from the equilibrium E_1 of the system (3.1), and use normal form theory to study stability of the bifurcating limit cycles. Assume that $k_0 = k_{0H} + \mu = 0.000176806\cdots + \mu$, where μ is a small perturbation (bifurcation) parameter.

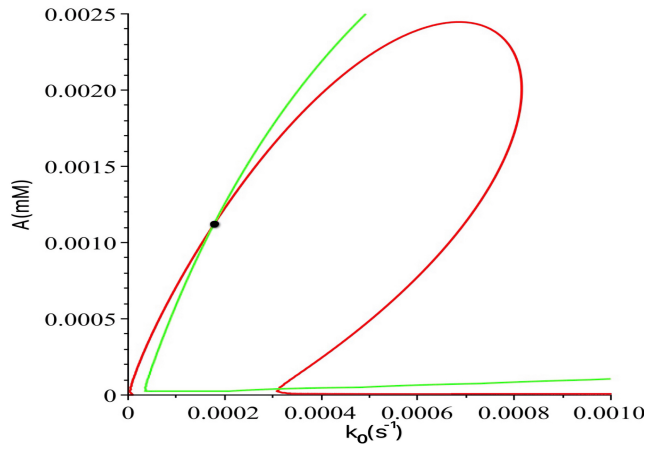

Figure 3.3: The graph of $\Delta_2 = 0$, showing Hopf bifurcation.

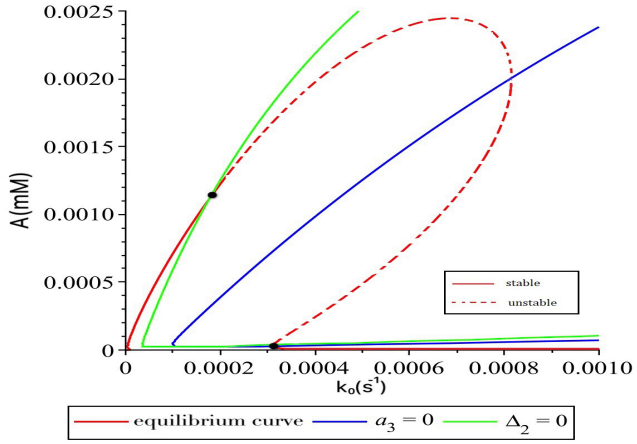

Figure 3.4: Bifurcation diagram

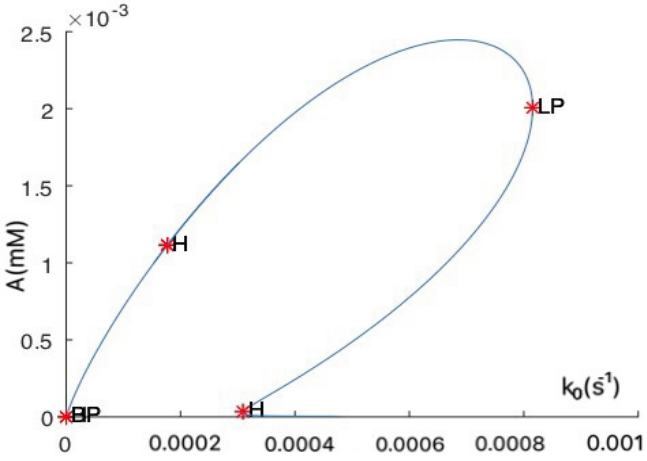

Figure 3.5: Numerical bifurcation diagram obtained by using MATCONT in Matlab, confirming the result shown in Figure 3.1.

Based on the values given in (3.5), we introduce the following transformation,

$$\begin{aligned} A &= A_1 + x_1 + x_3, \\ I &= -0.004737302\cdots x_1 + 0.000015401\cdots x_2 + 1.002113047\cdots x_3 \\ &\quad + \frac{0.000176806\cdots + \mu}{100(300A_1 + 0.000176806\cdots + \mu)}, \\ S &= -1.514185916\cdots x_1 + 3.134552877\cdots x_2 + 0.012529174\cdots x_3 \\ &\quad + \frac{0.000176806\cdots + \mu}{20(0.25A_1 + 0.000246806\cdots + \mu)}, \end{aligned} \tag{3.11}$$

into system (3.1) to obtain

$$\frac{dx_i}{dt} = G_i(x_1, x_2, x_3; \mu, A_1), \quad i = 1, 2, 3, \tag{3.12}$$

where

$$\begin{aligned} G_1(x_1, x_2, x_3; \mu, A_1) = [&-6.685965797 \times 10^{-13}x_1 + 1.270633803 \times 10^{-13}x_2 \\ &+ 1.451973290 \times 10^{-15} - 2.174775067 \times 10^{-10}x_1^2 + 4.537921451 \times 10^{-10}x_1x_2 \\ &- 5.827487976 \times 10^{-10}x_1x_3 + 4.537921451 \times 10^{-10}x_3x_2 - 3.652712909 \times 10^{-10}x_3^2 \\ &- 5.038382521 \times 10^{-13}x_3 + (1.642442597 \times 10^{-11} + 0.000004405x_3x_2 \\ &+ 0.000004405x_1x_2 - 0.000005657x_1x_3 - 0.000002111x_1^2 - 0.000003545x_3^2 \\ &+ 1.246098433 \times 10^{-9}x_1 + 1.233487325 \times 10^{-9}x_2 + 3.427342293 \times 10^{-9}x_3)\mu \\ &+ (7.294389852 \times 10^{-10} + 0.000770440x_1x_2 + 0.000770440x_3x_2 - 0.000989380x_1x_3 \\ &- 0.000369229x_1^2 - 0.000620151x_3^2 + 0.000005074x_1 + 2.16179759310^{-7}x_2 \\ &+ 0.000005354x_3)A_1 - 0.9953022834A_1^3\mu - 3.984526808A_1^2\mu^2 - 0.0132706971A_1\mu^3 \\ &+ (4.64474398910^{-8} + 0.000002911x_2 + 0.0103992451x_3x_2 + 0.0103992451x_1x_2 \\ &- 0.0133544568x_1x_3 - 0.0049837837x_1^2 - 0.0083706731x_3^2 + 0.000026078x_1 \\ &+ 0.000035502x_3)\mu^2 + (0.000878680x_2 + 0.035797988x_3 + 0.033677967x_1 \\ &- 1.496381068x_1^2 - 2.513294604x_3^2 + 3.122373365x_1x_2 + 3.122373365x_3x_2 \\ &- 4.009675672x_1x_3 - 0.000002893)A_1\mu + (0.779943388x_3x_2 + 0.779943388x_1x_2 \\ &- 1.001584265x_1x_3 - 0.004135088x_1 + 0.000988827x_2 - 0.004102836x_3 \\ &+ 0.3424094672^{-5} - 0.3737837804x_1^2 - 0.6278004841x_3^2)A_1^2 + (3.122373365x_2 \\ &- 2.513294604x_3 - 2.496381068x_1 + 0.0241785817)A_1^2\mu + (-0.0083706731x_3 \\ &+ 0.0103992451x_2 - 4.008317117x_1 - 0.0397006230)A_1\mu^2 + (-0.3737837804x_1 \\ &+ 0.7799433885x_2 - 0.6278004841x_3 - 0.0036595339)A_1^3 - 0.0133333333x_1\mu^3]/[(A_1 \\ &+ 0.000987226 + 4\mu)(A_1 + 5.893552658 \times 10^{-7} + 0.003333333\mu)], \end{aligned}$$

$$G_2(x_1, x_2, x_3; \mu, A_1) = \{5.046435823 \times 10^{-12}x_1 - 8.222154554 \times 10^{-14}x_2$$

$$
\begin{aligned}
&+ 7.013669022 \times 10^{-16} - 3.808463387 \times 10^{-11} x_1^2 + 7.375550314 \times 10^{-11} x_1 x_2 \\
&+ 4.825811507 \times 10^{-10} x_1 x_3 + 7.375550314 \times 10^{-11} x_3 x_2 + 5.206657845 \times 10^{-10} x_3^2 \\
&+ 5.056493269 \times 10^{-12} x_3 - [0.0133333333(-5.950289605 \times 10^{-10} - 0.0000536994 x_3 x_2 \\
&- 0.0000536994 x_1 x_2 - 0.0003513548 x_1 x_3 + 0.0000277284 x_1^2 - 0.0003790832 x_3^2 \\
&- 0.3775567185 \times 10^{-5} x_1 + 1.035004006 \times 10^{-7} x_2 - 0.3782889752 \times 10^{-5} x_3)]\mu \\
&- [0.0133333333(-2.642633124 \times 10^{-8} - 0.0093915594 x_1 x_2 - 0.0093915594 x_3 x_2 \\
&- 0.0614488327 x_1 x_3 + 0.0048494565 x_1^2 - 0.0662982892 x_3^2 + 0.0000183015 x_1 \\
&+ 0.0000104640 x_2 + 0.0000169789 x_3)]A_1 - 0.4807747388 A_1^3 \mu - 1.924701537 A_1^2 \mu^2 \\
&- 0.0064103298 A_1 \mu^3 - [0.0133333333(-0.1682711586 \times 10^{-5} + 0.0005649292 x_2 \\
&- 0.1267653433 x_3 x_2 - 0.1267653433 x_1 x_2 - 0.8294237395 x_1 x_3 + 0.0654569690 x_1^2 \\
&- 0.8948807086 x_3^2 - 0.0092468712 x_1 - 0.0092641571 x_3)]\mu^2 \\
&- [0.0133333333(0.1164626449 x_2 - 0.1039722264 x_3 - 0.0983753008 x_1 \\
&+ 19.65345496 x_1^2 - 268.6879328 x_3^2 - 38.06129433 x_1 x_2 - 38.06129433 x_3 x_2 \\
&- 249.0344778 x_1 x_3 + 0.000104818)]A_1 \mu - [0.01333333333(-9.507400748 x_3 x_2 \\
&- 9.507400748 x_1 x_2 - 62.20678047 x_1 x_3 + 0.1323386341 x_1 + 0.0012071504 x_2 \\
&+ 0.05989444020 x_3 - 0.0001240491 + 4.909272679 x_1^2 - 67.11605314 x_3^2)]A_1^2 \\
&- (0.01333333333(36.93870567 x_2 - 268.6879328 x_3 + 19.65345496 x_1 \\
&- 0.8759488090))A_1^2 \mu - (0.01333333333(-0.8948807086 x_3 + 300.1232347 x_2 \\
&+ 0.06545696905 x_1 + 1.438285911))A_1 \mu^2 - [0.01333333333(4.909272679 x_1 \\
&- 9.507400748 x_2 - 67.11605314 x_3 + 0.1325786792)]A_1^3 - 0.01333333333 x_2 \mu^3\}/[(A_1 \\
&+ 0.000987226 + 4\mu)(A_1 + 5.893552658 \times 10^{-7} + 0.003333333\mu)],
\end{aligned}
$$

$$
\begin{aligned}
G_3(x_1, x_2, x_3; \mu, A_1) = \{&-1.741803333 \times 10^{-9} x_1 + 6.003510305 \times 10^{-16} x_2 \\
&+ 8.241160714 \times 10^{-10} x_1^2 - 5.385351495 \times 10^{-13} x_1 x_2 - 1.737257276 \times 10^{-7} x_1 x_3 \\
&- 5.385351495 \times 10^{-13} x_3 x_2 - 1.745498436 \times 10^{-7} x_3^2 + 6.853153162 \times 10^{-18} \\
&- 1.741905912 \times 10^{-9} x_3 - [0.0133333333(-5.814110402 \times 10^{-12} \\
&+ 3.920934653 \times 10^{-7} x_3 x_2 + 3.920934653 \times 10^{-7} x_1 x_2 + 0.1264851934 x_1 x_3 \\
&- 0.0006000175 x_1^2 + 0.1270852109 x_3^2 + 0.0012681588 x_1 - 4.371000039 \times 10^{-10} x_2 \\
&+ 0.0012682771 x_3)]\mu - [0.0133333333(-2.582153434 \times 10^{-10} + 0.0000685736 x_1 x_2 \\
&+ 0.000068573 x_3 x_2 + 22.12113583 x_1 x_3 - 0.1049377304 x_1^2 + 22.22607356 x_3^2 \\
&+ 0.0001304019 x_1 - 7.640451461 \times 10^{-8} x_2 + 0.0001566166 x_3)]A_1 - 0.0046977165 A_1^3 \mu \\
&- 0.0188065253 A_1^2 \mu^2 - 0.0000626362 A_1 \mu^3 - (0.0133333333(-1.644200801 \times 10^{-8} \\
&- 0.1031837643 \times 10^{-5} x_2 + 0.0009255932 x_3 x_2 + 0.0009255932 x_1 x_2 \\
&+ 298.5865536 x_1 x_3 - 1.416427958 x_1^2 + 300.0029816 x_3^2 + 2.993662281 x_1 \\
&+ 2.994262198 x_3))\mu^2 - [0.0133333333(-0.0003094171 x_2 + 0.9899843300 x_3
\end{aligned}
$$

$$
\begin{aligned}
&+ 0.7352776462x_1 - 425.2824944x_1^2 + 90075.89521x_3^2 + 0.2779093621x_1x_2 \\
&+ 0.2779093621x_3x_2 + 89650.61272x_1x_3 + 0.1024198492 \times 10^{-5})]A_1\mu \\
&- [0.0133333333(0.0694194909x_3x_2 + 0.0694194909x_1x_2 + 22393.99152x_1x_3 \\
&- 0.1036671966x_1 - 0.8814161928 \times 10^{-5}x_2 + 22.24056690x_3 - 0.1212101079 \times 10^{-5} \\
&- 106.2320969x_1^2 + 22500.22362x_3^2)]A_1^2 - [0.0133333333(0.2779093621x_2 \\
&+ 90150.89521x_3 - 425.2824944x_1 - 0.0085590171)]A_1^2\mu \\
&- [0.0133333333(600.2529816x_3 + 0.0009255932x_2 - 1.416427958x_1 \\
&+ 0.0140536908)]A_1\mu^2 - [0.0133333333(-106.2320969x_1 + 0.0694194909x_2 \\
&+ 22500.22362x_3 + 0.0012954446)]A_1^3 - 0.0133333333x_3\mu^3\}/[(A_1 + 0.0009872263 \\
&+ 4\mu)(A_1 + 5.893552659 \times 10^{-7} + 0.0033333333\mu)].
\end{aligned}
$$

Note in the above equations that we have used digits format for convenience. Similarly, with $k_0 = k_{0H} + \mu = 0.000176806\cdots + \mu$, we can rewrite (3.6) as

$$
\begin{aligned}
F(\mu, A_1) = \quad & -0.2757604935\cdots A_1^3 - 75 \times A_1^3\mu + 0.0002580192\cdots A_1^2 \\
& +1.821952649\cdots A_1^2\mu - 300.25A_1^2\mu^2 + 5.496613923\cdots \times 10^{-8}A_1 \\
& -0.0002180204\cdots A_1\mu - 2.991600420\cdots A_1\mu^2 - A_1\mu^3 \\
& +1.094119833 \times 10^{-13} + 1.237646058\cdots \times 10^{-9}\mu \\
& +0.35 \times 10^{-5}\mu^2.
\end{aligned} \tag{3.13}
$$

Now, the Jacobian of system (3.12) evaluated at the origin, $x_i = 0,\ i = 1, 2, 3$, at the critical point, $\mu = 0,\ A_1 = 0.001114785\cdots$ (corresponding to the positive equilibrium E_1 for model (3.1)) is in the Jordan canonical form:

$$
\begin{bmatrix}
0 & 0.001087856\cdots & 0 \\
-0.001087856\cdots & 0 & 0 \\
0 & 0 & -0.336194209\cdots
\end{bmatrix}. \tag{3.14}
$$

To obtain the normal form of Hopf bifurcation, we need to find v_0 and τ_0 from linear analysis. The following theorem gives formulas for computing v_0 and τ_0.

Theorem 3.3.1 [59] *For the two-dimensional linear system,*

$$
\begin{pmatrix} \dot{x_1} \\ \dot{x_2} \end{pmatrix} = \begin{bmatrix} a_{11}\mu & \omega + a_{12}\mu \\ -\omega + a_{21}\mu & a_{22}\mu \end{bmatrix} \begin{pmatrix} x_1 \\ x_2 \end{pmatrix}, \tag{3.15}
$$

the following hold:

$$
v_0 = \frac{1}{2}(a_{11} + a_{22}),\ \tau_0 = \frac{1}{2}(a_{12} - a_{21}). \tag{3.16}
$$

Based on the center manifold theory, the system on the center manifold of system (3.12) is

a two-dimensional dynamical system. Then, applying the formula (3.16), we obtain

$$\begin{aligned}
v_0 &= \frac{1}{2}\left(\frac{\partial^2 G_1}{\partial x_1 \partial \mu} + \frac{\partial^2 G_2}{\partial x_2 \partial \mu}\right)\Bigg|_{x_i=0,\mu=0} \\
&= \frac{1}{2}\left[\left(\frac{\partial(\frac{\partial G_1}{\partial x_1})}{\partial \mu} + \frac{\partial(\frac{\partial G_1}{\partial x_1})}{\partial A_1}\frac{\partial A_1}{\partial \mu}\right) + \left(\frac{\partial(\frac{\partial G_2}{\partial x_2})}{\partial \mu} + \frac{\partial(\frac{\partial G_2}{\partial x_2})}{\partial A_1}\frac{\partial A_1}{\partial \mu}\right)\right]\Bigg|_{x_i=0,\mu=0} \\
&= \frac{1}{2}\left[\left(\frac{\partial(\frac{\partial G_1}{\partial x_1})}{\partial \mu} + \frac{\partial(\frac{\partial G_1}{\partial x_1})}{\partial A_1}\frac{\frac{\partial F(\mu,A_1)}{\partial \mu}}{\frac{\partial F(\mu,A_1)}{A_1}}\right) + \left(\frac{\partial(\frac{\partial G_2}{\partial x_2})}{\partial \mu} + \frac{\partial(\frac{\partial G_2}{\partial x_2})}{\partial A_1}\frac{\frac{\partial F(\mu,A_1)}{\partial \mu}}{\frac{\partial F(\mu,A_1)}{A_1}}\right)\right]\Bigg|_{x_i=0,\mu=0} \\
&= 1.455701498\cdots, \\
\tau_0 &= \frac{1}{2}\left(\frac{\partial^2 G_1}{\partial x_2 \partial \mu} - \frac{\partial^2 G_2}{\partial x_1 \partial \mu}\right)\Bigg|_{x_i=0,\mu=0} \\
&= \frac{1}{2}\left[\left(\frac{\partial(\frac{\partial G_1}{\partial x_2})}{\partial \mu} + \frac{\partial(\frac{\partial G_1}{\partial x_2})}{\partial A_1}\frac{\partial A_1}{\partial \mu}\right) - \left(\frac{\partial(\frac{\partial G_2}{\partial x_1})}{\partial \mu} + \frac{\partial(\frac{\partial G_2}{\partial x_1})}{\partial A_1}\frac{\partial A_1}{\partial \mu}\right)\right]\Bigg|_{x_i=0,\mu=0} \\
&= \frac{1}{2}\left[\left(\frac{\partial(\frac{\partial G_1}{\partial x_2})}{\partial \mu} + \frac{\partial(\frac{\partial G_1}{\partial x_2})}{\partial A_1}\frac{\frac{\partial F(\mu,A_1)}{\partial \mu}}{\frac{\partial F(\mu,A_1)}{A_1}}\right) - \left(\frac{\partial(\frac{\partial G_2}{\partial x_1})}{\partial \mu} + \frac{\partial(\frac{\partial G_2}{\partial x_1})}{\partial A_1}\frac{\frac{\partial F(\mu,A_1)}{\partial \mu}}{\frac{\partial F(\mu,A_1)}{A_1}}\right)\right]\Bigg|_{x_i=0,\mu=0} \\
&= 1.538917076\cdots.
\end{aligned} \tag{3.17}$$

Next, substituting $\mu = 0$, and $A_1 = A_H = 0.001114785$ into system (3.12), and then applying the Maple program [58] to the resulting system yields

$$v_1 = 36.64582372\cdots, \quad \tau_1 = -54130.35015\cdots. \tag{3.18}$$

Therefore, the normal form associated with this Hopf bifurcation, up to third-order terms, is given by

$$\begin{aligned}
\dot{r} &= r(v_0\mu + v_1 r^2) \\
&= r(1.455701498\cdots\mu + 36.64582372\cdots r^2), \\
\dot{\theta} &= w_c + \tau_0\mu + \tau_1 r^2 \\
&= 0.001087856\cdots + 1.538917076\cdots\mu - 54130.35015\cdots r^2.
\end{aligned} \tag{3.19}$$

The steady-state solutions of Eq. (3.19) are determined from $\dot{r} = \dot{\theta} = 0$, yielding

$$\bar{r} = 0, \quad \bar{r}^2 \approx -0.039723530\cdots\mu. \tag{3.20}$$

The equilibrium $\bar{r} = 0$ represents the equilibrium E_1 of model (3.2). A linear analysis on the first differential equation of (3.19) shows that $\frac{d}{dr}(\frac{dr}{dt})|_{\bar{r}=0} = v_0\mu$, and thus $\bar{r} = 0$ (ie. the equilibrium E_1) is stable (unstable) for $\mu < 0$ (> 0), as expected. When μ is increased from negative to cross zero, a Hopf bifurcation occurs and the amplitude of the bifurcating limit cycles is approximated by the nonzero steady state solution,

$$\bar{r} = 0.1993076279\cdots\sqrt{-\mu} \ \ (\mu < 0). \tag{3.21}$$

Since $\frac{d}{dr}(\frac{dr}{dt})|_{(3.21)} = 2v_1\bar{r}^2 = -2v_0\mu > 0 \ \ (\mu < 0, v_0 > 0, v_1 > 0)$, the Hopf bifurcation is subcritical and so the bifurcating limit cycles are unstable. Equation (3.21) gives the approximate amplitude of the bifurcating limit cycles, while the phase of the motion is determined by

$\theta = \omega t$, where ω is given by

$$\omega = \left.\frac{d\theta}{dt}\right|_{(3.21)} = 0.001087856\cdots + 2151.787535\cdots\mu. \tag{3.22}$$

3.4 Simulations

In this section, we present simulation to demonstrate the behavior changes of solutions, showing a good agreement with the experimental results reported in [54].

Based on the given parameter values in (3.5), the system (3.1) can be rewritten as

$$\begin{aligned}
\frac{dA}{dt} &= 0.25SA - 300IA - 0.0035A - k_0A + 0.00007S,\\
\frac{dI}{dt} &= 0.01k_0 - Ik_0 - 300IA,\\
\frac{dS}{dt} &= -0.25SA - k_0S - 0.00007S + 0.05k_0.
\end{aligned} \tag{3.23}$$

We use the ode45 package in Matlab to simulate the above system to obtain the results, as shown in Figure 3.6.

It is seen from Figure 3.6 that the solutions of A are oscillating when the values of k_0 are chosen between k_{0H} and k_{0sn}. The period of oscillation increases with the increase of k_0, as shown in Figure 3.7. This shows the interesting recurrence phenomenon, which has been also studied by Zhang *et al* for a recurrent autoimmune disease model [60]. From a biological point of view, the subtypes of some diseases are classified based on the patterns of this recurrent behavior [61]. Therefore, an improved understanding of recurrence phenomenon in autoimmune disease is crucial to promoting correct diagnosis, patient management, and treatment decisions. For the recurrence phenomenon studied in this chapter, it can be used to realistically explain complex dynamics in organic reactions and promote correct classification, management and utilization of energy resources.

By simulation, we also find that the stable region before the Hopf critical point as shown in Figure 3.4 (i.e. for $k_0 \in (0, k_{0H})$) can be divided into two parts: globally asymptotic stable and locally asymptotic stable. The approximate value of the dividing point can be obtained as follows: Recall $k_{0H} = 0.000176806$, we choose $k_0 = 0.00014466350$ and two initial points $(A, I, S) = (1, 1, 1)$ and $(0.001, 0.000005, 0.016)$ for simulation and obtain the results as shown in Figures **??** and 3.9, respectively. It is seen that the trajectory starting from the first initial point converges a large stable limit cycle, while that starting from the second critical point converges to the equilibrium E_1. We also choose $k_0 = 0.00014466348$ and the initial point $(A, I, S) = (1, 1, 1)$ to obtain the result depicted in Figure **??**. It is shown that the trajectory eventually converges to the equilibrium E_1 even from a far away initial point, showing that the E_1 is globally asymptotically stable for this value of k_0. Thus, the approximate dividing point for globally asymptotic stability and locally asymptotic stability is $k_0 \approx 0.00014466348$.

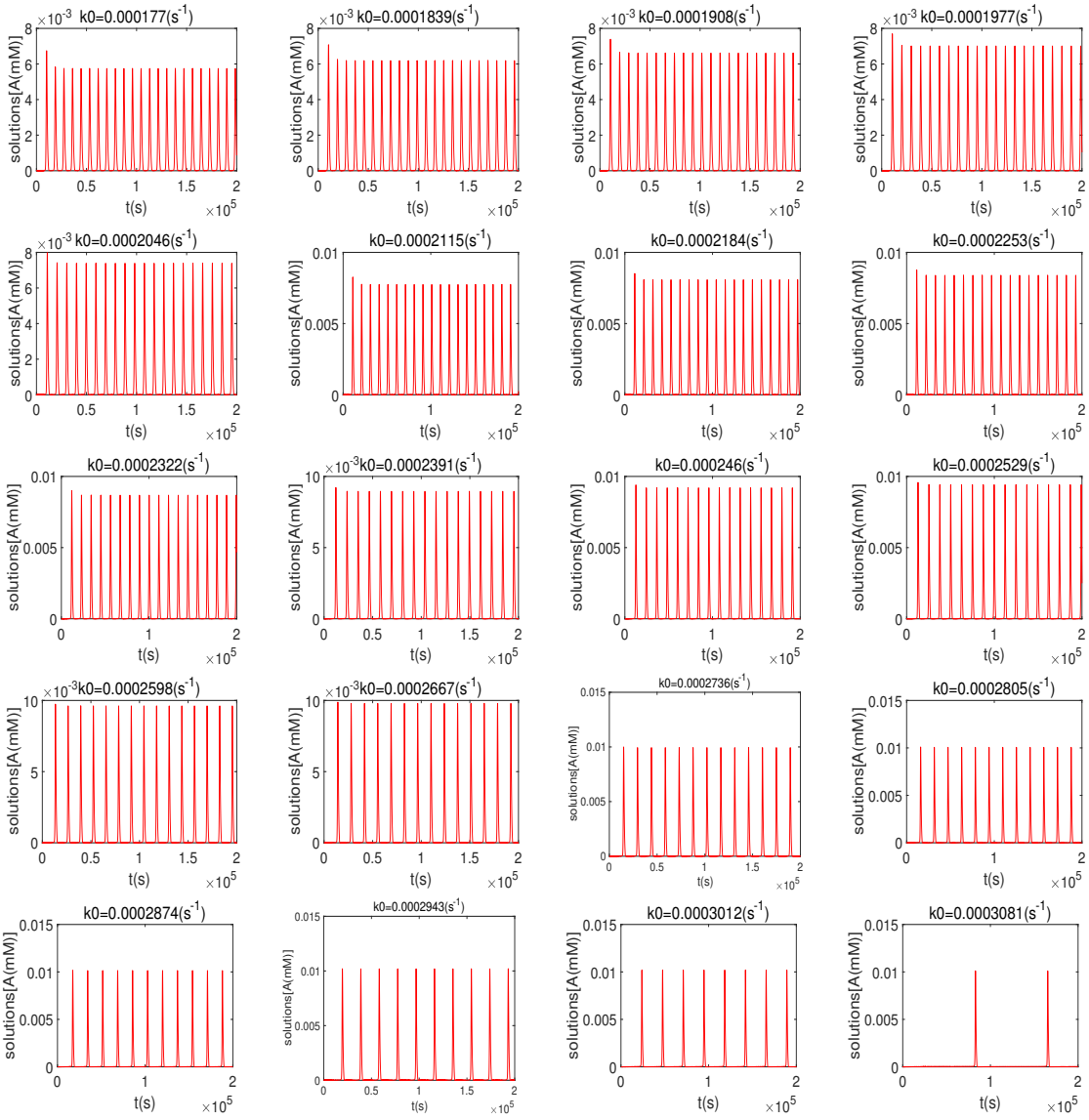

Figure 3.6: Simulated component A of system (3.23) for $k_0 = k_{0H} + 0.0000069\,j$, $j = 1, 2, \ldots 20$.

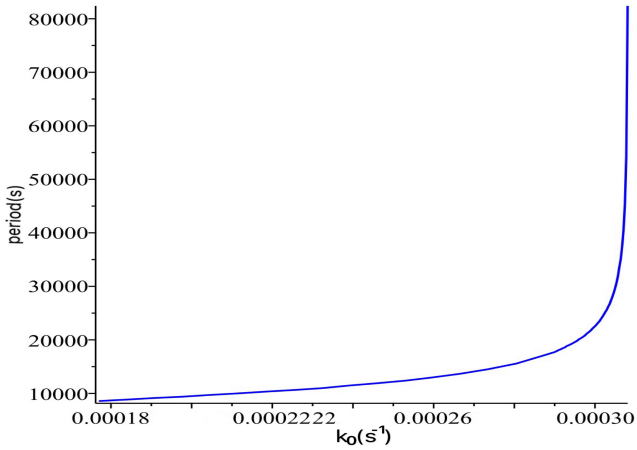

Figure 3.7: The period of oscillation with respect to k_0.

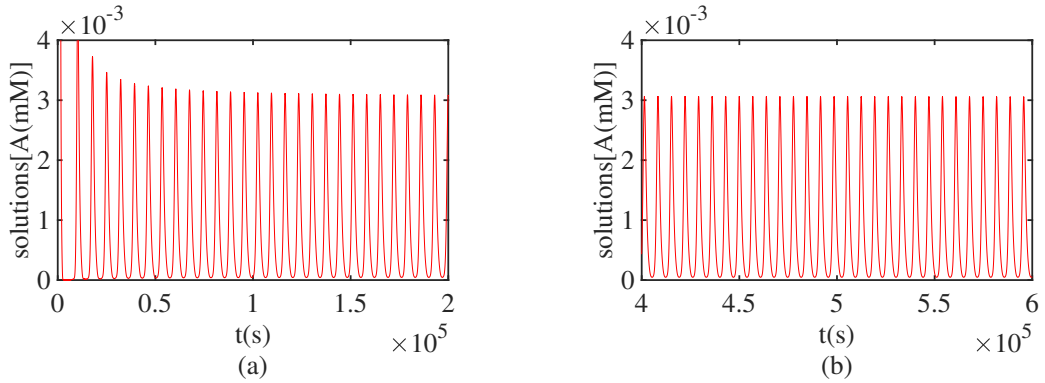

Figure 3.8: Simulated trajectory of system (3.23), starting from $t = 0$ and ended at $t = 6 \times 10^6$, converging to a large stable limit cycle starting from the initial point (1, 1, 1) for $k_0 = 0.00014466350$: (a) showing time history for $t \in (0, 2 \times 10^5)$; and (b) showing time history for $t \in (4 \times 10^5, 6 \times 10^5)$.

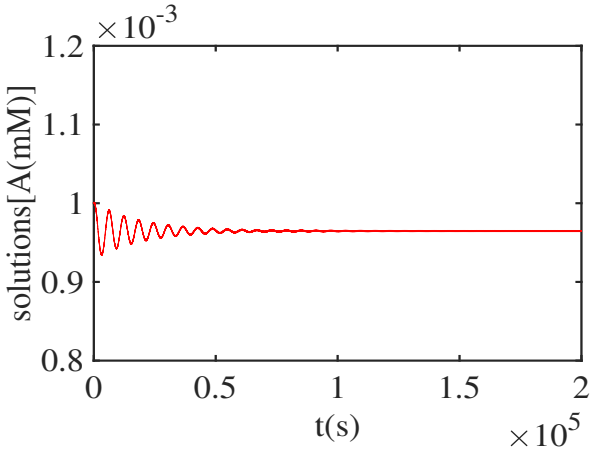

Figure 3.9: Simulated trajectory of system (3.23), converging to the equilibrium E_1 starting from the initial point(0.001, 0.000005, 0.016) for $k_0 = 0.00014466350$.

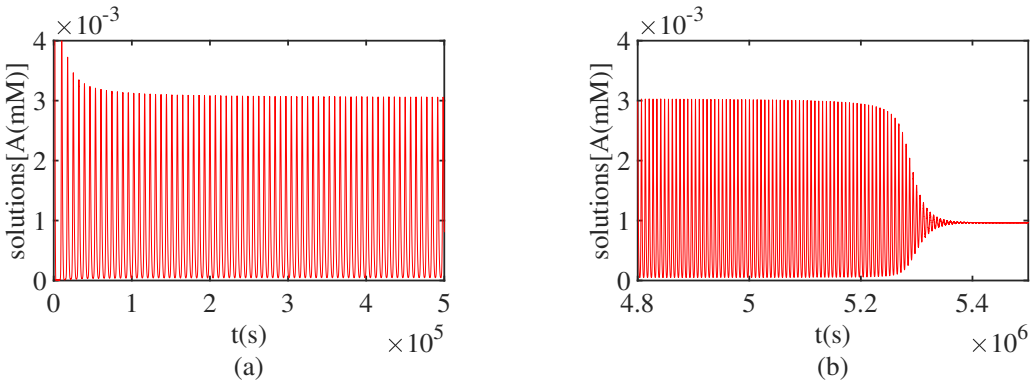

Figure 3.10: Simulated trajectory of system (3.23), starting from $t = 0$ and ended at $t = 6\times10^6$, converging to the equilibrium E_1 starting from the initial point(1, 1, 1) for $k_0 = 0.00014466348$: (a) showing time history for $t \in (0, 5\times10^5)$; and (b) showing time history for $t \in (4.8\times10^6, 5.5\times 10^6)$.

3.5 Conclusion and discussion

In this chapter, we have analyzed the stability and bifurcation in a kinetic model, which was constructed to enable qualitative analysis of dynamic behaviors in oscillating networks of biologically relevant organic reactions. In particular, a Hopf bifurcation is identified to be subcritical, and recurrence phenomenon is induced from the Hopf bifurcation for a pretty large internal of parameter. Simulations are given to verify the theoretical predictions and to show a very good agreement. The recurrence phenomenon studied in this chapter for a kinetic model which characterizes oscillating networks of biologically relevant organic reactions may be one of the sources of generating complex dynamics in biological systems or even more generally in real physical systems. It is anticipated that the method developed in this chapter can be applied to study other nonlinear dynamical systems, and promote further development in this field.

Chapter 4

Conclusion and Future work

4.1 Conclusion

In this thesis, we have applied nonlinear dynamical system theory to study two practical biological models: a tritrophic food chain model with Holling functional response types III and IV for the predator and superpredator, respectively and an oscillating networks model of biologically relevant organic reactions. In particular, we have used stability and bifurcation theory to investigate the dynamical behavior arising from Hopf bifurcation and multiple limit cycle bifurcation, which may explain how complex dynamical behavior occurs in such systems. Simulations are given to verify the theoretical predictions.

For the tritrophic food chain model studied in Chapter 2, we focus on the stability and bifurcation of the positive equilibrium when the prey has linear growth. Center manifold theory and normal form theory are applied to analyze Hopf bifurcation. Moreover, bifurcation of multiple limit cycles is explored to show that the food chain model can exhibit at least three limit cycles due to Hopf bifurcation, which may explain the complex dynamical behavior occurring in such food chain systems. The multiple cycle bifurcation, confirmed by simulation, indicates that a new bistable phenomenon consisting of two stable oscillations (the inner-most and outer-most limit cycles), can occur in such a food chain model. Since periodic and quasi-periodic oscillations are often observed in practical biological systems, it is anticipated that the multiple limit cycle bifurcation studied in this thesis can establish a good method for investigating such complex dynamical behaviors.

For the oscillating networks model studied in Chapter 3, a Hopf bifurcation is identified to be subcritical, and recurrence phenomenon is induced from the Hopf bifurcation for a pretty large interval of a parameter. Simulations are given to verify the theoretical predictions and to show a very good agreement. The recurrence phenomenon studied in this thesis may explain how complex dynamics occurs in biological systems or even more generally in real physical systems. It is expected that the method developed in this thesis can be applied to consider other nonlinear dynamical systems and promote further development in this field.

4.2 Future work

There are some interesting but also challenging problems that are worth to study further.

In Chapter 2, we obtain at least three limit cycles in the food chain model due to Hopf bifurcation. However, this result is based on the assumption that the prey has a linear growth, which is a unbounded function. More realistically, the linear growth should be modified as a bounded function, for example, the logistic equation. Certainly, studying such an nonlinear growth function is much more challenging, but exhibit more interesting results. Also, to make the complex algebraic computation manageable, we have set fixed values for some parameters. It would be interesting to see what the maximal number of limit cycles can be achieved if all parameters are chosen free.

In Chapter 3, we study the recurrence phenomenon in the oscillating networks model, and use the method of normal forms to analytically determine the Hopf critical point, and show that the Hopf bifurcation is subcritical by using just one bifurcation parameter. If we choose more parameters, say two parameters, as bifurcation parameters, can we analytically determine the generalized Hopf bifurcation? Also, in this thesis, we use numerical simulation to show the critical point which divides the interval of the parameter corresponding to the stable equilibrium into two parts: one is locally asymptotically stable and the other is globally asymptotically stable. Thus, as a future work, we will try to use an analytical approach such as Lyapunov function method to give a rigorous mathematical proof and find the algebraic expression to determine this critical point.

References

[1] J. Guckenheimer and J.S. Labouriau. Bifurcation of the Hodgkin and Huxley equations: A new twist. Bulletin of Mathematical Biology, 55(5): 937-952, 1993.

[2] J.M.T. Thompson, M. Thompson, and H.B. Stewart. Nonlinear dynamics and chaos. John Wiley & Sons, LTD, 2002.

[3] A. Bazykin. Nonlinear Dynamics of Interacting Populations. World Scientific, River edge, NJ, 1998.

[4] G. Blé, V. Castellanos, and J. Llibre. Existence of limit cycles in a tritrophic food chain model with Holling functional responses of type II and III. Math. Meth. Appl. Sci.39: 3996-4006, 2016.

[5] J. Carr. Applications of Centre Manifold Theory. Springer-Verlag, New York, 2012.

[6] V. Castellanos and R. E. Chan-Lòpez. Existence of limit cycles in a three level trophic chain with Lotka-Volterra and Holling type II functional responses. Chaos Solit. Fract.95: 157-167, 2017.

[7] V. Castellanos, F. Eduardo, C. Santos, M. A. Dela-Rosa, and I. Loreto-Hernàndez. Hopf and bautin bifurcation in a tritrophic food chain model with holling functional response types III and IV. Int. J. Bifur. Chaos28(03),1850035(24 pages), 2018.

[8] V. Castellanos, J. Llibre, and I. Quilantan. Simultaneous periodic orbits bifurcating from two zero-Hopf equilibria in a tritrophic food chain model. J. Appl. Math. Phys.1: 31-38, 2013.

[9] F. E. Castillo-Santos, M. A. Dela Rosa, and I. Loreto-Hernandez. Existence of a limit cycle in an intraguild food web model with Holling type II and logistic growth for the common prey. Appl. Math.8: 358-376, 2017.

[10] S. N. Chow, C. Li, and D. Wang. Normal Forms and Bifurcation of Planar Vector Fields. Cambridge University Press, Cambridge, 1994.

[11] J. P. Francois and J. Llibre. Analytical study of a triple Hopf bifurcation in a tritrophic food chain model. Appl. Math. Comput.217: 7146-7154, 2011.

[12] H. I. Freedman and J. W.-H. So. Global stability and persistence of simple food chains. Math. Bio. Sci.76: 69-76, 1985.

[13] T. Gard. Persistence in food chains with general interactions. Math. Bio.Sci.51: 165-174, 1980.

[14] E. Gonzàlez-Olivares, B. Gonzàlez-Yañez, J. Mena Lorca, A. Rojas-Palma, and J. D. Flores. Consequence of double Allee effect on the number of limit cycles in a predator-prey model. Comput. Math. Appl.62: 3449-3463, 2011.

[15] J. Guckenheimer and Y. A. Kuznetsov. Bautin bifurcation. Scholarpedia.2: 1853, $http : //www.scholarpedia.org/article/Bautin - bifurcation$, 2007.

[16] J. Guckenheimer and P. J. Holmes. Nonlinear Oscillations, Dynamical Systems, and Bifurcations of Vector Fields. 1st Ed, Springer-Verlag, New York, 1983.

[17] M. Han and P. Yu. Normal Forms, Melnikov Functions and Bifurcations of Limit Cycles. Springer-Verlag, New York, 2012.

[18] A. Hastings and T. Powell. Chaos in a three-species food chain. Ecology.72, 896-903, 1991.

[19] D. Hinrichsen and A. J. Pritchard. Mathematical Systems Theory I: Modelling, State Space Analysis, Stability and Robustnes. 2nd edition, Springer-Verlag, NY, 2005.

[20] P. Hogeweg and B. Hesper. Interactive instruction on population interactions. Comp. Biol. Med.8: 319-327, 1978.

[21] Y. Kuang and E. Beretta. Global quantities analysis of a ratio-dependent predator-prey system. J. Math. Biol.36: 389-406, 1998.

[22] Y. A. Kuznetsov. Elements of Applied Bifurcation Theory. 3rd edition, Springer-Verlag, 2004.

[23] Y. Liu and J. Li. Theory of values of singular point in complex autonomous differential systems. Sci. China (Ser. A).33(1): 10-23, 1990.

[24] A. Lotka. Elements of physical biology. Williams and Wilkins, Baltimore, MD, 1925.

[25] J. E. Marsden and M. McCracken. The Hopf Bifurcation and Its Applications. Springer-Verlag, NY, 1976.

[26] S. Muratori and S. Rinaldi. A separation condition for the existence of limit cycles in slow-fast systems. Appl. Math. Model.15: 312-318, 1991.

[27] L. Perko. Differential Equations and Dynamical Systems. 3rd edition, Springer-Verlag, 2001.

[28] P. W. Price, C. E. Bouton, P. Gross, B. A. Mcpheropn, J. N.Thompson, and A. E. Weis. Iteractions among three trophic levels: influence of plants on interactions between insect herbivores and natural enemies. Annu. Rev Ecol.Syst.11: 41-65, 1980.

[29] Y. Tian and P. Yu. An explicit recursive formula for computing the normal form and center manifold of general n-dimensional differential systems associated with Hopf bifurcation. Int. J. Bifur. Chaos.23(06),1350104(18 pages), 2013.

[30] V. Volterra. Variazioni e fluttuazioni del numero di individui in specie animali conviventi. Mem. Accad. Lincei.2: 31-113 (in Italian),1926.

[31] P. Yu. Closed-form conditions of bifurcation points for general differential equations. Int. J. Bifurcation and Chaos.15: 1467-1483, 2005.

[32] P. Yu. Computation of normal forms via a perturbation technique. J. Sound Vib.211(1): 19-38, 1998.

[33] P. Yu and W. Lin. Complex dynamics in biological systems arising from multiple limit cycle bifurcation. J. Biol. Dyn.10(1): 263-285, 2016.

[34] P. Yu, A. Nadeem, and L. M. Wahl. The impact of prophage on the equilibria and stability of phage and host. J. Nonlin. Sci.27: 817-846, 2017.

[35] W. Zhang, L. M. Wahl, and P. Yu. Modeling and analysis of recurrent autoimmune disease. SIAM J. Appl. Math. 74: 1998-2025, 2014.

[36] W. Zhang, L. M. Wahl, and P. Yu. Backward bifurcations, turning points and rich dynamics in simple disease models. J. Math. Biol.73: 947-976, 2016 .

[37] B. P. Belousov. Periodicheski deistvuyushchaya reaktsia i ee mechanism in Russian. in Sbornik. Referatov po Radiatsionni Meditsine: 145-147, Moscow: Medgiz, 1958.

[38] F. J. Dyson. A model for the origin of life. J. Mol. Evol.18: 344-350, 1982.

[39] I. R. Epstein and J. A. Pojman. An introduction to Nonlinear Chemical Dynamics: Oscillations, Waves, Patterns, and Chaos. Chs.2 and 4: 17-47 and 62-83 (Oxford Univ. Press), 1998.

[40] J. E. Ferrell, T. Y. C. Tasi, and Q. O. Yang. Modeling the cell cycle:why do certain circuits oscillate. Cell.244: 874-885, 2011.

[41] R. FitzHugh. Impulses and physiological states in theoretical models of nerve membrane. Biophys. J1: 445-466, 1961.

[42] D.M. Fergusson, L.J. Horwood, and F.T. Shannon. Early solid feeding and recurrent childhood eczema: A 10-year longitudinal study. Pediatrics.86: 541-546, 1990.

[43] A. Goldbeter. A model for circadian oscillations in the Drosophila period protein(PER). Proc. R. Soc. Lond. B261: 319-324, 1995.

[44] L. Gyorgyi, T. Turányi, and R. J. Field. Mechanistic details of the oscillatory Belousov-Zhabotinskii reaction. J. Phys. Chem.94: 7162-7170, 1990.

[45] H.J. Girschick, C. Zimmer, G. Klaus, K. Darge, A. Dick, and H. Morbach. Chronic recuurent multifocal osteomyelitis: What is it and how should it be treated? Nat. Clin. Practice Rheumatol.3: 733-738, 2007.

[46] D. Hinrichsen and A. J. Pritchard. Mathematical Systems Theory I: Modelling, State Space Analysis, Stability and Robustnes. 2nd edition, Springer-Verlag, NY, 2005.

[47] R.S. Iyer, M.M. Thapa, and F.S. Chew. Chronic recurrent multifocal osteomyelitis: Review. Amer. J. Roentgenol.196: S87-S91, 2011.

[48] I. U. A. Kuznetsov. Elements of Applied Bifurcation Theory. 3rd edition, Ch.3: 77-115, Springer, 2004.

[49] A. D. Lander. Pattern, growth, and control. Cell.144: 955-969, 2011.

[50] M. T. Laub and W. F. A. Loomis. molecular network that produces spontaneous oscillations in excitable cells of dictyostelium. Mol. Biol. Cell.9: 3521-3532, 1998.

[51] D.D. Munro. Recurrent subacute discoid lupus erythematosus. Proc. Roy. Soc. Med.56: 78-79, 1963.

[52] P. Nghe et al. Prebiotic network evolution:six key parameters. Mol. Biosyst.11: 3206-3217, 2015.

[53] B. H. Patel, C. Percivalle, D. J. Ritson, C. D. Duffy, and J. D. Sutherland. Common origins of RNA, protein and lipid precursors in a cyanosulfidic protometabolism. Nat. Chem.7: 301-307, 2015.

[54] N. S. Semenov, J. K. Lewis, A. Alar, Z. Mengxia, B. Mostafa , E. C. Victoria, K. Kyungtae, M.F. Jerome and M. W. George. Autocatalytic, bistable, oscillatory networks of biologically relevant organic reactions. Nature.573:656-660, 2016.

[55] J. J. Tyson, K. C. Chen, B. Novak, and B. Sniffers. toggles and blinkers:dynamics of regulatory and signaling pathways in the cell. Curr. Opin. Cell Biol.15: 221-231, 2003.

[56] J. J. Tyson. Modeling the cell -division cycle: cdc2 and cyclin interactions. Proc. Natl Acad. Sci. USA.88: 7328-7332,1991.

[57] P. Yu. Closed-form conditions of bifurcation points for general differential equations. Int. J. Bifurcation and Chaos.15: 1467-1483, 2005.

[58] P. Yu. Computation of normal forms via a perturbation technique. J. Sound Vib.211(1):19-38, 1998.

[59] W. Zhang and P. Yu. Hopf and generalized Hopf bifurcations in a recurrent autoimmune disease model. Int. J. Bifurcation and Chaos.26: 1650079 (24 pages), 2016.

[60] W. Zhang, L.M. Wahl, and Yu P. Modeling and analysis of recurrent autoimmune disease. Siam J. Appl. Math.74: 1998-2025, 2016.

[61] T. Vollmer. The natural history of relapses in multiple sclerosis. J. Neurolog. Sci.256: s5-s13, 2007.

[62] J.H.P. Dawes and M.O. Souza. A derivation of Holling'type I, II and III functional responses in predator-prey systems. J. Theoretical Biology. 327: 11-22, 2013.

Appendix A

In Section 2.2 of Chapter 2, the V_{1a} and V_{2a} are given below.

$$
\begin{aligned}
V_{1a} = {} & 190B_1^9 d_2^7 + 5823B_1^9 d_2^6\rho + 74616B_1^9 d_2^5\rho^2 + 516841B_1^9 d_2^4\rho^3 + 2082330B_1^9 d_2^3\rho^4 + 4855896B_1^9 d_2^2\rho^5 + 6029856B_1^9 d_2\rho^6 + 3048192B_1^9\rho^7 + 2660B_1^8 X_0 d_2^7 + 78636B_1^8 X_0 d_2^6\rho + 972132B_1^8 X_0 d_2^5\rho^2 + 6499616B_1^8 X_0 d_2^4\rho^3 \\
& + 25307088B_1^8 X_0 d_2^3\rho^4 + 57179952B_1^8 X_0 d_2^2\rho^5 + 69149376B_1^8 X_0 d_2\rho^6 + 34380288B_1^8 X_0\rho^7 + 15960B_1^7 X_0^2 d_2^7 + 455172B_1^7 X_0^2 d_2^6\rho + 5428668B_1^7 X_0^2 d_2^5\rho^2 + 35023680B_1^7 X_0^2 d_2^4\rho^3 + 131680092B_1^7 X_0^2 d_2^3\rho^4 \\
& + 287756400B_1^7 X_0^2 d_2^2\rho^5 + 337626432B_1^7 X_0^2 d_2\rho^6 + 163759104B_1^7 X_0^2\rho^7 + 53200B_1^6 X_0^3 d_2^7 + 1465344B_1^6 X_0^3 d_2^6\rho + 16871464B_1^6 X_0^3 d_2^5\rho^2 + 105038400B_1^6 X_0^3 d_2^4\rho^3 + 381078184B_1^6 X_0^3 d_2^3\rho^4 + 804123776B_1^6 X_0^3 d_2^2\rho^5 \\
& + 912658304B_1^6 X_0^3 d_2\rho^6 + 429576192B_1^6 X_0^3\rho^7 + 106400B_1^5 X_0^4 d_2^7 + 2839440B_1^5 X_0^4 d_2^6\rho + 31619552B_1^5 X_0^4 d_2^5\rho^2 + 190070544B_1^5 X_0^4 d_2^4\rho^3 + 664935376B_1^5 X_0^4 d_2^3\rho^4 + 1352318144B_1^5 X_0^4 d_2^2\rho^5 + 1480145152B_1^5 X_0^4 d_2\rho^6 \\
& + 672995328B_1^5 X_0^4\rho^7 + 127680B_1^4 X_0^5 d_2^7 + 3327936B_1^4 X_0^5 d_2^6\rho + 35998592B_1^4 X_0^5 d_2^5\rho^2 + 209153920B_1^4 X_0^5 d_2^4\rho^3 + 704389664B_1^4 X_0^5 d_2^3\rho^4 + 1375463936B_1^4 X_0^5 d_2^2\rho^5 + 1443665408B_1^4 X_0^5 d_2\rho^6 + 629407744B_1^4 X_0^5\rho^7 \\
& + 85120B_1^3 X_0^6 d_2^7 + 2215872B_1^3 X_0^6 d_2^6\rho + 23511744B_1^3 X_0^6 d_2^5\rho^2 + 132067456B_1^3 X_0^6 d_2^4\rho^3 + 425126784B_1^3 X_0^6 d_2^3\rho^4 + 786673152B_1^3 X_0^6 d_2^2\rho^5 + 777416704B_1^3 X_0^6 d_2\rho^6 + 317521920B_1^3 X_0^6\rho^7 + 24320B_1^2 X_0^7 d_2^7 \\
& + 689664B_1^2 X_0^7 d_2^6\rho + 7351936B_1^2 X_0^7 d_2^5\rho^2 + 39342592B_1^2 X_0^7 d_2^4\rho^3 + 115571456B_1^2 X_0^7 d_2^3\rho^4 + 187174912B_1^2 X_0^7 d_2^2\rho^5 + 154066944B_1^2 X_0^7 d_2\rho^6 + 48758784B_1^2 X_0^7\rho^7 + 43008B_1 X_0^8 d_2^6\rho + 483328B_1 X_0^8 d_2^5\rho^2 \\
& + 1412096B_1 X_0^8 d_2^4\rho^3 - 2496512B_1 X_0^8 d_2^3\rho^4 - 20799488B_1 X_0^8 d_2^2\rho^5 - 38469632B_1 X_0^8 d_2\rho^6 - 23592960B_1 X_0^8\rho^7 - 65536X_0^9 d_2^5\rho^2 - 917504X_0^9 d_2^4\rho^3 - 4980736X_0^9 d_2^3\rho^4 - 13107200X_0^9 d_2^2\rho^5 - 16777216X_0^9 d_2\rho^6 \\
& - 8388608X_0^9\rho^7,
\end{aligned}
$$

$$
\begin{aligned}
V_{2a} = {} & 1566767862220559410419204096X_0^{30}\rho^{26} + 1615491072B_1^{30} d_2^{26} + 561691514549715124145356 8B_1^{30}\rho^{26} - 5149357466192649866204184523571 2B_1^3 X_0^{27} d_2^6\rho^{20} \\
& - 279714346584047374955773092167 68B_1^3 X_0^{27} d_2^5\rho^{21} - 6660479065380721153124423696384B_1^3 X_0^{27} d_2^4\rho^{22} + 3499605027152561581515314561024B_1^3 X_0^{27} d_2^3\rho^{23} \\
& + 4025658451720501600221954834432B_1^3 X_0^{27} d_2^2\rho^{24} + 1619394882390787724957901127680B_1^3 X_0^{27} d_2\rho^{25} - 4783139463616266 24B_1^2 X_0^{28} d_2^{24}\rho^2 - 3551302930851377971 2B_1^2 X_0^{28} d_2^{23}\rho^3 \\
& - 1264667219894558785536B_1^2 X_0^{28} d_2^{22}\rho^4 - 2848777540923901870080 0B_1^2 X_0^{28} d_2^{21}\rho^5 - 4525439133814326978150 40B_1^2 X_0^{28} d_2^{20}\rho^6 - 5366009482230572936855552B_1^2 X_0^{28} d_2^{19}\rho^7 \\
& - 4911390059423169674582425 6B_1^2 X_0^{28} d_2^{18}\rho^8 - 3541580167112741300071301 12B_1^2 X_0^{28} d_2^{17}\rho^9 - 2034763617195911230259200000B_1^2 X_0^{28} d_2^{16}\rho^{10} - 9341207982479964524943245312B_1^2 X_0^{28} d_2^{15}\rho^{11} \\
& - 3400268491106837209303062937 6B_1^2 X_0^{28} d_2^{14}\rho^{12} - 9552054696479362989693914316 8B_1^2 X_0^{28} d_2^{13}\rho^{13} - 1911470509192839626564262952 96B_1^2 X_0^{28} d_2^{12}\rho^{14} - 1891853724379949690792097873 92B_1^2 X_0^{28} d_2^{11}\rho^{15} \\
& + 3514555533583270942414135623 68B_1^2 X_0^{28} d_2^{10}\rho^{16} + 2237901898958601484596454359040B_1^2 X_0^{28} d_2^9\rho^{17} + 6190483300810719699247478865920B_1^2 X_0^{28} d_2^8\rho^{18} \\
& + 1181163282114304313759214075904 0B_1^2 X_0^{28} d_2^7\rho^{19} + 1689626921252772253174768389324 8B_1^2 X_0^{28} d_2^6\rho^{20} + 1846808250026607035657679693414 4B_1^2 X_0^{28} d_2^5\rho^{21} \\
& + 1531102183939033006086898791 2192B_1^2 X_0^{28} d_2^4\rho^{22} + 9362195266082360040017914494976B_1^2 X_0^{28} d_2^3\rho^{23} + 3993281674537398031306828283904B_1^2 X_0^{28} d_2^2\rho^{24} \\
& + 1062982802402942553927758905344B_1^2 X_0^{28} d_2\rho^{25} - 2963931504763207686B_1 X_0^{29} d_2^{23}\rho^3 - 1723640167385373081 6B_1 X_0^{29} d_2^{22}\rho^4 - 4413832331485375361 2B_1 X_0^{29} d_2^{21}\rho^5 \\
& - 6276260491537378443264B_1 X_0^{29} d_2^{20}\rho^6 - 4647857269932065135001 6B_1 X_0^{29} d_2^{19}\rho^7 + 2333991689079661736755 2B_1 X_0^{29} d_2^{18}\rho^8 + 5095746646859631921463296B_1 X_0^{29} d_2^{17}\rho^9 \\
& + 7087813320352296301756416 0B_1 X_0^{29} d_2^{16}\rho^{10} + 6108706590903038344094023 68B_1 X_0^{29} d_2^{15}\rho^{11} + 3874971782820400278433431552B_1 X_0^{29} d_2^{14}\rho^{12} + 1920251291287886627357904076 8B_1 X_0^{29} d_2^{13}\rho^{13} \\
& + 7647846326284527539187823 4112B_1 X_0^{29} d_2^{12}\rho^{14} + 2485228676836324588984027054 08B_1 X_0^{29} d_2^{11}\rho^{15} + 6640563548421428040575012044 80B_1 X_0^{29} d_2^{10}\rho^{16} \\
& + 1463012460280402356107539906560B_1 X_0^{29} d_2^9\rho^{17} + 2654038698987177867057762926592B_1 X_0^{29} d_2^8\rho^{18} + 3943336193681313519067226701824B_1 X_0^{29} d_2^7\rho^{19} \\
& + 4751697548206931438690377924608B_1 X_0^{29} d_2^6\rho^{20} + 4571912680230561391877717753856B_1 X_0^{29} d_2^5\rho^{21} + 3429831522985365858215666909184B_1 X_0^{29} d_2^4\rho^{22} \\
& + 1933332273919627056975043362816B_1 X_0^{29} d_2^3\rho^{23} + 7702687104615310858219935498 24B_1 X_0^{29} d_2^2\rho^{24} + 1933938278682091028501558722256B_1 X_0^{29} d_2\rho^{25} \\
& - 3115142450923633789995836034252 8B_1^5 X_0^{25} d_2^{12}\rho^{14} - 1379034845710954282284701670440 96B_1^5 X_0^{25} d_2^{11}\rho^{15} - 4130109975720628643410787434496 00B_1^5 X_0^{25} d_2^{10}\rho^{16} \\
& - 9450101175229631141953097988833 28B_1^5 X_0^{25} d_2^9\rho^{17} - 1714571463347991579063666130026496B_1^5 X_0^{25} d_2^8\rho^{18} - 2494313501467179283894785347158016B_1^5 X_0^{25} d_2^7\rho^{19} \\
& - 2904392748435716607068350843977728B_1^5 X_0^{25} d_2^6\rho^{20} - 2676352796714457972412647682867200B_1^5 X_0^{25} d_2^5\rho^{21} - 1910119684964937806903419317780480B_1^5 X_0^{25} d_2^4\rho^{22}
\end{aligned}
$$

$$
\begin{aligned}
&- 10186831879923992122207652072652 80 B_1^5 X_0^{25} d_2^3 \rho^{23} - 382049104069562282675128907071488 B_1^5 X_0^{25} d_2^2 \rho^{24} - 898360376912288692290571531714 56 B_1^5 X_0^{25} d_2 \rho^{25} + 120713957745969070 08 B_1^4 X_0^{26} d_2^{25} \rho \\
&+ 541939357894752337920 B_1^4 X_0^{26} d_2^{24} \rho^2 + 140580373234457646202 88 B_1^4 X_0^{26} d_2^{23} \rho^3 + 241587900619202469298176 B_1^4 X_0^{26} d_2^{22} \rho^4 + 291811266571728169887334 4 B_1^4 X_0^{26} d_2^{21} \rho^5 \\
&+ 250058103478442056587673 60 B_1^4 X_0^{26} d_2^{20} \rho^6 + 141962863804646860531957760 B_1^4 X_0^{26} d_2^{19} \rho^7 + 32930287926254695151461990 4 B_1^4 X_0^{26} d_2^{18} \rho^8 - 303631279978278548310641868 8 B_1^4 X_0^{26} d_2^{17} \rho^9 \\
&- 450345864956151463626963681 28 B_1^4 X_0^{26} d_2^{16} \rho^{10} - 338530483922776569680138076160 B_1^4 X_0^{26} d_2^{15} \rho^{11} - 183062439801550033165896875264 B_1^4 X_0^{26} d_2^{14} \rho^{12} \\
&- 774326761620582503613888200704 0 B_1^4 X_0^{26} d_2^{13} \rho^{13} - 264821736777056852848347877212 16 B_1^4 X_0^{26} d_2^{12} \rho^{14} - 743567194798702681823332732 1453 44 B_1^4 X_0^{26} d_2^{11} \rho^{15} \\
&- 172536584447637014495380318978048 B_1^4 X_0^{26} d_2^{10} \rho^{16} - 331227913401126437747757905084416 B_1^4 X_0^{26} d_2^9 \rho^{17} - 524428780445360973689097115664384 B_1^4 X_0^{26} d_2^8 \rho^{18} \\
&- 679826014748666196171174921109504 B_1^4 X_0^{26} d_2^7 \rho^{19} - 712956424631799410515902422056960 B_1^4 X_0^{26} d_2^6 \rho^{20} - 594083947292389762932420030496768 B_1^4 X_0^{26} d_2^5 \rho^{21} \\
&- 382921257750577104992540186116096 B_1^4 X_0^{26} d_2^4 \rho^{22} - 183268590354500126170744004542464 B_1^4 X_0^{26} d_2^3 \rho^{23} - 609360037731923119384972587171 84 B_1^4 X_0^{26} d_2^2 \rho^{24} \\
&- 124480108396946059085698207580 16 B_1^4 X_0^{26} d_2 \rho^{25} + 29314739215112601 6 B_1^3 X_0^{27} d_2^{25} \rho + 14871272997670354944 B_1^3 X_0^{27} d_2^{24} \rho^2 + 283596221613170753536 B_1^3 X_0^{27} d_2^{23} \rho^3 \\
&+ 717675492476880683008 B_1^3 X_0^{27} d_2^{22} \rho^4 - 84774444782032257024000 B_1^3 X_0^{27} d_2^{21} \rho^5 - 228733637859650720864665 6 B_1^3 X_0^{27} d_2^{20} \rho^6 - 348522131906048650756751 36 B_1^3 X_0^{27} d_2^{19} \rho^7 \\
&- 376802989577267701117616128 B_1^3 X_0^{27} d_2^{18} \rho^8 - 311772890287192398145309900 8 B_1^3 X_0^{27} d_2^{17} \rho^9 - 204807735266902157650705776 64 B_1^3 X_0^{27} d_2^{16} \rho^{10} - 109066470415065330002918637568 B_1^3 X_0^{27} d_2^{15} \rho^{11} \\
&- 476752737266513411894438526976 B_1^3 X_0^{27} d_2^{14} \rho^{12} - 172290899417958998646304066764 8 B_1^3 X_0^{27} d_2^{13} \rho^{13} - 516389909296598725461153729740 8 B_1^3 X_0^{27} d_2^{12} \rho^{14} \\
&- 128320423444091707642446757232 64 B_1^3 X_0^{27} d_2^{11} \rho^{15} - 263330141180079200645901199605 76 B_1^3 X_0^{27} d_2^{10} \rho^{16} - 442562808527781320539976583086 08 B_1^3 X_0^{27} d_2^9 \rho^{17} \\
&- 600361242166991906882350156349 44 B_1^3 X_0^{27} d_2^8 \rho^{18} - 641230542585460047515016746762 24 B_1^3 X_0^{27} d_2^7 \rho^{19} + 626705236743314857750582788096 B_1^7 X_0^{23} d_2^{18} \rho^8 \\
&+ 380062712229040017084197634048 0 B_1^7 X_0^{23} d_2^{17} \rho^9 + 193299125849787216593296891576 32 B_1^7 X_0^{23} d_2^{16} \rho^{10} + 829116100782073040120010726440 96 B_1^7 X_0^{23} d_2^{15} \rho^{11} \\
&+ 300855854659790768576248682643456 B_1^7 X_0^{23} d_2^{14} \rho^{12} + 924344921229693210576999686340608 B_1^7 X_0^{23} d_2^{13} \rho^{13} + 240136865473299029566687814667468 8 B_1^7 X_0^{23} d_2^{12} \rho^{14} \\
&+ 525539634980358142153564984495308 8 B_1^7 X_0^{23} d_2^{11} \rho^{15} + 962460388763846733040660930101248 0 B_1^7 X_0^{23} d_2^{10} \rho^{16} + 145946514822187325972326494681169 92 B_1^7 X_0^{23} d_2^9 \rho^{17} \\
&+ 180238604376308029079230871670620 16 B_1^7 X_0^{23} d_2^8 \rho^{18} + 176446918938856619718922165372846 08 B_1^7 X_0^{23} d_2^7 \rho^{19} + 130349015414677993982564911420538 88 B_1^7 X_0^{23} d_2^6 \rho^{20} \\
&+ 648375120837626421072488342487040 0 B_1^7 X_0^{23} d_2^5 \rho^{21} + 131212499893895434568105473553203 2 B_1^7 X_0^{23} d_2^4 \rho^{22} - 854799580790680820286543924035584 B_1^7 X_0^{23} d_2^3 \rho^{23} \\
&- 854967780102472762641486937325568 B_1^7 X_0^{23} d_2^2 \rho^{24} - 320811170792346239739126500818944 B_1^7 X_0^{23} d_2 \rho^{25} + 790871587542165094400 B_1^6 X_0^{24} d_2^{25} \rho + 330854588867058975375 36 B_1^6 X_0^{24} d_2^{24} \rho^2 \\
&+ 864286020773571974922240 B_1^6 X_0^{24} d_2^{23} \rho^3 + 158938231706237913624739 84 B_1^6 X_0^{24} d_2^{22} \rho^4 + 219502018238578875183398912 B_1^6 X_0^{24} d_2^{21} \rho^5 + 236842935193928693347201843 2 B_1^6 X_0^{24} d_2^{20} \rho^6 \\
&+ 204867491853341139580590488 960 B_1^6 X_0^{24} d_2^{19} \rho^7 + 144517447655298001671441874944 B_1^6 X_0^{24} d_2^{18} \rho^8 + 840732632271797109927945699328 B_1^6 X_0^{24} d_2^{17} \rho^9 + 406010348453821616409142099968 0 B_1^6 X_0^{24} d_2^{16} \rho^{10} \\
&+ 163164939051881226345104728391688 B_1^6 X_0^{24} d_2^{15} \rho^{11} + 544631747450272929024188067348488 B_1^6 X_0^{24} d_2^{14} \rho^{12} + 149847713337254981348378428833792 B_1^6 X_0^{24} d_2^{13} \rho^{13} \\
&+ 334045495765532401622955715461120 B_1^6 X_0^{24} d_2^{12} \rho^{14} + 580966589397219866782114800205824 B_1^6 X_0^{24} d_2^{11} \rho^{15} + 712657795396571667575566692777984 B_1^6 X_0^{24} d_2^{10} \rho^{16} \\
&+ 371259362691453726529665923809280 B_1^6 X_0^{24} d_2^9 \rho^{17} - 778942583153857354933506362310656 B_1^6 X_0^{24} d_2^8 \rho^{18} - 263140407306535586436048712053555 2 B_1^6 X_0^{24} d_2^7 \rho^{19} \\
&- 440329744246227852394912739334553 6 B_1^6 X_0^{24} d_2^6 \rho^{20} - 506677023413758176961128773242060 8 B_1^6 X_0^{24} d_2^5 \rho^{21} - 423731026631460800367010069558067 2 B_1^6 X_0^{24} d_2^4 \rho^{22} \\
&- 255905670426477093490175636825702 4 B_1^6 X_0^{24} d_2^3 \rho^{23} - 106547156100954465973992146180505 6 B_1^6 X_0^{24} d_2^2 \rho^{24} - 274866489375591382460436509097984 B_1^6 X_0^{24} d_2 \rho^{25} + 133159238317832667136 B_1^5 X_0^{25} d_2^{25} \rho \\
&+ 568415277207006268620 8 B_1^5 X_0^{25} d_2^{24} \rho^2 + 148586118195118973386752 B_1^5 X_0^{25} d_2^{23} \rho^3 + 269377077207294017955430 4 B_1^5 X_0^{25} d_2^{22} \rho^4 + 361776731760540321820180 48 B_1^5 X_0^{25} d_2^{21} \rho^5 \\
&+ 374071829273980952362614784 B_1^5 X_0^{25} d_2^{20} \rho^6 + 304574470997060950756530585 6 B_1^5 X_0^{25} d_2^{19} \rho^7 + 197411263675670999750986956800 B_1^5 X_0^{25} d_2^{18} \rho^8 + 101781363210569743400066613248 B_1^5 X_0^{25} d_2^{17} \rho^9 \\
&+ 409950668780249937227072667648 B_1^5 X_0^{25} d_2^{16} \rho^{10} + 121597396291397179565740864307 2 B_1^5 X_0^{25} d_2^{15} \rho^{11} + 210029303852733899342342415974 4 B_1^5 X_0^{25} d_2^{14} \rho^{12} \\
&- 194314331422801476363258272153 6 B_1^5 X_0^{25} d_2^{13} \rho^{13} + 818477882856701750673408 B_1^9 X_0^{21} d_2^{24} \rho^2 + 216906811643274611507855360 B_1^9 X_0^{21} d_2^{23} \rho^3 + 409590385128780825760890880 B_1^9 X_0^{21} d_2^{22} \rho^4 \\
&+ 587044967821023108386730803 2 B_1^9 X_0^{21} d_2^{21} \rho^5 + 664065548394541587081304473 60 B_1^9 X_0^{21} d_2^{20} \rho^6 + 608538485860052691420612395008 B_1^9 X_0^{21} d_2^{19} \rho^7 + 460026402725185184604579744972 88 B_1^9 X_0^{21} d_2^{18} \rho^8 \\
&+ 290599677877923184242561468334088 B_1^9 X_0^{21} d_2^{17} \rho^9 + 154812696077991771144295741915136 B_1^9 X_0^{21} d_2^{16} \rho^{10} + 699967965502286165760247758585856 B_1^9 X_0^{21} d_2^{15} \rho^{11} \\
&+ 269709480134526400689970021295718 4 B_1^9 X_0^{21} d_2^{14} \rho^{12} + 887607116334601308882688284819456 0 B_1^9 X_0^{21} d_2^{13} \rho^{13} + 249612244841655633015887166795939 84 B_1^9 X_0^{21} d_2^{12} \rho^{14} \\
&+ 599136023254296169097725695135580 16 B_1^9 X_0^{21} d_2^{11} \rho^{15} + 122390833095404838891957477399592960 B_1^9 X_0^{21} d_2^{10} \rho^{16} + 211769139263776700017237064568274944 B_1^9 X_0^{21} d_2^9 \rho^{17} \\
&+ 308193141753113576039177847736107008 B_1^9 X_0^{21} d_2^8 \rho^{18} + 373569105299207676678507365020991488 B_1^9 X_0^{21} d_2^7 \rho^{19} + 372077932678146204024814789327847424 B_1^9 X_0^{21} d_2^6 \rho^{20} \\
&+ 298855229227770149935372232359411712 B_1^9 X_0^{21} d_2^5 \rho^{21} + 188475880552032644171326544683204608 B_1^9 X_0^{21} d_2^4 \rho^{22} + 896911303618232605499610132161495 04 B_1^9 X_0^{21} d_2^3 \rho^{23} \\
&+ 302110417663093814263936436970455 04 B_1^9 X_0^{21} d_2^2 \rho^{24} + 640245280850123658758837142080716 8 B_1^9 X_0^{21} d_2 \rho^{25} + 888298516727751245824 0 B_1^8 X_0^{22} d_2^{25} \rho + 369484723504010749804544 B_1^8 X_0^{22} d_2^{24} \rho^2 \\
&+ 972078736100058687812403 2 B_1^8 X_0^{22} d_2^{23} \rho^3 + 181878781213338079399510016 B_1^8 X_0^{22} d_2^{22} \rho^4 + 257856838995889227581882368 0 B_1^8 X_0^{22} d_2^{21} \rho^5 + 288081615270473824612814684 16 B_1^8 X_0^{22} d_2^{20} \rho^6 \\
&+ 260329630660480491603445678080 B_1^8 X_0^{22} d_2^{19} \rho^7 + 193760065391924414736224380518 4 B_1^8 X_0^{22} d_2^{18} \rho^8 + 120308338313123353379857739284488 B_1^8 X_0^{22} d_2^{17} \rho^9 \\
&+ 628837351355009837177570181775368 B_1^8 X_0^{22} d_2^{16} \rho^{10} + 278403381506218919932656661561344 B_1^8 X_0^{22} d_2^{15} \rho^{11} + 104807781967425855432755852292915 2 B_1^8 X_0^{22} d_2^{14} \rho^{12} \\
&+ 336152792366515171818741731793305 6 B_1^8 X_0^{22} d_2^{13} \rho^{13} + 918695445133078759708273810604032 0 B_1^8 X_0^{22} d_2^{12} \rho^{14} + 213603313831182214903837151629148 16 B_1^8 X_0^{22} d_2^{11} \rho^{15} \\
&+ 421075340935390114077649849339084 80 B_1^8 X_0^{22} d_2^{10} \rho^{16} + 699914243175377236231742506968023 04 B_1^8 X_0^{22} d_2^9 \rho^{17} + 973207771746168663201746698874388 48 B_1^8 X_0^{22} d_2^8 \rho^{18} \\
&+ 111947482931027858925652745031516160 B_1^8 X_0^{22} d_2^7 \rho^{19} + 104904227923872140321402345362554880 B_1^8 X_0^{22} d_2^6 \rho^{20} + 783807539664922467797104174605271 04 B_1^8 X_0^{22} d_2^5 \rho^{21} \\
&+ 452749445713873783312746207929958 40 B_1^8 X_0^{22} d_2^4 \rho^{22} + 192989289867408160873880130043248 64 B_1^8 X_0^{22} d_2^3 \rho^{23} + 562740970889545336508942926636646 4 B_1^8 X_0^{22} d_2^2 \rho^{24}
\end{aligned}
$$

$$+ 974765020576242915324899478208512B_1^8X_0^{22}d_2\rho^{25} + 3105173757646759526400B_1^7X_0^{23}d_2^{25}\rho + 1290633907739277624606672B_1^7X_0^{23}d_2^{24}\rho^2 + 337848667614041739152588 8B_1^7X_0^{23}d_2^{23}\rho^3$$
$$+ 626774124278629025647165 44B_1^7X_0^{23}d_2^{22}\rho^4 + 878419510472172297930145792B_1^7X_0^{23}d_2^{21}\rho^5 + 967379031347499920945210982 4B_1^7X_0^{23}d_2^{20}\rho^6 + 859251576399800230652726476 80B_1^7X_0^{23}d_2^{19}\rho^7$$
$$+ 238792538060172555657811387821431193 6B_1^{12}X_0^{18}d_2^5\rho^{21} + 163819294704885894978184876815653273 6B_1^{12}X_0^{18}d_2^4\rho^{22} + 85385445664265745622095235478506700 8B_1^{12}X_0^{18}d_2^3\rho^{23}$$
$$+ 317581254773735552716753532463611904B_1^{12}X_0^{18}d_2^2\rho^{24} + 750527367497545625249056947846512 64B_1^{12}X_0^{18}d_2\rho^{25} + 496493276063384731648000B_1^{11}X_0^{19}d_2^{25}\rho + 211059236840732705895219 2B_1^{11}X_0^{19}d_2^{24}\rho^2$$
$$+ 570032655411727911249510 40B_1^{11}X_0^{19}d_2^{23}\rho^3 + 109892360018421141266549964 8B_1^{11}X_0^{19}d_2^{22}\rho^4 + 161043300466630358114857123 84B_1^{11}X_0^{19}d_2^{21}\rho^5 + 186528278626602254521046401024 B_1^{11}X_0^{19}d_2^{20}\rho^6$$
$$+ 175256999565869707232055708876 8B_1^{11}X_0^{19}d_2^{19}\rho^7 + 136026694125947468892942043709 44B_1^{11}X_0^{19}d_2^{18}\rho^8 + 883528131086440121153209247989 76B_1^{11}X_0^{19}d_2^{17}\rho^9$$
$$+ 484718136765151601616501325430784B_1^{11}X_0^{19}d_2^{16}\rho^{10} + 226071584081095850985109060161 39936B_1^{11}X_0^{19}d_2^{15}\rho^{11} + 900199138888394308409224580405657 6B_1^{11}X_0^{19}d_2^{14}\rho^{12}$$
$$+ 306757648798988549567999071643238 40B_1^{11}X_0^{19}d_2^{13}\rho^{13} + 895169362713778328385132740361584 64B_1^{11}X_0^{19}d_2^{12}\rho^{14} + 223483071794936313228416396457672704B_1^{11}X_0^{19}d_2^{11}\rho^{15}$$
$$+ 476054218726675849627610167570857984B_1^{11}X_0^{19}d_2^{10}\rho^{16} + 861340127558197871814638376901935104B_1^{11}X_0^{19}d_2^9\rho^{17} + 131487064548044017562217039714582528 0B_1^{11}X_0^{19}d_2^8\rho^{18}$$
$$+ 167755507996112504483683741429294694 4B_1^{11}X_0^{19}d_2^7\rho^{19} + 176552355698687920776720380408417484 8B_1^{11}X_0^{19}d_2^6\rho^{20} + 150508591925467246876508986517802188 8B_1^{11}X_0^{19}d_2^5\rho^{21}$$
$$+ 101262734618849862801466669375737036 8B_1^{11}X_0^{19}d_2^4\rho^{22} + 517209799018856072930786736032710656B_1^{11}X_0^{19}d_2^3\rho^{23} + 188348832562108713035158827451809792B_1^{11}X_0^{19}d_2^2\rho^{24}$$
$$+ 435405626614194595179721817849856 00B_1^{11}X_0^{19}d_2\rho^{25} + 344678282439906715238 40B_1^{10}X_0^{20}d_2^{25}\rho + 145171064277377536858521 6B_1^{10}X_0^{20}d_2^{24}\rho^2 + 388158957526976125112156 16B_1^{10}X_0^{20}d_2^{23}\rho^3$$
$$+ 740338406660275135756369920B_1^{10}X_0^{20}d_2^{22}\rho^4 + 107279153887243291870762106 88B_1^{10}X_0^{20}d_2^{21}\rho^5 + 122801971869349191304237547520B_1^{10}X_0^{20}d_2^{20}\rho^6 + 113974998210048953653285040947 2B_1^{10}X_0^{20}d_2^{19}\rho^7$$
$$+ 873402747476142495898048187596 8B_1^{10}X_0^{20}d_2^{18}\rho^8 + 559807760842239693303635226132 48B_1^{10}X_0^{20}d_2^{17}\rho^9 + 302894745735741169377931335565312B_1^{10}X_0^{20}d_2^{16}\rho^{10}$$
$$+ 139241434253425872710783879820083 2B_1^{10}X_0^{20}d_2^{15}\rho^{11} + 546129088337404045717502326472704 0B_1^{10}X_0^{20}d_2^{14}\rho^{12} + 183179631909221304287218687782420 48B_1^{10}X_0^{20}d_2^{13}\rho^{13}$$
$$+ 525749242730039765780450098093752 32B_1^{10}X_0^{20}d_2^{12}\rho^{14} + 128988531751291449528418563509977088B_1^{10}X_0^{20}d_2^{11}\rho^{15} + 269780560340003500304666024690581504B_1^{10}X_0^{20}d_2^{10}\rho^{16}$$
$$+ 478809467114081785640063321432391680B_1^{10}X_0^{20}d_2^9\rho^{17} + 716240944815022252474441702779650048B_1^{10}X_0^{20}d_2^8\rho^{18} + 894456111331193272340598584030265344B_1^{10}X_0^{20}d_2^7\rho^{19}$$
$$+ 920317735150538231178950956636176384B_1^{10}X_0^{20}d_2^6\rho^{20} + 766008115966408291750574080072351744B_1^{10}X_0^{20}d_2^5\rho^{21} + 502452273998435029745213671068401664B_1^{10}X_0^{20}d_2^4\rho^{22}$$
$$+ 249790744129298777185630582111993856B_1^{10}X_0^{20}d_2^3\rho^{23} + 883765343479812624137992830336368 64B_1^{10}X_0^{20}d_2^2\rho^{24} + 198069916846369332746181047589273 60B_1^{10}X_0^{20}d_2\rho^{25}$$
$$+ 195804959682031989555520B_1^9X_0^{21}d_2^{25}\rho + 393340087758057041993051207542767616B_1^{14}X_0^{16}d_2^{11}\rho^{15} + 874608660032116124153070758393806848B_1^{14}X_0^{16}d_2^{10}\rho^{16}$$
$$+ 165364404150738491790274692179715686 4B_1^{14}X_0^{16}d_2^9\rho^{17} + 264098904658557623574340990970049331 2B_1^{14}X_0^{16}d_2^8\rho^{18} + 352948997691469438766191904206041907 2B_1^{14}X_0^{16}d_2^7\rho^{19}$$
$$+ 389605274837898396426455345506182758 4B_1^{14}X_0^{16}d_2^6\rho^{20} + 348837834314040819419867350029251379 2B_1^{14}X_0^{16}d_2^5\rho^{21} + 246859782558613886027852130286777139 2B_1^{14}X_0^{16}d_2^4\rho^{22}$$
$$+ 132821850981478491714217395692450611 2B_1^{14}X_0^{16}d_2^3\rho^{23} + 510355675826814863769812212320829440B_1^{14}X_0^{16}d_2^2\rho^{24} + 124699513076252064267889692584706048B_1^{14}X_0^{16}d_2\rho^{25}$$
$$+ 601900743683037619814404B_1^{13}X_0^{17}d_2^{25}\rho + 261461244469069994577100 8B_1^{13}X_0^{17}d_2^{24}\rho^2 + 722131980810327379662602 24B_1^{13}X_0^{17}d_2^{23}\rho^3 + 142447390947962269682059392B_1^{13}X_0^{17}d_2^{22}\rho^4$$
$$+ 213703448545632994433151795 20B_1^{13}X_0^{17}d_2^{21}\rho^5 + 253501831358699379147727962112B_1^{13}X_0^{17}d_2^{20}\rho^6 + 244036367536820319847084143411 2B_1^{13}X_0^{17}d_2^{19}\rho^7$$
$$+ 194143765455091290731056694558 72B_1^{13}X_0^{17}d_2^{18}\rho^8 + 129309100636190788955281338007552B_1^{13}X_0^{17}d_2^{17}\rho^9 + 727805998288318399726468053860352B_1^{13}X_0^{17}d_2^{16}\rho^{10}$$
$$+ 348435040055471499626894375505100 8B_1^{13}X_0^{17}d_2^{15}\rho^{11} + 142502309440529407967178909532815 36B_1^{13}X_0^{17}d_2^{14}\rho^{12} + 499081231288498809955924407961518 08B_1^{13}X_0^{17}d_2^{13}\rho^{13}$$
$$+ 149790930724364056089045040537534464B_1^{13}X_0^{17}d_2^{12}\rho^{14} + 384917227692821694409183939325329408B_1^{13}X_0^{17}d_2^{11}\rho^{15} + 844664653988603225985491099520598016B_1^{13}X_0^{17}d_2^{10}\rho^{16}$$
$$+ 157577547137984894607516374330140262 4B_1^{13}X_0^{17}d_2^9\rho^{17} + 248258501605470465061866887094206464 0B_1^{13}X_0^{17}d_2^8\rho^{18} + 327214168000838863020575571738781286 4B_1^{13}X_0^{17}d_2^7\rho^{19}$$
$$+ 356139071939470219664025970181511577 6B_1^{13}X_0^{17}d_2^6\rho^{20} + 314325967202689944767559798553051136 0B_1^{13}X_0^{17}d_2^5\rho^{21} + 219205651650243347190878504144286515 2B_1^{13}X_0^{17}d_2^4\rho^{22}$$
$$+ 116196839747080303494057073852389785 60B_1^{13}X_0^{17}d_2^3\rho^{23} + 439739632740975936986371787644207104B_1^{13}X_0^{17}d_2^2\rho^{24} + 105792632871833802468085914113409024B_1^{13}X_0^{17}d_2\rho^{25}$$
$$+ 595407822246775881728008B_1^{12}X_0^{18}d_2^{25}\rho + 255758361189125093484134 4B_1^{12}X_0^{18}d_2^{24}\rho^2 + 698316118459046420241448968B_1^{12}X_0^{18}d_2^{23}\rho^3 + 136147731106154812981431500 8B_1^{12}X_0^{18}d_2^{22}\rho^4$$
$$+ 201843197920666870342656983048B_1^{12}X_0^{18}d_2^{21}\rho^5 + 236574487415943986591819890688B_1^{12}X_0^{18}d_2^{20}\rho^6 + 224992437387137153439071705497 6B_1^{12}X_0^{18}d_2^{19}\rho^7$$
$$+ 176809315289498969686866343215104B_1^{12}X_0^{18}d_2^{18}\rho^8 + 116309726800238124634151089864704B_1^{12}X_0^{18}d_2^{17}\rho^9 + 646452719531440495031674977124352B_1^{12}X_0^{18}d_2^{16}\rho^{10}$$
$$+ 305559647759253225383996936211660 8B_1^{12}X_0^{18}d_2^{15}\rho^{11} + 123354981482143409140194893071646 72B_1^{12}X_0^{18}d_2^{14}\rho^{12} + 426346301867707785996348061384704 00B_1^{12}X_0^{18}d_2^{13}\rho^{13}$$
$$+ 126245977273699580641260838351536128B_1^{12}X_0^{18}d_2^{12}\rho^{14} + 319973050582757215114474296082169856B_1^{12}X_0^{18}d_2^{11}\rho^{15} + 692320757230509014528310969674760192B_1^{12}X_0^{18}d_2^{10}\rho^{16}$$
$$+ 127305683619331913406279125026891366 4B_1^{12}X_0^{18}d_2^9\rho^{17} + 197620806449145522642999196832602521 6B_1^{12}X_0^{18}d_2^8\rho^{18} + 256550063714185936796201357152354034 0B_1^{12}X_0^{18}d_2^7\rho^{19}$$
$$+ 274915742291080829231249238191295692 8B_1^{12}X_0^{18}d_2^6\rho^{20} + 694735811784598071279017959096 32B_1^{16}X_0^{14}d_2^{17}\rho^9 + 405717094173087087373517104807936B_1^{16}X_0^{14}d_2^{16}\rho^{10}$$
$$+ 201546792299628366600640879366963 2B_1^{16}X_0^{14}d_2^{15}\rho^{11} + 855407586161579822592243633989222 4B_1^{16}X_0^{14}d_2^{14}\rho^{12} + 310952375831278190076435924058112 00B_1^{16}X_0^{14}d_2^{13}\rho^{13}$$
$$+ 968898466944889660937234022591365 12B_1^{16}X_0^{14}d_2^{12}\rho^{14} + 258554927526222433604917184075137024B_1^{16}X_0^{14}d_2^{11}\rho^{15} + 589396856573694528145759394175385600B_1^{16}X_0^{14}d_2^{10}\rho^{16}$$
$$+ 114267308610628472860739023578700185 6B_1^{16}X_0^{14}d_2^9\rho^{17} + 187163323607701034052088221490007244 8B_1^{16}X_0^{14}d_2^8\rho^{18} + 256589444464751467296186102618836172 8B_1^{16}X_0^{14}d_2^7\rho^{19}$$
$$+ 290624038476447221013342509656650547 2B_1^{16}X_0^{14}d_2^6\rho^{20} + 267069621758934490999556020960336281 6B_1^{16}X_0^{14}d_2^5\rho^{21} + 194028483407188544827111701874572436 8B_1^{16}X_0^{14}d_2^4\rho^{22}$$
$$+ 107207046322637783238099575086723891 2B_1^{16}X_0^{14}d_2^3\rho^{23} + 423148741737321541122802117546868736B_1^{16}X_0^{14}d_2^2\rho^{24} + 106238284831126521119706177104510976B_1^{16}X_0^{14}d_2\rho^{25}$$
$$+ 380941140543498774118408B_1^{15}X_0^{15}d_2^{25}\rho + 169478194291593532617523 2B_1^{15}X_0^{15}d_2^{24}\rho^2 + 479518333172881857309573 12B_1^{15}X_0^{15}d_2^{23}\rho^3 + 969162064232764430001111040B_1^{15}X_0^{15}d_2^{22}\rho^4$$
$$+ 148987713210094372707589160 96B_1^{15}X_0^{15}d_2^{21}\rho^5 + 181110174887112607446962012160B_1^{15}X_0^{15}d_2^{20}\rho^6 + 178671637585542015298978263859 2B_1^{15}X_0^{15}d_2^{19}\rho^7$$

$$+ 14567284583391338280231583875072B_1^{15}X_0^{15}d_2^{18}\rho^8 + 9943923938154035597376018212454 4B_1^{15}X_0^{15}d_2^{17}\rho^9 + 57365015825284979873300636709683 2B_1^{15}X_0^{15}d_2^{16}\rho^{10}$$

$$+ 28151327097770944594890507907563 52B_1^{15}X_0^{15}d_2^{15}\rho^{11} + 11803296033319173240468746502799360B_1^{15}X_0^{15}d_2^{14}\rho^{12} + 42387037437493082651539526869057536B_1^{15}X_0^{15}d_2^{13}\rho^{13}$$

$$+ 13047323981234308852988919459033907 2B_1^{15}X_0^{15}d_2^{12}\rho^{14} + 34394432339579596162500353357 4074864B_1^{15}X_0^{15}d_2^{11}\rho^{15} + 77449172653503369097427539437027328 0B_1^{15}X_0^{15}d_2^{10}\rho^{16}$$

$$+ 14831321823468154749444813829124915 20B_1^{15}X_0^{15}d_2^{9}\rho^{17} + 23993693728249059342540259406727086 08B_1^{15}X_0^{15}d_2^{8}\rho^{18} + 32486155738480714417270731894413066 24B_1^{15}X_0^{15}d_2^{7}\rho^{19}$$

$$+ 36335801317900152401576607256076615 68B_1^{15}X_0^{15}d_2^{6}\rho^{20} + 32970724301879153099257059232773570 56B_1^{15}X_0^{15}d_2^{5}\rho^{21} + 23649653211161620990676678294162636 80B_1^{15}X_0^{15}d_2^{4}\rho^{22}$$

$$+ 12900024766695443880192236190947082 24B_1^{15}X_0^{15}d_2^{3}\rho^{23} + 50259672244587938659307975900292710 4B_1^{15}X_0^{15}d_2^{2}\rho^{24} + 12454260845290231592400180871377715 2B_1^{15}X_0^{15}d_2\rho^{25}$$

$$+ 51754933159688950251520B_1^{14}X_0^{16}d_2^{25}\rho + 22747769195613571524853 76B_1^{14}X_0^{16}d_2^{24}\rho^2 + 63580264202993419542331392B_1^{14}X_0^{16}d_2^{23}\rho^3 + 12693559367590214693362073 60B_1^{14}X_0^{16}d_2^{22}\rho^4$$

$$+ 19275146026590076447834046464B_1^{14}X_0^{16}d_2^{21}\rho^5 + 23144568658658151452274 2947840B_1^{14}X_0^{16}d_2^{20}\rho^6 + 22554043728299401100995598745 60B_1^{14}X_0^{16}d_2^{19}\rho^7$$

$$+ 18164140113260456095452469919744B_1^{14}X_0^{16}d_2^{18}\rho^8 + 12247988293235523671278667359846 4B_1^{14}X_0^{16}d_2^{17}\rho^9 + 69794970160691920466428746131046 4B_1^{14}X_0^{16}d_2^{16}\rho^{10}$$

$$+ 33832915134244298606460175137505 28B_1^{14}X_0^{16}d_2^{15}\rho^{11} + 14011796202308502353527998646976512B_1^{14}X_0^{16}d_2^{14}\rho^{12} + 49699517155933938581199028051771392B_1^{14}X_0^{16}d_2^{13}\rho^{13}$$

$$+ 15109138905955236059581761931024793 6B_1^{14}X_0^{16}d_2^{12}\rho^{14} + 83866593398336389236654 08B_1^{18}X_0^{12}d_2^{23}\rho^3 + 17601411065080463670904422 4B_1^{18}X_0^{12}d_2^{22}\rho^4 + 28095338509884814279975321 60B_1^{18}X_0^{12}d_2^{21}\rho^5$$

$$+ 35456938717218257583636455424B_1^{18}X_0^{12}d_2^{20}\rho^6 + 36308985886291326611714825 4208B_1^{18}X_0^{12}d_2^{19}\rho^7 + 30722283459278562656524779192 32B_1^{18}X_0^{12}d_2^{18}\rho^8$$

$$+ 21760184153347131778105847709696B_1^{18}X_0^{12}d_2^{17}\rho^9 + 13022617061177192110895394776678 4B_1^{18}X_0^{12}d_2^{16}\rho^{10} + 66285839962853533453494858240409 6B_1^{18}X_0^{12}d_2^{15}\rho^{11}$$

$$+ 28822524866234313526677349905776 64B_1^{18}X_0^{12}d_2^{14}\rho^{12} + 10732954113359799095765479065468928B_1^{18}X_0^{12}d_2^{13}\rho^{13} + 34255645947391208320311185455939584B_1^{18}X_0^{12}d_2^{12}\rho^{14}$$

$$+ 93628400081281657664074648076812288B_1^{18}X_0^{12}d_2^{11}\rho^{15} + 21859812948451369072778296221394534 4B_1^{18}X_0^{12}d_2^{10}\rho^{16} + 43404794188099231897053780958406246 4B_1^{18}X_0^{12}d_2^{9}\rho^{17}$$

$$+ 72814246708643263420900453093736448 0B_1^{18}X_0^{12}d_2^{8}\rho^{18} + 10224115037389747238791813187596451 84B_1^{18}X_0^{12}d_2^{7}\rho^{19} + 11861197570352672957193621832571289 60B_1^{18}X_0^{12}d_2^{6}\rho^{20}$$

$$+ 11164933874961766161182689288047820 80B_1^{18}X_0^{12}d_2^{5}\rho^{21} + 83092275491639417455769184379915468 8B_1^{18}X_0^{12}d_2^{4}\rho^{22} + 47034158929279738137004643270944358 4B_1^{18}X_0^{12}d_2^{3}\rho^{23}$$

$$+ 19019984529119262042874832334146764 8B_1^{18}X_0^{12}d_2^{2}\rho^{24} + 48927873361868717111917108449509376B_1^{18}X_0^{12}d_2\rho^{25} + 13142134086009723289600B_1^{17}X_0^{13}d_2^{25}\rho + 59945643067814909365452 8B_1^{17}X_0^{13}d_2^{24}\rho^2$$

$$+ 17390624227228436624310272B_1^{17}X_0^{13}d_2^{23}\rho^3 + 36039278913788581781445017 6B_1^{17}X_0^{13}d_2^{22}\rho^4 + 56804413603904483335762247 68B_1^{17}X_0^{13}d_2^{21}\rho^5 + 70793397163647616415254020096B_1^{17}X_0^{13}d_2^{20}\rho^6$$

$$+ 71594497463182803147480008294 4B_1^{17}X_0^{13}d_2^{19}\rho^7 + 59831131405082712906312975646 72B_1^{17}X_0^{13}d_2^{18}\rho^8 + 41858216189366405192558518337536B_1^{17}X_0^{13}d_2^{17}\rho^9$$

$$+ 24745567283166156895116982943744 0B_1^{17}X_0^{13}d_2^{16}\rho^{10} + 12443320925600509084702892293242 88B_1^{17}X_0^{13}d_2^{15}\rho^{11} + 53456056966422945224040747426111968B_1^{17}X_0^{13}d_2^{14}\rho^{12}$$

$$+ 19668129787792396358724090412302336B_1^{17}X_0^{13}d_2^{13}\rho^{13} + 62026921874242383947244139852464128B_1^{17}X_0^{13}d_2^{12}\rho^{14} + 16752542560045647582885527843320627 2B_1^{17}X_0^{13}d_2^{11}\rho^{15}$$

$$+ 38650990872847805538723308005805260 8B_1^{17}X_0^{13}d_2^{10}\rho^{16} + 75841031683601040016098991992628838 4B_1^{17}X_0^{13}d_2^{9}\rho^{17} + 12573090599631338261221563650979921 92B_1^{17}X_0^{13}d_2^{8}\rho^{18}$$

$$+ 17446702398569588807469444032637173 76B_1^{17}X_0^{13}d_2^{7}\rho^{19} + 20002185830482732275350011373420544 00B_1^{17}X_0^{13}d_2^{6}\rho^{20} + 18606427014172348250285159281443471 36B_1^{17}X_0^{13}d_2^{5}\rho^{21}$$

$$+ 13684220988285543248691774121700229 12B_1^{17}X_0^{13}d_2^{4}\rho^{22} + 76545390093267130861571251456337510 4B_1^{17}X_0^{13}d_2^{3}\rho^{23} + 30588315742277880809275773297465753 6B_1^{17}X_0^{13}d_2^{2}\rho^{24}$$

$$+ 77756351129945546161052490242457600B_1^{17}X_0^{13}d_2\rho^{25} + 24103548375914879385600B_1^{16}X_0^{14}d_2^{25}\rho + 10857200413780036382883 84B_1^{16}X_0^{14}d_2^{24}\rho^2 + 31103602496100615745699840B_1^{16}X_0^{14}d_2^{23}\rho^3$$

$$+ 63651643054370880914659737 6B_1^{16}X_0^{14}d_2^{22}\rho^4 + 99075564410296470358679879 68B_1^{16}X_0^{14}d_2^{21}\rho^5 + 12194077516833291336526171340 8B_1^{16}X_0^{14}d_2^{20}\rho^6 + 12179621100111517985516448645 12B_1^{16}X_0^{14}d_2^{19}\rho^7$$

$$+ 10053299372992674716593085153280B_1^{16}X_0^{14}d_2^{18}\rho^8 + 74743629003277368676732488250294272B_1^{21}X_0^{9}d_2^{4}\rho^{22} + 43761596425203102873825041530748928B_1^{21}X_0^{9}d_2^{3}\rho^{23}$$

$$+ 18300682568205904476137382979043328B_1^{21}X_0^{9}d_2^{2}\rho^{24} + 48673400772749126855185923424911 36B_1^{21}X_0^{9}d_2\rho^{25} + 87150343318999662592 0B_1^{20}X_0^{10}d_2^{25}\rho + 41297049722811426013184B_1^{20}X_0^{10}d_2^{24}\rho^2$$

$$+ 12446366294968478355619 84B_1^{20}X_0^{10}d_2^{23}\rho^3 + 26794504593099037740830720B_1^{20}X_0^{10}d_2^{22}\rho^4 + 43867480377787801566194483 2B_1^{20}X_0^{10}d_2^{21}\rho^5 + 56776687679768102488715776 00B_1^{20}X_0^{10}d_2^{20}\rho^6$$

$$+ 59618500037213463848671877120B_1^{20}X_0^{10}d_2^{19}\rho^7 + 51718583335870187789109608857 6B_1^{20}X_0^{10}d_2^{18}\rho^8 + 37549420478007058595345173053 44B_1^{20}X_0^{10}d_2^{17}\rho^9$$

$$+ 23030525264015294852545724078080B_1^{20}X_0^{10}d_2^{16}\rho^{10} + 12011774551708791127206813986304 0B_1^{20}X_0^{10}d_2^{15}\rho^{11} + 53507671454740844139709078153011 2B_1^{20}X_0^{10}d_2^{14}\rho^{12}$$

$$+ 20408941399227979715009434201047 04B_1^{20}X_0^{10}d_2^{13}\rho^{13} + 66707457501897915460526594102394 88B_1^{20}X_0^{10}d_2^{12}\rho^{14} + 18668957671816148930994472055537664B_1^{20}X_0^{10}d_2^{11}\rho^{15}$$

$$+ 44623579145697302064570760796176384B_1^{20}X_0^{10}d_2^{10}\rho^{16} + 90699030988563690279201449867476992B_1^{20}X_0^{10}d_2^{9}\rho^{17} + 15573127445545607586182228950804070 4B_1^{20}X_0^{10}d_2^{8}\rho^{18}$$

$$+ 22378590960956018756639410710852403 2B_1^{20}X_0^{10}d_2^{7}\rho^{19} + 26566882129287452246885867432234188 8B_1^{20}X_0^{10}d_2^{6}\rho^{20} + 25587858921823896473900399746822963 2B_1^{20}X_0^{10}d_2^{5}\rho^{21}$$

$$+ 19483477638417457866676756493107200 0B_1^{20}X_0^{10}d_2^{4}\rho^{22} + 11282600178767732514670996636041216 0B_1^{20}X_0^{10}d_2^{3}\rho^{23} + 46671890745104112306793948410544128B_1^{20}X_0^{10}d_2^{2}\rho^{24}$$

$$+ 12280199557465310624799390645092352B_1^{20}X_0^{10}d_2\rho^{25} + 25032590784077601177 60B_1^{19}X_0^{11}d_2^{25}\rho + 11711778423065860059955 2B_1^{19}X_0^{11}d_2^{24}\rho^2 + 34850724681853594716733 44B_1^{19}X_0^{11}d_2^{23}\rho^3$$

$$+ 74077856893970750514954240B_1^{19}X_0^{11}d_2^{22}\rho^4 + 11975001617754424316486369 28B_1^{19}X_0^{11}d_2^{21}\rho^5 + 15304443264851347085106462720B_1^{19}X_0^{11}d_2^{20}\rho^6 + 15869888676673309038716867788 8B_1^{19}X_0^{11}d_2^{19}\rho^7$$

$$+ 13596297234578281474336007946 24B_1^{19}X_0^{11}d_2^{18}\rho^8 + 97498533346745715566900002160 64B_1^{19}X_0^{11}d_2^{17}\rho^9 + 59069272037706085531004060844032B_1^{19}X_0^{11}d_2^{16}\rho^{10}$$

$$+ 30434859062883921735194314469580 8B_1^{19}X_0^{11}d_2^{15}\rho^{11} + 13394612447463239763868008725626 88B_1^{19}X_0^{11}d_2^{14}\rho^{12} + 50480944596968321143605623966760 96B_1^{19}X_0^{11}d_2^{13}\rho^{13}$$

$$+ 16304809227582422369417192175566848B_1^{19}X_0^{11}d_2^{12}\rho^{14} + 45095703062958182060194955883839488B_1^{19}X_0^{11}d_2^{11}\rho^{15} + 10653450351271337735891713245524787 2B_1^{19}X_0^{11}d_2^{10}\rho^{16}$$

$$+ 21402959786614384783187128811310284 8B_1^{19}X_0^{11}d_2^{9}\rho^{17} + 36326568120896184978594296102702288 4B_1^{19}X_0^{11}d_2^{8}\rho^{18} + 51604604095725173613163735535950233 6B_1^{19}X_0^{11}d_2^{7}\rho^{19}$$

$$+ 60566372401600386410571277658593689 6B_1^{19}X_0^{11}d_2^{6}\rho^{20} + 57674940110295114722491838603722752 00B_1^{19}X_0^{11}d_2^{5}\rho^{21} + 43421876686379558467937320392720384 0B_1^{19}X_0^{11}d_2^{4}\rho^{22}$$

$$+ 24863805210468006483390901956221337 6B_1^{19}X_0^{11}d_2^{3}\rho^{23} + 10170898378724176073760675996260438 4B_1^{19}X_0^{11}d_2^{2}\rho^{24} + 26465938653853257431535800429838336B_1^{19}X_0^{11}d_2\rho^{25}$$

$$+ 61792321242617033523 20B_1^{18}X_0^{12}d_2^{25}\rho + 28544782488375901657497 6B_1^{18}X_0^{12}d_2^{24}\rho^2 + 12493196538751467927946012873195 52B_1^{23}X_0^{7}d_2^{10}\rho^{16} + 26287802291209761439084235536465 92B_1^{23}X_0^{7}d_2^{9}\rho^{17}$$

$$+ 467106912779963069502298504455782 4B_1^{23}X_0^7d_2^8\rho^{18} + 69439363157721063101208743187578 88B_1^{23}X_0^7d_2^7\rho^{19} + 85248248490104130807917729997127 68B_1^{23}X_0^7d_2^6\rho^{20}$$

$$+ 84875673935304803907196447862292 48B_1^{23}X_0^7d_2^5\rho^{21} + 66779412674265554071505805697351 68B_1^{23}X_0^7d_2^4\rho^{22} + 39941122483243763384922794297917 44B_1^{23}X_0^7d_2^3\rho^{23}$$

$$+ 17056505314883842127777147199160 32B_1^{23}X_0^7d_2^2\rho^{24} + 46304856397548554502049502330880 0B_1^{23}X_0^7d_2\rho^{25} + 65727358762799923200B_1^{22}X_0^8d_2^{25}\rho + 31947636670055387381 76B_1^{22}X_0^8d_2^{24}\rho^2$$

$$+ 98767248772034183880704B_1^{22}X_0^8d_2^{23}\rho^3 + 21810075231512663863326 72B_1^{22}X_0^8d_2^{22}\rho^4 + 36624284702745060082919936B_1^{22}X_0^8d_2^{21}\rho^5 + 48615034686148431784852019 2B_1^{22}X_0^8d_2^{20}\rho^6$$

$$+ 52348171533117890236258181 12B_1^{22}X_0^8d_2^{19}\rho^7 + 46560911930345028795734607872B_1^{22}X_0^8d_2^{18}\rho^8 + 34654328924552173881994724300 8B_1^{22}X_0^8d_2^{17}\rho^9 + 21784870810090989186930687185 92B_1^{22}X_0^8d_2^{16}\rho^{10}$$

$$+ 11643057829255535122226810717440B_1^{22}X_0^8d_2^{15}\rho^{11} + 53136457974708950118308674714112B_1^{22}X_0^8d_2^{14}\rho^{12} + 20759612707995542224948990956032 0B_1^{22}X_0^8d_2^{13}\rho^{13}$$

$$+ 69486402368678841618778721928601 6B_1^{22}X_0^8d_2^{12}\rho^{14} + 19910240637662844015125302925885 44B_1^{22}X_0^8d_2^{11}\rho^{15} + 48714324099495542463300166557040 64B_1^{22}X_0^8d_2^{10}\rho^{16}$$

$$+ 10132961445752319265684839477673984B_1^{22}X_0^8d_2^9\rho^{17} + 17801529097912657268067225928728576B_1^{22}X_0^8d_2^8\rho^{18} + 26167865071374262571151603801784320B_1^{22}X_0^8d_2^7\rho^{19}$$

$$+ 31771350484246205183576780864225280B_1^{22}X_0^8d_2^6\rho^{20} + 31288997908782698957299004139896832B_1^{22}X_0^8d_2^5\rho^{21} + 24354856800687763984902529304494080B_1^{22}X_0^8d_2^4\rho^{22}$$

$$+ 14413906363974069130145270650109952B_1^{22}X_0^8d_2^3\rho^{23} + 60920503840864031634503680131070200B_1^{22}X_0^8d_2^2\rho^{24} + 16372608586188130061849826730967 04B_1^{22}X_0^8d_2\rho^{25}$$

$$+ 25960076070672465920 0B_1^{21}X_0^9d_2^{25}\rho + 12459031795538888491008B_1^{21}X_0^9d_2^{24}\rho^2 + 38031127532319362670592 0B_1^{21}X_0^9d_2^{23}\rho^3 + 82921576355688651255685 12B_1^{21}X_0^9d_2^{22}\rho^4$$

$$+ 13749128201048288542968729 6B_1^{21}X_0^9d_2^{21}\rho^5 + 18021507386042153678909173 76B_1^{21}X_0^9d_2^{20}\rho^6 + 19162937267923475475222992896B_1^{21}X_0^9d_2^{19}\rho^7 + 16832688353845956532135630438 4B_1^{21}X_0^9d_2^{18}\rho^8$$

$$+ 12373636147414361808647875491 84B_1^{21}X_0^9d_2^{17}\rho^9 + 76832190565964099517930336890 88B_1^{21}X_0^9d_2^{16}\rho^{10} + 40564627300779132608739306765824B_1^{21}X_0^9d_2^{15}\rho^{11}$$

$$+ 18289910593992361982418748500377 6B_1^{21}X_0^9d_2^{14}\rho^{12} + 70603286222762285436160466320793 6B_1^{21}X_0^9d_2^{13}\rho^{13} + 23352938920259526670994844493168 64B_1^{21}X_0^9d_2^{12}\rho^{14}$$

$$+ 66130895711587220575422761446932 48B_1^{21}X_0^9d_2^{11}\rho^{15} + 15992684641533757778375429460066304B_1^{21}X_0^9d_2^{10}\rho^{16} + 32884320732109969362651443990626304B_1^{21}X_0^9d_2^9\rho^{17}$$

$$+ 57114851892207770064198165162098688B_1^{21}X_0^9d_2^8\rho^{18} + 83014039257614446942111974099517440B_1^{21}X_0^9d_2^7\rho^{19} + 99669894603366260994320827479490560B_1^{21}X_0^9d_2^6\rho^{20}$$

$$+ 97077974949003893931814617310298112B_1^{21}X_0^9d_2^5\rho^{21} + 16696593884441033189583658880B_1^{25}X_0^5d_2^{16}\rho^{10} + 92574262118202745850181555424B_1^{25}X_0^5d_2^{15}\rho^{11}$$

$$+ 43816122408012206118176239411 2B_1^{25}X_0^5d_2^{14}\rho^{12} + 17747388799174863289430216794888B_1^{25}X_0^5d_2^{13}\rho^{13} + 61564920735779388356418909824008B_1^{25}X_0^5d_2^{12}\rho^{14}$$

$$+ 18275181960131726143639180772352B_1^{25}X_0^5d_2^{11}\rho^{15} + 46303721224513840414484179476480B_1^{25}X_0^5d_2^{10}\rho^{16} + 99696544033167006318173687390208B_1^{25}X_0^5d_2^9\rho^{17}$$

$$+ 18121026188754625869561309570662 4B_1^{25}X_0^5d_2^8\rho^{18} + 27545925771252914385664292585472 0B_1^{25}X_0^5d_2^7\rho^{19} + 34566197036323303841107509352857 6B_1^{25}X_0^5d_2^6\rho^{20}$$

$$+ 35162098584064868052205720 6726656B_1^{25}X_0^5d_2^5\rho^{21} + 28251907610636471013427836141 4484 8B_1^{25}X_0^5d_2^4\rho^{22} + 17246424857331449199558943309824 0B_1^{25}X_0^5d_2^3\rho^{23}$$

$$+ 75122024081045665084225703903232B_1^{25}X_0^5d_2^2\rho^{24} + 20786571688653929198031690792960B_1^{25}X_0^5d_2\rho^{25} + 24832094525957734 40B_1^{24}X_0^6d_2^{25}\rho + 12378360169516521062 4B_1^{24}X_0^6d_2^{24}\rho^2$$

$$+ 39247604723208511457 28B_1^{24}X_0^6d_2^{23}\rho^3 + 88886593419407841988480B_1^{24}X_0^6d_2^{22}\rho^4 + 15307886001028974100981 76B_1^{24}X_0^6d_2^{21}\rho^5 + 20838067421279481553206720B_1^{24}X_0^6d_2^{20}\rho^6$$

$$+ 23008566455029356669388147 2B_1^{24}X_0^6d_2^{19}\rho^7 + 20982577002685987515586425 60B_1^{24}X_0^6d_2^{18}\rho^8 + 16009619955668973155936834560B_1^{24}X_0^6d_2^{17}\rho^9 + 10315528920701418581105119539 2B_1^{24}X_0^6d_2^{16}\rho^{10}$$

$$+ 56498171736477167358806285344 0B_1^{24}X_0^6d_2^{15}\rho^{11} + 26418046117265175108779040469 76B_1^{24}X_0^6d_2^{14}\rho^{12} + 10572336901849002025528835223552B_1^{24}X_0^6d_2^{13}\rho^{13}$$

$$+ 36240301806787949793799139877888B_1^{24}X_0^6d_2^{12}\rho^{14} + 10631619352111895036585217090150 4B_1^{24}X_0^6d_2^{11}\rho^{15} + 26625359449774263078981678954905 6B_1^{24}X_0^6d_2^{10}\rho^{16}$$

$$+ 56672198808122986001341387702272 0B_1^{24}X_0^6d_2^9\rho^{17} + 10184933887822396570023113720463 36B_1^{24}X_0^6d_2^8\rho^{18} + 15310910314356722176323370867752 96B_1^{24}X_0^6d_2^7\rho^{19}$$

$$+ 19004449734432654110142204047523 84B_1^{24}X_0^6d_2^6\rho^{20} + 19126759653452975922767054713651 20B_1^{24}X_0^6d_2^5\rho^{21} + 15208754958396429714605662871224 32B_1^{24}X_0^6d_2^4\rho^{22}$$

$$+ 91908841583354163358906975046860 8B_1^{24}X_0^6d_2^3\rho^{23} + 39645295144527994278719416329830 4B_1^{24}X_0^6d_2^2\rho^{24} + 10868089960248071865414862661224 4B_1^{24}X_0^6d_2\rho^{25} + 14012931278171668480B_1^{23}X_0^7d_2^{25}\rho$$

$$+ 68978540771159667507 2B_1^{23}X_0^7d_2^{24}\rho^2 + 21596753457631850059776B_1^{23}X_0^7d_2^{23}\rho^3 + 48298395210110917739724 8B_1^{23}X_0^7d_2^{22}\rho^4 + 82136616103839942866713 60B_1^{23}X_0^7d_2^{21}\rho^5$$

$$+ 11041173486756929904785612 8B_1^{23}X_0^7d_2^{20}\rho^6 + 12039301536115193138453245 44B_1^{23}X_0^7d_2^{19}\rho^7 + 10842975191934024262885429760B_1^{23}X_0^7d_2^{18}\rho^8 + 81710584867377942426062314496B_1^{23}X_0^7d_2^{17}\rho^9$$

$$+ 52003372267069482602387083980 8B_1^{23}X_0^7d_2^{16}\rho^{10} + 28135652945735676574915420235 52B_1^{23}X_0^7d_2^{15}\rho^{11} + 12997211757347974946492526606848B_1^{23}X_0^7d_2^{14}\rho^{12}$$

$$+ 51392026859607558576868457461760B_1^{23}X_0^7d_2^{13}\rho^{13} + 17407802885420466629337680857497 6B_1^{23}X_0^7d_2^{12}\rho^{14} + 50470172725325563693969070860288 0B_1^{23}X_0^7d_2^{11}\rho^{15} + 14566908060850144633 6B_1^{27}X_0^3d_2^{22}\rho^4$$

$$+ 26045256052663094775 52B_1^{27}X_0^3d_2^{21}\rho^5 + 36808299442209454417824B_1^{27}X_0^3d_2^{20}\rho^6 + 42191609170174226808997 6B_1^{27}X_0^3d_2^{19}\rho^7 + 39939073444967813193273 92B_1^{27}X_0^3d_2^{18}\rho^8$$

$$+ 31627056303229498118246112B_1^{27}X_0^3d_2^{17}\rho^9 + 21145878971431743631264412 8B_1^{27}X_0^3d_2^{16}\rho^{10} + 12015041313175804031359665 52B_1^{27}X_0^3d_2^{15}\rho^{11} + 58268076211124871204535768 64B_1^{27}X_0^3d_2^{14}\rho^{12}$$

$$+ 24177128564103129909709580864B_1^{27}X_0^3d_2^{13}\rho^{13} + 85896500480112510336099741696B_1^{27}X_0^3d_2^{12}\rho^{14} + 26107164276157213085723226112B_1^{27}X_0^3d_2^{11}\rho^{15} + 67707660121405620891246423244 8B_1^{27}X_0^3d_2^{10}\rho^{16}$$

$$+ 14916813513529451563030384926 72B_1^{27}X_0^3d_2^9\rho^{17} + 27732062466183418127718013992 96B_1^{27}X_0^3d_2^8\rho^{18} + 43098790073033249121485416366 08B_1^{27}X_0^3d_2^7\rho^{19}$$

$$+ 55264104828997477489122438021 12B_1^{27}X_0^3d_2^6\rho^{20} + 57410308212790854467863220060 16B_1^{27}X_0^3d_2^5\rho^{21} + 47074100830988744252462538424328B_1^{27}X_0^3d_2^4\rho^{22}$$

$$+ 29301725659441511445545908961 28B_1^{27}X_0^3d_2^3\rho^{23} + 13001484893291259159743865815 04B_1^{27}X_0^3d_2^2\rho^{24} + 36603644044443550745082671923 2B_1^{27}X_0^3d_2\rho^{25} + 41325359006310400B_1^{26}X_0^4d_2^{25}\rho$$

$$+ 21120062524274063 36B_1^{26}X_0^4d_2^{24}\rho^2 + 68660238820954409216B_1^{26}X_0^4d_2^{23}\rho^3 + 15944324541524864585 66B_1^{26}X_0^4d_2^{22}\rho^4 + 28155735938422470450256B_1^{26}X_0^4d_2^{21}\rho^5 + 39299013365004360988296 0B_1^{26}X_0^4d_2^{20}\rho^6$$

$$+ 44490166151215010193571 68B_1^{26}X_0^4d_2^{19}\rho^7 + 41595718526151938951497792B_1^{26}X_0^4d_2^{18}\rho^8 + 32534118621051474591592576B_1^{26}X_0^4d_2^{17}\rho^9 + 21486162236421703949105878 08B_1^{26}X_0^4d_2^{16}\rho^{10}$$

$$+ 12059818745430695737034793872B_1^{26}X_0^4d_2^{15}\rho^{11} + 57778290986836963904782396512B_1^{26}X_0^4d_2^{14}\rho^{12} + 23686458836158255332765522016 0B_1^{26}X_0^4d_2^{13}\rho^{13} + 83153866857283876905413790220 8B_1^{26}X_0^4d_2^{12}\rho^{14}$$

$$+ 24976771091859307579763955471 36B_1^{26}X_0^4d_2^{11}\rho^{15} + 64025188195277162743123477340 16B_1^{26}X_0^4d_2^{10}\rho^{16} + 13944485005445325675900628832256B_1^{26}X_0^4d_2^9\rho^{17}$$

$$+ 25633655287606721702972397625344B_1^{26}X_0^4d_2^8\rho^{18} + 39400149175264035866516634501120B_1^{26}X_0^4d_2^7\rho^{19} + 49980379037881764983981625704448B_1^{26}X_0^4d_2^6\rho^{20}$$

$$+ 51381828328643167037863162281984B_1^{26}X_0^4d_2^5\rho^{21} + 41709014042786041325414101549056B_1^{26}X_0^4d_2^4\rho^{22} + 25713776190848719676451116285952B_1^{26}X_0^4d_2^3\rho^{23}$$

$$
\begin{aligned}
&+ 1130646494844615820715534529331 2B_1^{26}X_0^4d_2^2\rho^{24} + 3156506843574437419711520047104B_1^{26}X_0^4d_2\rho^{25} + 359192001472020480B_1^{25}X_0^5d_2^{25}\rho + 1813045977980412928 8B_1^{25}X_0^5d_2^{24}\rho^2\\
&+ 582110282344016424448B_1^{25}X_0^5d_2^{23}\rho^3 + 133500150867002513690888B_1^{25}X_0^5d_2^{22}\rho^4 + 232816685656201956095392B_1^{25}X_0^5d_2^{21}\rho^5 + 320924530964333359671596 8B_1^{25}X_0^5d_2^{20}\rho^6\\
&+ 358813068227106172454723 52B_1^{25}X_0^5d_2^{19}\rho^7 + 331322582155314691982956800B_1^{25}X_0^5d_2^{18}\rho^8 + 255953480356906940482031750 4B_1^{25}X_0^5d_2^{17}\rho^9 + 93179312573 44B_1^{29}X_0d_2^{25}\rho + 4940216669895 68B_1^{29}X_0d_2^{24}\rho^2\\
&+ 16663826166766240B_1^{29}X_0d_2^{23}\rho^3 + 4015575207878764 88B_1^{29}X_0d_2^{22}\rho^4 + 735896668892634495 4B_1^{29}X_0d_2^{21}\rho^5 + 1066002371242483671 80B_1^{29}X_0d_2^{20}\rho^6 + 1252469787405591862576B_1^{29}X_0d_2^{19}\rho^7\\
&+ 1215235104016087531985 6B_1^{29}X_0d_2^{18}\rho^8 + 9863298019964254457065 0B_1^{29}X_0d_2^{17}\rho^9 + 6758606226231907693377 96B_1^{29}X_0d_2^{16}\rho^{10} + 3935301795397406938974588B_1^{29}X_0d_2^{15}\rho^{11}\\
&+ 1955436361583719160903810 4B_1^{29}X_0d_2^{14}\rho^{12} + 8311914777968516391076569 6B_1^{29}X_0d_2^{13}\rho^{13} + 3024550820303297550337749 12B_1^{29}X_0d_2^{12}\rho^{14} + 9412829135723171868434288 64B_1^{29}X_0d_2^{11}\rho^{15}\\
&+ 2498829496237743814953441792B_1^{29}X_0d_2^{10}\rho^{16} + 5633130403406428091114471424B_1^{29}X_0d_2^9\rho^{17} + 1071113463306671041097607168 0B_1^{29}X_0d_2^8\rho^{18} + 1701624679344487752215932108 8B_1^{29}X_0d_2^7\rho^{19}\\
&+ 2228975151056409626289812275 2B_1^{29}X_0d_2^6\rho^{20} + 2363598248394371068399111372 8B_1^{29}X_0d_2^5\rho^{21} + 1976379649724411599156936704 0B_1^{29}X_0d_2^4\rho^{22} + 1253061696949478281077954969 6B_1^{29}X_0d_2^3\rho^{23}\\
&+ 5654893508257880566545776640B_1^{29}X_0d_2^2\rho^{24} + 1616236718259482768638476288B_1^{29}X_0d_2\rho^{25} + 230153379237888B_1^{28}X_0^2d_2^{25}\rho + 1205507809619097 6B_1^{28}X_0^2d_2^{24}\rho^2 + 4016967463416393 60B_1^{28}X_0^2d_2^{23}\rho^3\\
&+ 9562017885032001960B_1^{28}X_0^2d_2^{22}\rho^4 + 1730935656825064866 00B_1^{28}X_0^2d_2^{21}\rho^5 + 2476705040104763699988B_1^{28}X_0^2d_2^{20}\rho^6 + 2874292338654584069475 6B_1^{28}X_0^2d_2^{19}\rho^7 + 2754692136446661823067 28B_1^{28}X_0^2d_2^{18}\rho^8\\
&+ 2208471224449272764326896B_1^{28}X_0^2d_2^{17}\rho^9 + 1494850701908661075556760 4B_1^{28}X_0^2d_2^{16}\rho^{10} + 8598268091488261587844962 0B_1^{28}X_0^2d_2^{15}\rho^{11} + 4220826713477408079815346 0B_1^{28}X_0^2d_2^{14}\rho^{12}\\
&+ 1772607729810981675582608544B_1^{28}X_0^2d_2^{13}\rho^{13} + 6373473125969582684966022336B_1^{28}X_0^2d_2^{12}\rho^{14} + 1960178559016866816124328601 6B_1^{28}X_0^2d_2^{11}\rho^{15} + 5143289155394793829181933414 4B_1^{28}X_0^2d_2^{10}\rho^{16}\\
&+ 1146215088833023824560141414 40B_1^{28}X_0^2d_2^9\rho^{17} + 2155084870347517406112307077 12B_1^{28}X_0^2d_2^8\rho^{18} + 3386313724472055006625720074 24B_1^{28}X_0^2d_2^7\rho^{19} + 4388858437539218939509122662 40B_1^{28}X_0^2d_2^6\rho^{20}\\
&+ 4606643806555560602715000668 16B_1^{28}X_0^2d_2^5\rho^{21} + 3814784610043130302957847838 72B_1^{28}X_0^2d_2^4\rho^{22} + 2396842014324012474080962805 76B_1^{28}X_0^2d_2^3\rho^{23} + 1072774988898673828853490647 04B_1^{28}X_0^2d_2^2\rho^{24}\\
&+ 3044044487718886279757797785 6B_1^{28}X_0^2d_2\rho^{25} + 3637892889190400B_1^{27}X_0^3d_2^{25}\rho + 1882287865781760 00B_1^{27}X_0^3d_2^{24}\rho^2 + 6195469019085494912B_1^{27}X_0^3d_2^{23}\rho^3 + 8808618864830054400B_1^6X_0^{24}d_2^{26}\\
&- 3319779597671044220526824679014 4B_1^6X_0^{24}\rho^{26} + 1409379018372808704B_1^5X_0^{25}d_2^{26} - 995633047727020916431236838195 2B_1^5X_0^{25}\rho^{26} + 1084137706440622 08B_1^4X_0^{26}d_2^{26}\\
&- 1159311825098565628512109068288B_1^4X_0^{26}\rho^{26} + 2601201862503836564907695800 32B_1^3X_0^{27}\rho^{26} + 1331140664191295592836628480 00B_1^2X_0^{28}\rho^{26} + 2301190297636446634053206016 0B_1X_0^{29}\rho^{26}\\
&+ 3647915698170101 76X_0^{30}d_2^{22}\rho^4 + 2407624360792267161 6X_0^{30}d_2^{21}\rho^5 + 7500114675437729218 56X_0^{30}d_2^{20}\rho^6 + 1467921276943648948224 0X_0^{30}d_2^{19}\rho^7 + 2026665228600967094599 68X_0^{30}d_2^{18}\rho^8\\
&+ 2100487369001695809896448X_0^{30}d_2^{17}\rho^9 + 1697731794597201458076057 6X_0^{30}d_2^{16}\rho^{10} + 1097250084154304958289674 24X_0^{30}d_2^{15}\rho^{11} + 5767909201993052738027520 00X_0^{30}d_2^{14}\rho^{12}\\
&+ 2494799296794587014946095104X_0^{30}d_2^{13}\rho^{13} + 8946354375737687862128148480X_0^{30}d_2^{12}\rho^{14} + 2671446517543963074184504934 4X_0^{30}d_2^{11}\rho^{15} + 6653021704857761955068038348 8X_0^{30}d_2^{10}\rho^{16}\\
&+ 1380341379107510347248540057 60X_0^{30}d_2^9\rho^{17} + 2376618015893572121843780812 80X_0^{30}d_2^8\rho^{18} + 3371777389838126174448868392 96X_0^{30}d_2^7\rho^{19} + 3898276036019018138923051253 76X_0^{30}d_2^6\rho^{20}\\
&+ 3612731063082580736609102069 76X_0^{30}d_2^5\rho^{21} + 2618828000953817858274911846 40X_0^{30}d_2^4\rho^{22} + 1430165289233204386823279738 88X_0^{30}d_2^3\rho^{23} + 5532649013466350418042814464 0X_0^{30}d_2^2\rho^{24}\\
&+ 1351337281165232491486563532 8X_0^{30}d_2\rho^{25} + 181347630848B_1^{30}d_2^{25}\rho + 9731240857440B_1^{30}d_2^{24}\rho^2 + 332243351248752B_1^{30}d_2^{23}\rho^3 + 8104259504656662B_1^{30}d_2^{22}\rho^4 + 1503439628339722 77B_1^{30}d_2^{21}\rho^5\\
&+ 2204678113972047567B_1^{30}d_2^{20}\rho^6 + 2622291068760588526B_1^{30}d_2^{19}\rho^7 + 2575748899312698682 0B_1^{30}d_2^{18}\rho^8 + 2116370954248422936813B_1^{30}d_2^{17}\rho^9 + 1468059028638350465854 7B_1^{30}d_2^{16}\rho^{10}\\
&+ 8652954104451554486342 4B_1^{30}d_2^{15}\rho^{11} + 4352166314031760478973 00B_1^{30}d_2^{14}\rho^{12} + 1872427616358319291200048B_1^{30}d_2^{13}\rho^{13} + 6895467653392951543763136B_1^{30}d_2^{12}\rho^{14}\\
&+ 2171535661060072383373977 6B_1^{30}d_2^{11}\rho^{15} + 5832551648792028464240716 8B_1^{30}d_2^{10}\rho^{16} + 1330030099043477741619947 52B_1^{30}d_2^9\rho^{17} + 2557589598437618072263311 36B_1^{30}d_2^8\rho^{18}\\
&+ 4107819861818143546096189 44B_1^{30}d_2^7\rho^{19} + 5438028069135509079328358 40B_1^{30}d_2^6\rho^{20} + 5824970885841828397268336 64B_1^{30}d_2^5\rho^{21} + 4917183413129142983637073 92B_1^{30}d_2^4\rho^{22}\\
&+ 3144970118364747271703101 44B_1^{30}d_2^3\rho^{23} + 1430359452532868871188643 84B_1^{30}d_2^2\rho^{24} + 411484910362810327593123 84B_1^{30}d_2\rho^{25} + 84005535744B_1^{29}X_0d_2^{26} + 2195564246668478301591306 24B_1^{29}X_0\rho^{26}\\
&+ 2100138393600B_1^{28}X_0^2d_2^{26} + 4110799484977331043362144256B_1^{28}X_0^2\rho^{26} + 33602214297600B_1^{27}X_0^3d_2^{26} + 4909518147026101593060252057 6B_1^{27}X_0^3\rho^{26} + 386425464422400B_1^{26}X_0^4d_2^{26}\\
&+ 4201676485709152932525464616 96B_1^{26}X_0^4\rho^{26} + 34005440869171 20B_1^{25}X_0^5d_2^{26} + 2744159346796478422587052916736B_1^{25}X_0^5\rho^{26} + 2380380860841984 0B_1^{24}X_0^6d_2^{26}\\
&+ 1422126095814127528171291017216 0B_1^{24}X_0^6\rho^{26} + 136021763476684800B_1^{23}X_0^7d_2^{26} + 6002726152944355776274828256870 4B_1^{23}X_0^7\rho^{26} + 6461033765142528 00B_1^{22}X_0^8d_2^{26}\\
&+ 2101741461390529821578574189035 52B_1^{22}X_0^8\rho^{26} + 2584413506057011200B_1^{21}X_0^9d_2^{26} + 6184596786563500322050211441541 12B_1^{21}X_0^9\rho^{26} + 8787005920593838080B_1^{20}X_0^{10}d_2^{26}\\
&+ 1543872460167804519649359144419328B_1^{20}X_0^{10}\rho^{26} + 2556219904172752896 0B_1^{19}X_0^{11}d_2^{26} + 3290852247714599958878934269952000B_1^{19}X_0^{11}\rho^{26} + 6390549760431882240 0B_1^{18}X_0^{12}d_2^{26}\\
&+ 6014669877925376282695324693168128B_1^{18}X_0^{12}\rho^{26} + 1376426102246866944 00B_1^{17}X_0^{13}d_2^{26} + 9445429802381703663998493328932864B_1^{17}X_0^{13}\rho^{26} + 2556219904172752896 00B_1^{16}X_0^{14}d_2^{26}\\
&+ 1274530023991863452865303192954470 4B_1^{16}X_0^{14}\rho^{26} + 4089951846676404633 60B_1^{15}X_0^{15}d_2^{26} + 1474511798703870514496249477568921 6B_1^{15}X_0^{15}\rho^{26} + 5623683789180056371 20B_1^{14}X_0^{16}d_2^{26}\\
&+ 1455480117109743848486689522581504 0B_1^{14}X_0^{16}\rho^{26} + 6616098575505948672 00B_1^{13}X_0^{17}d_2^{26} + 1215431108857861392057710480562585 6B_1^{13}X_0^{17}\rho^{26} + 6616098575505948672 00B_1^{12}X_0^{18}d_2^{26}\\
&+ 8465687725152077722932471543103488B_1^{12}X_0^{18}\rho^{26} + 5571451432005009408 00B_1^{11}X_0^{19}d_2^{26} + 4799148627124431791002083139780608B_1^{11}X_0^{19}\rho^{26} + 3900016002403056858 60B_1^{10}X_0^{20}d_2^{26}\\
&+ 2111452847706797695144892911583232B_1^{10}X_0^{20}\rho^{26} + 2228580572802003763 20B_1^9X_0^{21}d_2^{26} + 6397373405191856455511690969088 00B_1^9X_0^{21}\rho^{26} + 1012991169455456256 00B_1^8X_0^{22}d_2^{26}\\
&+ 7113138166311052068754149290803 2B_1^8X_0^{22}\rho^{26} + 3523447545932021760 0B_1^7X_0^{23}d_2^{26} - 4869134141380426772086130108006 4B_1^7X_0^{23}\rho^{26},
\end{aligned}
$$

Appendix B

In Section 2.3 of Chapter 2, F_5 is given by

$$
\begin{aligned}
F_5 = &-864464377694645416623129992344153559007022296693513484920422400B + 22283066366582715976802171907121249298330669930861578212380337367941 12B^9 \\
&- 40435209964788672146644072100858576391561470115673355682305802240B^3 - 89184359981934452621413047075255825750882685632079770476661964 80B^2 \\
&+ 28336681879102319547678392631806571805416368090813987595137140654 08B^5 + 78718308342022918287936146803681132485676509344598352818037 850112B^4 \\
&+ 27081297340361231405196066604128902110172584960204378361661197647872B^6 + 17408748436599085271743967185504894462868371450317178835086686447 2064B^7 \\
&+ 79865949659552648027543041406808376964334626247264562886174004215808 0B^8 - 85274469173669110941629675256329160807260329583656542113243351062937 6B^{10} \\
&- 49199497352029688521240172293846721419180371919411141607100881543223936144113664B^{28} - 16147183674470087554218532691689097007161921517412184941680970441195738825228288B^{27} \\
&- 13140527082058504663939304395248075445138360271431724813462277570151689015315660 8B^{29} - 43049614777452207641182816303984047130786065977594128856812449102012140916571 6B^{26} \\
&- 69139261002437626062314382845547238655004259399670570301396273984861675244748 8B^{25} - 31749271376670395282934694413242201959073423615517283921137902177788431451344076 8B^{31} \\
&+ 13323926648163643202333083037727671752308663661041008328056586907443809956659 2B^{24} + 18746446329280954428219774763591054437035933447641570911336724107035436856115 2B^{23} \\
&+ 10795897666882091387927568008732670613292509848417236697159300703704961358233 6B^{22} + 46612618781269434279626994261138858794741358277175328648141259923815053393920B^{21} \\
&+ 16494827270600767238354142611397787650055480300946358362589293929199090728 96B^{20} + 48183493682018618778240350552887378176222332339579553718279668006236129853 44B^{19} \\
&+ 11085956834812050085962148352344040412116025144872349204801249401995358371 84B^{18} + 16566984197528435843046296003279324072880616245105628835427281573697814528 0B^{17} \\
&- 48323847449406709893572171440566347366749176603148554380320187244420792 32B^{16} - 14178377202552699290952826200991320221928521549329002584615928618582802432B^{15} \\
&- 60683907528670032426695101509831343618551755441583768299208843409940807 68B^{14} - 17489718778095550453872392465523373787770463020002470222483106592918077 44B^{13} \\
&- 37436109303655953032377264529353792882015751318555042311035476348869017 6B^{12} - 53106130597903514386047931702617243249438598624499369291523039395053568B^{11} \\
&- 34313945632736272058442969453574860833977262463190895375155200 - 33683119304032183110184323317919313893520717898668783216904818332349136497893441536B^{46} \\
&- 17003144062760968660378327971680603042297257407408497731219251030899994346506813 44B^{47} - 13495727674687537492374038552618566931652720303415534075194167102152527979321753 6B^{48} \\
&+ 14598890496414185672815357588603844868395540369528038737624096019537196853839790080B^{49} + 25424557460646419148144180225350840615902048737132715932645573075791321948655452160B^{50} \\
&+ 31474737963311881579881757559731529639809699796442780369269232486327042788219158528B^{51} + 32873453628273140083345243605651374606435678446495047563671111348512552717581182566 4B^{52} \\
&+ 30546159339109793682256860679103923049408985544494515968285366876963144727938465792B^{53} + 25851123443670042870386347400498524374342901691811192170171770593704842582510534656B^{54} \\
&+ 20177113058915606384468292494734631280216959459146300939875379474618849998451769344B^{55} + 14636671542146177243998956991980750867108444885539449434620662948387567111505969152B^{56} \\
&+ 99211386187765625379843209572783317011599482814392159251197702316347771256265768 96B^{57} + 63103207661911268609707275511614437170111126526012445613875968331644295111738654 72B^{58} \\
&+ 37802333587833495059275336513219789856794022734561299657486550942650792981896888 32B^{59} + 21403228940562508621098397790982512428121832701917124587343611246537973985087324 16B^{60} \\
&+ 11492459911223578159449014226661526746036250565672975163949397070288664353959 78912B^{61} + 58715506935285542723830767218549617130038439040142957141805854589308548417585152 0B^{62} \\
&+ 28630518995395517944325405140767252264442239147963113463866929379060662715862220 8B^{63} + 13359441039330138572545427762059169525309567189461559502219132175037178492066201 6B^{64} \\
&+ 59773636951182552650757868176629574034267681878494188791146472074744794349305856B^{65} + 25677040000419505167533313221126178157135865410136068517703108022651829481373696B^{66} \\
&+ 10594502811397965438295255403787098812491725225528791828913137507428106835066880B^{67} + 41967339708645597668344780648709578613531324269145635689948616849218691136716 80B^{68} \\
&+ 15936949182291883484214595550070845723675759683001986730876128737539477020999 68B^{69} + 57870146929429559124682738179306038179857733654735502153456880152556406935552 0B^{70} \\
&+ 20019155731977077642168977550357718835799817231566956149834056297188390174310 4B^{71} + 65658766542693861484359458767644475310768417586505388593791370222847605429248B^{72} \\
&+ 20304229537682847837317954520997667919386328220424826875768975758404783750144B^{73} + 58869026441120897616208725457782483551217881888685112239789836025354753822 72B^{74} \\
&+ 15928186270349520586853186522147024917628734155688450815536518772944626862 08B^{75} + 40124146554368021338779030639875734727123258748027882955388944838770269772 8B^{76} \\
&+ 94249923916521150078631218433850868235096101060610524854527623145144260096B^{77} + 20779989489319877399703583527515752404274744627420873836464639501307364608B^78
\end{aligned}
$$

$$+ 434529759977506928269757953238840065119571267082649494659522021554259968 0B^{79} + 868972384463904100851813025901258804307166316085191317833898103884890816B^{80}$$
$$+ 165484192416576952892901312705393490193724491190309149387567938234737024B^{81} + 292450755873375766333440085377131231208886882747499056718347970321872 32B^{82}$$
$$+ 455566371274324188042136274145086023311058177219184284007445408742723 2B^{83} + 571203288451571386296560176966060474242703259416798380702889700896704B^{84}$$
$$+ 453196134266127523438258108076912531627146599120187435068668309503 20B^{85} - 116679462059785165113204966425220043008712602114025685368008206784 0B^{86}$$
$$- 116738136857616364612212593949335094677675269169918073394494887611 2B^{87} - 232014361115239982403914227205551240816761671666820553619417342976B^{88}$$
$$- 290897115293553036617269720818458788365590169367402766941972560 84B^{89} - 253100517718560826650854207167312314027879549581509093330593216 6B^{90}$$
$$- 149549367622987447906965545183008044019692794618873264044429134B^{91} - 538856072378233129763385978581578943126210316619512796652127 9B^{91}$$
$$- 843261582198818058364736025143056412132125659185882188993 17B^{93} + 359098678279423005492281073288668612343391930044438789855B^{94}$$
$$- 705270480874162918169608110073368268522537624966304359348574139956490396827123712B^{31} - 145395876079056930879194995836638019706362322629251776324578572196117131571914342 4B^{32}$$
$$- 279799626256210901545734245994354296554784027837749146573347114772829822346539827 2B^{33} - 504497457591737148450113273682058623690452576348645546191007164452355037298950144 0B^{34}$$
$$- 854340987028971845069946438607167386684175149052487871239861146768114325398120038 4B^{35} - 136086174232455234058949141506423097024004800482303508329360360266653748540368486 40B^{36}$$
$$- 204059973038631777256931945219936986070098529853215095645277237494852082394673971 20B^{37} - 288102423684594632699713686145872506241255718851538819014447907681531399657970728 96B^{38}$$
$$- 382808055556844890347107603969402038467021714346903721062539582766365840377611550 72B^{39} - 478083920319785454683084706987058682033901023579185401211527165349995238696985559 04B^{40}$$
$$- 559836821690422995858383249225621741244983516212369485995020495519860156118136258 56B^{41} - 612123546104472276870520647225710853827066011869339897861177639961224846507612569 60B^{42}$$
$$- 620535625391652513763377177183950362115562238363006200381195311325536982744873041 92B^{43} - 576062920593551733195333798305066777841597200918343177082440750169024181597854760 96B^{44}$$
$$- 478300581266344189366135752785429181038617168250944072872657781198907366137879592 96B^{45}.$$

Curriculum Vitae

Name:	Xiangyu Wang
Post-Secondary Education and Degrees:	University of Western Ontario London, Ontario, Canada, 2017-2018 Master of Science, Applied Mathematics
	Hefei University of Technology Hefei, Anhui, china, 2012-2016 Bachelor of Science, Mathematics and Applied Mathematics
Honours and Awards:	Excellent Bachelor's Thesis, 2016 The first prize scholarship, 2015 The first prize scholarship, 2014 The third prize scholarship, 2013 Hefei University of Technology, China
Related Work Experience:	Teaching Assistant Department of Applied Mathematics 2017 - 2018 Research Assitant Department of Applied Mathematics 2017-2018